Use of oyster shell (Crassostrea gigas) as aggregate replacement for producing environmentally-friendly concrete

Ana Claudia Pinto Dabes Guimaraes

Université de Pau et des Pays de l'Adour

École Doctorale des Sciences Exactes et leurs Applications

Thesis presented to obtain a PhD in Civil Engineering

Ana Cláudia Pinto Dabés Guimarães

Use of oyster shell (*Crassostrea gigas*) as aggregate replacement for producing environmentally-friendly concrete

Thesis defended on 9th May 2022 in front of the Jury members:

Mark G. Alexander	PR at University Cape Town	President
Alexandra Bourdot	MC at ENS Paris Saclay	Examiner
David Grégoire	PR at Université de Pau et des Pays de l'Adour	Director
Thibaut Lecompte	MC HDR at Université Bretagne Sud	Reviewer
Céline Perlot	MC HDR at Université de Pau et des Pays de l'Adour	Director
Brahim Safi	PR University M'Hamed Bougara of Boumerdes	Examiner
Nassim Sebaibi	MC HDR ESITC Caen	Reviewer

ACKNOWLEDGEMENTS

I would like to thank my kind thesis supervisors Professor David Grégoire and Professor Céline Perlot for guidance and support throughout my PhD. A special thank you to Olivier Nouaillettas for his dedication to the project and all his advice.

I wish to show my appreciation to the Jury Members for letting my PhD defence be an enjoyable moment, with a great scientific exchange and your brilliant comments that will contribute to the progress of the project BeCCoH.

I would like to thank Professor Fernando Soares Lameiras for his valuable contribution to the statistical part of this thesis.

I wish to show my appreciation to the Région Nouvelle-Aquitaine, the Comité Régional de Conchyliculture Arcachon-Aquitaine (CRCAA) and the Institut Universitaire de France for funding the project; Ovive and Cemex for their collaboration to the project; and, the UPPA and ISA BTP facilities where I could develop my experimental program.

I would like to thank the people from LFCR and SIAME laboratories and ISA BTP for their kindness and good moments, especially Bruno Fernandes for his friendship, help and motivation throughout the PhD.

Last but not the least, I would like to thank my parents Tânia and Geraldo; my boyfriend James; my brother Luiz and his wife Barbara; and my friends in Brazil especially Bruna, for their support, love and motivation throughout the PhD, even with the ocean setting us apart sometimes.

ABSTRACT

Due to the depletion of resources, by-products claim attention to be reused or reincorporated in other materials. Cementitious materials are on the top of the list of the most consumed materials which traditionally leads to a high demand for raw materials. In the actual context of net zero emissions target and circularity economy, building materials must be reinvented through a more sustainable approach. Based on this, bio-based materials have been attracting attention to be incorporated into building materials, improving materials properties and providing lower environmental burdens. Within this context, the Nouvelle-Aquitaine region (France), the Arcachon bay shellfish farming Comittee and France University Institute funded the BeCCoH project, which aims to assess the potential use of crushed oyster shells (OS) in concrete. The oyster farming activity is largely developed in this region and generates a high amount of waste (shells) due to the maintenance and cleaning process in the farming area on top of food consumption. In general, the shells represent over 70% of the oyster weight, leading to over 700 kilograms of waste per ton of production. Therefore, the BeCCoH project has been built to evaluate the reuse of crushed oyster shells as aggregate replacement in cementitious materials, raising awareness in the local community about alternative sustainable solutions for local by-products.

In this context, this PhD thesis aims to investigate the use of crushed oyster shells to fully replace fine and coarse aggregate in concrete and to characterise the change of material properties and the potential environmental benefits from this substitution. A new approach is developed to optimise the granular skeleton obtained after oyster shell crushing. This approach consists in combining particle classes in different proportions to obtain better particle packing. Because of the flatness of the crushed OS, traditional methods designed for spherical particles cannot be used for this purpose. Consequently, our strategy is to directly minimise the intergranular porosity, which can be estimated through loose bulk and oven-dried densities of particle classes. A statistical software is used to analyse the particle classes combination and to optimise the mixture proportion in order to decrease the intergranular porosity. The crushed OS is optimised into fine (0/4 mm) and coarse (4/10 mm) aggregates. Once this optimisation is determined, a self-compacting concrete formulation is set with a full replacement of conventional aggregate (sand and gravel) by OS. To limit further environmental impacts, low clinker cement (CEM V/A) is chosen for concrete mixes. As conventional aggregates are

substituted by OS, the formulation goes beyond the prescriptions of NF EN 206/CN for classical concretes. Therefore, the performance-based approach is applied to evaluate whether the concrete meets the performance and durability requirements or not. In this aim, the mechanical properties considered are the compressive strength, the flexural strength, the tensile splitting strength and the elastic modulus. In sequence, relevant durability indicators are chosen to evaluate the ageing of the OS concrete: carbonation, chloride migration, gas permeability, capillary water absorption and porosity accessible to water.

Going further on the sustainable approach, the environmental impacts related to the replacement of conventional aggregates by crushed OS in concrete are investigated. We aim to evaluate the potential environmental impacts and possibilities for improvement in these processes. The energy demand, fuel consumption, water used and solid waste were the main indicators chosen to be assessed.

RESUMÉ

Dans le contexte de la transition énergétique appliquée au Génie Civil, une attention particulière est portée à l'épuisement des ressources naturelles et à l'empreinte carbone des matériaux. Les matériaux cimentaires figurent en tête de liste des matériaux les plus consommés ce qui conduit à une forte demande en matières premières. Dans le contexte actuel de zéro émission nette et d'économie circulaire, les matériaux de construction doivent être réinventés à travers une approche plus durable et plus globale. Un des leviers est la réutilisation des sous-produits. Dans cette logique, les sous-produits biosourcés sont étudiés pour être incorporés dans les matériaux de construction, réduisant les charges environnementales tout en améliorant les propriétés hygrothermiques des matériaux. La région Nouvelle-Aquitaine (France), le comite de conchyliculture du Bassin d'Arcachon et l'Institut Universitaire de France ont financé le projet BeCCoH (Béton et Coulis pour la valorisation de COquilles d'Huîtres), qui vise à évaluer le potentiel de réutilisation des coquilles d'huîtres concassés (OS) dans le béton. L'activité ostréicole est largement développée dans cette région (dont le Bassin d'Arcachon) et génère une quantité importante de déchets (coquilles) due au processus d'entretien et de nettoyage de la zone d'élevage en plus de la consommation alimentaire. En général, les coquilles représentent plus de 70 % du poids de l'huître, ce qui entraîne plus de 700 kilogrammes de déchets par tonne de production. Par conséquent, le projet BeCCoH a été construit pour évaluer la réutilisation des coquilles d'huîtres broyées comme granulats de substitution dans les matériaux cimentaires, sensibilisant la communauté locale aux solutions alternatives durables pour les sous-produits locaux, s'inscrivant dans une logique d'économie circulaire.

Dans ce contexte, cette thèse de doctorat vise à étudier l'utilisation de coquilles d'huîtres broyées pour remplacer complètement les granulats fins et grossiers dans un béton et à caractériser le changement des propriétés des matériaux et les avantages environnementaux potentiels de cette substitution. Pour cela, une nouvelle approche est développée pour optimiser le squelette granulaire obtenu après broyage des coquilles d'huîtres. Cette approche consiste à combiner des classes de particules dans différentes proportions pour obtenir un meilleur tassement des particules. En raison de la planéité de l'OS broyé, les méthodes traditionnelles conçues pour les particules sphériques ne peuvent pas être utilisées à cette fin. Par conséquent, notre stratégie consiste à minimiser directement la porosité intergranulaire,

qui peut être estimée à travers les masses volumiques en vrac et réelle séchée à l'étuve des classes de particules. Un logiciel statistique est utilisé pour analyser la combinaison des classes de particules et optimiser la proportion du mélange afin de diminuer la porosité intergranulaire. Finalement, l'OS concassé est optimisé en granulats fins (0/4 mm) et grossiers (4/10 mm). Une fois cette optimisation déterminée, une formulation de béton autoplaçant est définie avec un remplacement complet des granulats conventionnels (sable et gravier) par l'OS. Pour limiter les impacts environnementaux ultérieurs, le ciment à faible teneur en clinker (CEM V/A) est choisi. Les granulats conventionnels étant substitués par l'OS, la formulation va au-delà des prescriptions de la NF EN 206/CN pour les bétons classiques. Par conséquent, l'approche performantielle est appliquée pour évaluer si le béton répond ou non aux exigences de performance et de durabilité. Dans ce but, les propriétés mécaniques considérées sont la résistance à la compression, la résistance à la flexion, la résistance au fendage en traction et le module d'élasticité. Puis, des indicateurs de durabilité pertinents sont choisis pour évaluer la durabilité du béton OS: carbonatation, migration des chlorures, perméabilité au gaz, absorption d'eau capillaire et porosité accessible à l'eau.

Pour aller plus loin dans l'approche durable et valider la réutilisation des sous-produits coquillers, les impacts environnementaux liés au remplacement des granulats conventionnels par l'OS concassé dans le béton sont examinés. Nous visons à évaluer les impacts environnementaux potentiels et les possibilités d'amélioration de ces processus. La demande d'énergie, la consommation de carburant, l'eau utilisée et les déchets solides ont été les principaux indicateurs choisis pour être évalués.

SUMMARY

LIST OF FIGURES

LIST OF TABLES

CHAPTER 1 - INTRODUCTION

1.1 Context

Concrete is one of the most widely used material in the world and its demand continue to grow. However, the processes to obtain the raw materials for concrete (cement production and aggregates extraction) are associated with many environmental impacts such as resource depletion, climate change and others. More precisely, the processes to obtain the conventional aggregates are also harmful to the environment, generating impacts on the ecosystems, land losses, landscape changing and depletion of natural resources. Given this scenario and the current trend to develop sustainable construction materials, efforts have been made to limit clinker and conventional aggregate consumption. One of the solution is to reuse and recycle waste materials and by-products to produce environmentally-friendly concrete.

Shellfish aquaculture is the farming activity where oysters, mussels, clams and others types of molluscs are cultivated for food consumption. For instance, it is estimated that for 1 kg of oyster produced, about 70% represents the shell weight and is treated as a waste of the process. However, the shells can be seen as a by-product of shellfish farming, making them a promising option as aggregate for concrete due to the high content of calcium carbonate. Additionally, the recycling of shells goes into the principles of circularity, adding value to materials consider as waste, and reducing the disposal in landfills.

The Nouvelle Aquitaine region is the main Shellfish producer region in France. The main species cultivated in Arcachon Bay is the oyster shell (Crassostrea gigas), 315 farming points in the bay (Fig. 1-1). This activity generates a high amount of waste like dead shells, by-products from the process, farming cleaning areas and the waste from food consumption as well. The farming cleaning areas have their “oyster shell’s rocks” removed from the farming area and dumped at another point of the bay. The dead shells from the farming process generate about 9500 tonnes per year and have a high potential to be used as a by-product for producing aggregates. Looking for more sustainable management of these wastes and by-products from the oyster shell farming, the project BeCCoH was created (Beccoh – Béton et coulis pour la valorisation de coquilles d’huîtres / Valorisation of oyster shells in concrete and grout). The project is a join effort in partnership of academia (UPPA – Université de Pau et des Pays de l’Adour) with local community (COBAS – Communauté d’Agglomération du Bassin

d'Arcachon Sud), local committee (CRCAA – Comité Régional de la Conchyliculture Arcachon Aquitaine) and a company (OVIVE S.A). The Beccoh project aims to provide alternative solutions for using oyster shells in cementitious materials since their potential as an aggregate replacement and due to a demand for increasing the recycling of materials and decreasing the extraction of raw materials from nature.

Figure 1-1 – Oyster shells (*Crassostrea gigas*) from Arcachon Bay, France.

The efforts to produce more sustainable construction materials and the abundance of shells led up to several studies investigating the feasibility of their use as aggregate replacement in concrete. Because of this, some particularities of shells were found when compared to conventional aggregates. The shells have a flaky, elongated and irregular shape which is different from the shape of conventional aggregates (generally consider as spherical particles). The shells also tend to have a lighter density than conventional aggregates due to their nature and porosity. Correlating to the porosity, the crushed shells also tend to present higher water absorption than conventional aggregates, which need attention when batching concrete. All of these particularities do not limit their use as aggregate in concrete but show the need for adaptations.

One of the main adaptions concerns the optimisation of the granular skeleton. Conventional methods for granular packing often rely on particle diameter or an ideal gradation curve. These

methods are well established for spherical particles but offer limitations when applied to bio-based materials such as crushed shells (non-spherical). The main limitation is the particle shape and hence, a method to optimise the granular skeleton that bypasses this parameter rises as an important step to improve the use of crushed shells as aggregate in concrete.

The use of crushed shells as aggregate replacement in concrete also faces another challenge: the standards that prescribe concrete formulation specifications. The traditional prescriptive approach for designing concrete relies on conventional aggregates and only allows minimum variation of them from the traditional standard of concrete formulation. This approach establishes minimum contents for the mix design (binder content, water/cement ratio) and compressive strength to ensure the concrete durability. Therefore, this approach is not flexible when designing the concrete mix, limiting the use of by-products in concrete and innovation. Conversely, the performance-based approach arose from the need to validate innovative materials that were designed beyond the traditional prescriptive approach. This last approach opens new paths for sustainable materials in construction since the heart of the method is to demonstrate through mechanical and durability performance that the new material provides an equal or better performance than the traditional one.

Besides the several challenges bio-based by-products face to be used in concrete, their natural properties can add value to the final product and their use can reduce the environmental impacts of cementitious materials. The recycling of crushed shells turns this by-product into an avoided burden for the shellfish farming activities although the transportation to far locations can increase the carbon footprint. Therefore, an environmental analysis is often recommended as a way to better assess whether the alternative option bring environmental beneftis or not. Furthermore, this type of analysis allow to identify the hotspots of impacts and opportunities for improving the material use.

1.2 Research objectives

This thesis aimed to investigate the use of crushed oyster shells as aggregate replacement in cementitious materials and the properties of these materials. The use of seashells in cementitious materials faces a few challenges concerning the particle packing (due to the flaky and elongated shape); the amount of conventional aggregate replaced; the hardened properties of concrete and mortars, and the root question of whether recycling the oyster shells in concrete will have a positive balance in terms of decreasing environmental impacts. In order

to find answers to these questions, we developed an experimental investigation that was carried out through this thesis and is described below:

- To improve the particle packing of oyster shells, a granular skeleton optimisation methodology was developed bypassing the shape problem by relying on material's densities;
- The improvement of the particle packing of oyster shells allows for higher replacement rates of conventional aggregates. Therefore, a study was carried out using oyster shell's granular skeleton to replace 100% of sand in mortars and 100% of sand and gravel in a self-compacting concrete;
- To evaluate the effect of this replacement in mortars, two strategies of formulations were studied and compressive and flexural strength were investigated;
- To evaluate the effect of this replacement in concrete, mechanical (compressive, flexural, splitting tensile strength and elastic modulus) were investigated;
- The performance-based approach was used to validate the potential durability of the oyster shell concrete. For this, porosity accessible to water, gas permeability, chloride migration, capillary water absorption and carbonation were investigated;
- To evaluate the potential environmental impact of oyster shell aggregate production and conventional aggregate production processes, a preliminary analysis was carried out to identify potential impacts related to their processes and opportunities for improvement.

1.3 Outline of the thesis

This thesis manuscrit gathers all results of the experimental program and the development of oyster shell concrete. The manuscrit is organised into 6 chapters as follows:

Chapter 1 (current chapter) presents the context of the project, objectives and the experimental program, and the outline for the manuscrit.

Chapter 2 reports the state of the art on the use of seashells in concrete. The particularities of their use in concrete are presented, as well as an overview of the current methods of granular skeleton optimisation. The current concrete formulation apporaches (traditional and prescriptive) are also presented, as well as their differences, advantages and structure.

Chapter 3 presents the granular skeleton optimisation method. The method was applied to optimise separately the fine, coarse and after, the fine + coarse crushed oyster shells.

Chapter 4 presents the validation of the optimised granular skeleton of crushed oyster shells (fine) by comparison to other granular skeletons. Two strategies of formulation are investigated using oyster shell granular skeletons and sand to produce mortar, and the compressive and flexural strength are investigated.

Chapter 5 is focused on the use of the optimised fine + coarse crushed oyster shells granular skeletons to produce self-compacting concrete. To validate the oyster shell concrete, the mechanical and durability properties are investigated and compared to two other concretes made with conventional aggregates (sand and gravel). Hindsight analysis of concrete formulations studied are presented based on the knowledge acquired along with this thesis. To assess the use of OS concrete, the potential durability is evaluated based on the performance-based approach.

Chapter 6 consists of the preliminary environmental analysis of the potential environmental impacts related to the production of conventional and crushed oyster shells aggregates. The main impacts are discussed and opportunities for improvement to reduce the impacts related to these two aggregates production process are suggested in order to enhanced the valorisation of oyster shells.

Finally, general conclusions and perspectives are summarised and presented in the last part of this manuscrit.

Once establish the context, objectives and the outline of the thesis to guide the reader, we will enter in the chapter 2, state of the art.

CHAPTER 2 - STATE OF THE ART

The seashells are the heart of this thesis. Therefore, this chapter aims to present an overview of the studies that have been carried out using seashells to produce cementitious materials and the particularities of their use. We also present the ways to obtain a granular skeleton for concrete, and the methods for designing and validating a concrete formulation (traditional prescriptive approach and performance-based approach).

2.1 The use of seashells as an aggregate replacement in cementitious materials

The aquaculture industry is growing fast and provides a great variety of seafood for food consumption. The consumption of seafood and the cleaning of their farming areas generate large quantities of wastes. Seashells are the main by-product of the aquaculture industry. The seashell is a hard and protective shell created by a marine animal, usually a mollusc, mostly composed of calcium carbonate (calcite). Different uses of these co-products are considered in pharmaceuticals, cosmetics and agriculture. The local resource availability allied to the context of producing more sustainable materials, re-using by-products and decreasing the extraction of raw materials arose the interest in using seashells in cementitious materials for construction. Considering the chemical composition of seashells, studies have been increasing concerning their use in cementitious materials (Eziefula et al., 2018; Mo et al., 2018).

2.1.1 Generalities on the use of seashells

The main seashells studied for aggregate replacement are mussel shells, periwinkle shells, oyster shells, cockle shells, scallop shells, crepidula shell and clamshell. Mortar and concrete were produced using seashells as a partial or total aggregate replacement and physical, chemical, mechanical, and durability properties were investigated. In the sequence, we are going to point out some studies carried out using seashell and their findings.

Seashells in general

(Safi et al., 2015) investigated the use of seashells (the species were not identified) as fine aggregate replacement in self-compacting mortar, with replacement rates up to 100% (replacement by weight). Several properties were investigated in fresh and hardened states.

The authors found that mortar with 100% crushed seashells presented a suitable flowability allowing its use for self-compacting concrete. They also found a minimal reduction in compressive strength and elastic modulus and good adhesion between the seashell and cement paste matrix. They also related this improvement to the better distribution of seashells in the cement matrix due to the angular form of seashells.

(Georges et al., 2021, 2020) investigated concrete formulations incorporating oyster shell by-products in order to enhance marine organism colonisation. The authors tested the durability of these concretes after being immersed for 3 months in the Rance of Dinard (France). The authors found that the incorporation of shells in concrete affects strength, chloride penetration and porosity.

Seashells have been also investigated for other purposes than aggregate replacement, demonstrating the potential of this by-product as a "raw" resource for other materials. Some authors summarised the scientific research carried out using seashells in construction materials (Eziefula et al., 2018; Mo et al., 2018; Tayeh et al., 2019).

Some of the other potential uses for seashells and scientific research carried out on them are summarised below:

- Binder or cement replacement: (Bamigboye et al., 2021; Chen et al., 2019; Tayeh et al., 2019; Wang et al., 2019);
- Alkali-activated materials: (Hasnaoui et al., 2021; Monneron-Gyurits et al., 2018);
- Composite material: (Silva et al., 2019)

The main seashells studied for aggregate replacement are mussel shells, periwinkle shells, oyster shells, cockle shells, scallop shells, crepidula shell and clamshell, usually a "waste" from the food industry. Mortar and concrete were produced using seashells as a partial or total aggregate replacement and physical, chemical, mechanical, and durability properties were investigated. In the sequence, we are going to point out some studies carried out using seashell and their findings.

2.1.2 Particularities on using seashells as aggregate replacement in cementitious materials

Even though the chemical composition of oyster shells is similar to limestone, its use in cementitious materials brings some challenges. Several particularities were identified concerning the use of seashells as aggregate replacement in previous studies and are described below:

Inaccurate sieving

(Cuadrado-Rica, 2016) studied the use of queen scallop shells to replace aggregate in concrete. After comparing the sand equivalent and the particle size distribution, the author found that the traditional sieving process provides accurate results for spherical aggregates and is very imprecise for the shells. This is due to the flattened shape of particles over 4 mm and needle shape for particle sizes smaller than 2 mm. The author suggested that flattened particles are not retained in the sieve aperture of its lateral dimension and the needle particles might be retained in the sieve aperture bigger than its section (Fig. 2-1).

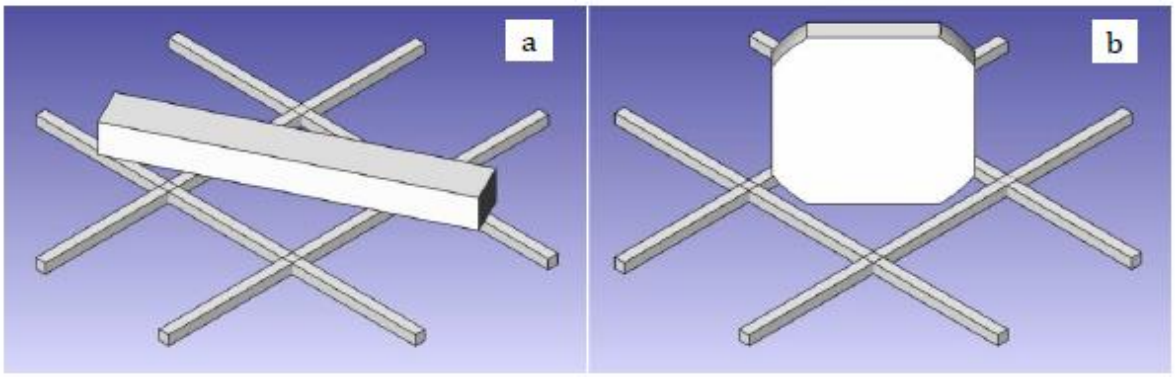

Figure 2-1 – Crushed queen scallop shells of different sizes and the sieving problem; a – needle shape; b – flatten shape (Cuadrado-Rica, 2016).

Seashell particle characteristics (shape, size, texture)

(Eziefula et al., 2018; Nguyen et al., 2013) suggest that the rough texture and the elongated, flaky, angular or irregular shape of seashells are directly related to the losses in workability in cementitious materials.

(Martínez-García et al., 2017; Yang et al., 2010) suggest that the improvement of the water permeability in concrete with mussel and oyster shells is due to the flaky and elongated shape, and the horizontal placement of shells works as a barrier to the water penetration.

(Foti and Cavallo, 2018) suggest that the flaky shape of mussel shells is also responsible for weakening the bond between the cement paste and the aggregate. This occurs due to the internal bleeding water that was stored below the mussel shell particles, increasing the porosity and reducing the mechanical properties.

(Mo et al., 2018) attribute the loss in strength of materials that use seashells as aggregate to the higher surface area of this type of aggregate (demanding a higher amount of cement paste to coat the particles) and the fact that seashell aggregates are weaker than conventional aggregates by their nature.

(Martínez-García et al., 2019) suggest that the smooth texture and flat surface of mussel shells reduce the bond between the mussel aggregates and the air lime matrix, which was confirmed by a high porosity in the interfacial transition zone of mortars made with a mussel shell. Additionally, the authors found micro-cracks around the mussel shell aggregate that were formed because of the irregular shape of the aggregate.

Granular skeleton packing

In terms of granular skeleton packing, (Varhen et al., 2017) discussed very important points concerning the use of crushed scallop shells (CSS) as fine aggregate in concrete. The authors found that the angularity of CSS contributes to creating more voids between the particles. Therefore, if replacing sand by weight and for constant weight, the volume of CSS is higher than sand since there are more voids between the particles.

Water absorption

Authors reported a water absorption for seashells varying from 1.8 to 13%. They reported the variation due to the high amount of internal pores in the seashells and the irregular surface. An extra amount of water corresponding to the water absorbed by the seashells can be added to the mixing water, although this can affect the concrete density (Eziefula et al., 2018; Mo et al., 2018).

Density

Concrete with seashells tends to be more lightweight than concrete with conventional aggregates. The reduction in density is related to the air entrapped in concrete or the poor particle packing that creates voids in the granular skeleton. Additionally, the lower specific gravity, the shape (irregular and angular), and the presence of organic matter contributes to decrese the density (Cuadrado-Rica, 2016; Martínez-García et al., 2017; Varhen et al., 2017).

All these drawback have to be taken into account to valorise seashells as aggregates replacement in concrete and to limit the losses in performances. As mentioned afore, the use of pozzolanic addition or supplementary materials could counterbalance these effects.

2.1.3 Focus on the use of the oyster shell in cementitious materials

Oyster shells (Fig. 2-2 and 2-3) are mostly composed of calcite ($CaCO_3$) with a small number of other minerals, specific gravity varying between 1.85 and 2.48; water absorption coefficient varying between 2.9 and 9.2%; porosity of about 55% and BET surface area of 1.75 m^2/g (Eziefula et al., 2018). The microstructure of an oyster shell shows the presence of two layers, one is a sheet layer and a porous bulk layer between the sheet layers (Yoon et al., 2003).

Figure 2-2 – Oyster shell (*Crassostrea gigas*).

Figure 2-3 - Pile of oyster shell from cleaning farming area in Arcachon Bay, France.

Several research studies have been carried out to investigate the use of the oyster shell in cementitious materials. We are going to summarise the conclusions of these researches below:

(Yoon et al., 2004) investigated the use of crushed oyster shells mixed with sand to produce mortar with fly ash. The authors found that fly ash contributed to improve the long-term compressive strength of mortars with oyster shell particles. They also found that mortars with oyster shells experience failure differently from control mortars (with sand). The sand mortars presented cracks in the vertical direction increasing until failure whereas the mortars containing oyster shells display the start of the fracture at the centre and increase around the outer edges of the specimen until failure.

(Yang et al., 2010, 2005) investigated the fine aggregate replacement by the crushed oyster shell in concrete. The aggregate was replaced up to 20% by weight, and fresh, hardened and durability properties were investigated. The authors found that workability is reduced with the increase in replacement rate and is associated to the shells' shape. The compressive strength was not affected in the concrete with 20% of fine aggregate replaced by oyster shells. However, the elastic modulus decreased (10-15%) as the elastic modulus of oyster shells is smaller than sand. In terms of durability, the authors found that the shrinkage increased with the replacement rate; no significant affect on freezing and thawing, carbonation and chemical attack resistant; and, improvement of permeability resistance.

(Kuo et al., 2013) studied the fine aggregate replacement by oyster shells to produce controlled low-strength materials. The replacement rates were 5, 10, 15 and 20% and the cement was also replaced by 20% with fly ash. Mechanical and durability properties were investigated and the authors suggested that there was no losses in compressive strength at a replacement rate of 20% due to the addition of fly ash. The authors explained that the pozzolanic reaction of the fly ash contributed to fill up the pores in the specimens, decreasing the absorption rates.

(Eo and Yi, 2015) investigated the effect of oyster shells as fine and coarse aggregate replacement in concrete. The coarse aggregate replacement included rates up to 100% whereas for the fine aggregate the maximum replacement rate was 50%. Fresh and hardened properties were investigated. The authors found that as the aggregate replacement rate increases, the workability and strength decrease. They related the strength reduction to the air content of the fresh state and also the particle size of the oyster shell, suggesting that as the particle size increases, the strength decreases.

(Chen et al., 2019) investigated the use of crushed oyster shells as fine aggregate replacement in mortars containing supplementary cementitious materials. Cement was replaced up to 40% by fly ash (FA) and ground granulated blast-furnace slag (GGBS), and 30% of sand was replaced by the crushed waste oyster shell. Mechanical and durability properties were investigated. Authors found the mortars containing crushed waste oyster shells, FA and GGBS provided about the same hardened density and mechanical behaviour as the control mortar.

(Liao et al., 2022) investigated the use of waste oyster shell powder (WOSP) to replace fine aggregate in eco-friendly mortar. Fresh, mechanical and durability properties, as well as microstructure, were studied. The replacement rates were 0, 10, 20 and 30% of river sand. Authors found that although workability was decreased with the increase of WOSP, properties like compressive and flexural strength, resistance to water penetration and chloride diffusion were improved. They also found a positive effect of using WOSP on the pore size distribution and suggested 10 to 30% as optimal replacement rates.

2.1.4 Use of other types of shells

Mussel shells

(Foti and Cavallo, 2018) studied the concrete formulations using mussel shells to replace coarse aggregate on 46.5% and 100%. The authors found good workability for the mixes and losses in compressive strength as the replacement rate increases.

(Martínez-García et al., 2019) investigated the pore structure and carbonation on air lime mortars containing mussel shells as aggregate replacement. The mussel shell was crushed and sieved, and the mussel shell sand was created to have an equivalent particle size distribution to the limestone sand. The aggregate was replaced by volume at rates of 25%, 50% and 75%. The authors found that the flaky particle shape of mussel aggregates increases the water demand affecting the mortar consistency. Additionally, the organic matter attached to the mussel shape creates irregular and bubble-like voids changing the pore size distribution. The pore size in mortars was mainly related to the poor cohesion between the binder and the aggregates, and these larges pores (> 50µm) were also the main reason for the higher carbonation degree and decrease in strength.

Scallop shells

(Cuadrado-Rica et al., 2016) investigated the fresh, mechanical and durability properties of ordinary concrete with fine aggregate replacement at different rates (20, 40 and 60%) per crushed queen scallop shell. The authors found that the air content increases while the slump decreases as the replacement rate of scallop shells increases. In terms of mechanical performance, the lowest compressive strength was found for the concrete with the highest replacement rate. In terms of durability, the authors found that the water absorption porosity and chloride diffusion coefficient increase with the replacement rate. The authors also concluded that soluble substances could have leached from the shells affecting the physical properties of the cement paste. Besides the concrete with scallop shells was less performing than the reference, yet has a potential application field.

(Varhen et al., 2017) studied the Peruvian scallop as a fine aggregate replacement in concrete. Different mix designs and water/cement ratios were tested and aggregate was replaced up to 60% by mass. The authors investigated fresh and hardened properties and found the properties are affected by the size particle distribution of the global aggregate (sand + crushed Peruvian

scallop) and the angular shape of the Peruvian scallop can contribute to the granular arrangement. They also found an optimal replacement rate of 5% to which losses in concrete properties were not considerable.

Crepidula shell

(Nguyen et al., 2013) studied the use of crepidula shell as a partial aggregate replacement to produce previous concrete pavers. The crushed crepidula sizes 2/4 mm and 4/6.3 mm were used to produce concrete pavers, and mechanical and hydrologic properties were investigated. Authors found that pervious concrete pavers with crepidula shells have the comparable mechanical strength to the reference ones. They also found that the crepidula shell crushed size affect considerably the granular arrangement of concrete matrix and hence, mechanical performance. Additionally, the authors found that the interconnected porous system is the reason for higher water permeability.

(Nguyen et al., 2017) investigated mechanical and durability properties of pervious concrete with crushed seashells (crepidula, scallop and queen scallop). The authors found that the compressive strength of pervious concretes is lower than the control concrete. The freeze-thaw is weaker for seashells pervious concrete than for the control one. They also found quicker leaching in the seashell pervious concrete than the control sample, especially in terms of calcium quantity in the leaching solution as it comes from the dissociation of calcium carbonation, releasing calcium.

Cockle shell

(Olivia et al., 2015) investigated the use of cockle shells as partial cement replacement in concrete (seashell powder made using sieve #200). Mechanical properties were studied and compared to a control ordinary Portland cement concrete. The cement was replaced by weight in proportions of 2, 4, 6 and 8%. The authors found that the concrete with seashells presented lower compressive strength and modulus of elasticity when compared to the control one. However, tensile strength and flexural strength were higher in the seashell concrete than in the control one. The authors related this improvement to the changement of the Interfacial

Transition Zone (ITZ) phase between the seashell aggregate and the cement paste, increasing the tension properties.

2.2 Producing a granular skeleton for concrete

As previously discussed, there are several particularities concerning the use of seashells as aggregate for cementitious materials. However, one of the main differences compared to conventional aggregates is their flaky and elongated shape. Because of that, it is expected that the granular skeleton will behave differently if compared to spherical materials like sand and gravel.

2.2.1 A brief discussion of current granular skeleton optimisation methods

The way particles pack (i.e how efficiently they fill a volume) will influence directly the properties of materials. Several particle packing theories have been developed to predict material packing density. The packing density means how well particles can be organised in a given volume. A high packing density means that there are fewer voids between particles. There are many methods for optimising aggregates particles to enhance the packing density. The most common method for optimising aggregate is to follow an ideal grading curve or area (Fennis et al., 2009; Kumar and Santhanam, 2003). This approach was initially developed by Fuller and Thompson (Fuller and Thompson, 1907), and Andreasen and Andersen (Andersen, 1991), and is widely used by European standards (NF EN 206/CN in France for example) as a trustful method for reaching good concrete mixtures. This method considers a continuous particle size distribution in which the voids left by larger particles are filled with smaller particles and so on. In line with this, Furnas (Furnas, 1931) also designed a model to predict the percentage of voids of binary mixtures.

As the studies progressed on this topic, structural and interaction effects between particles became clearer. The main effects are described below (Fennis et al., 2009; Kumar and Santhanam, 2003; Mehdipour and Khayat, 2018):

- The loosening effect occurs when the frame of coarse particles is loosened by a fine particle that disturbs the packing;
- The wall effect happens when additional voids are created by a coarse particle among a frame of fine particles;

- The filling effect, when fine particles tend to fill smaller voids created among coarse particles frame;
- The occupying effect is when coarse particles are placed in the bulk volume of fine particles.

A multi-component packing models were studied considering both loosening and wall effect, as proposed by De Larrard (De Larrard, 1999) and Goltermann (Goltermann et al., 1997). In addition to that, computer models (discrete element models) were also developed, allowing simulating particle packing in 2D or 3D structures. The models can calculate the theoretical packing density based on the particle size distribution and its geometry (Fennis et al., 2009).

The models aforementioned are very precise in estimating particle packing density of binary and ternary mixtures of mono-sized spherical particles. Some particle packing models tend to limit the number of particle classes on the mixture because the more particle classes are used; the higher are the interaction effects.

However, replacing conventional aggregates for non-spherical by-products remains very difficult so far, especially with high rates of replacement. A direct replacement of aggregate is not advisable and these theories are not perfectly suitable for non-spherical aggregates, leading to a tricky situation for concrete formulation.

Limited studies were conducted to develop models to predict the packing density of a blend with non-spherical particles (Mehdipour and Khayat, 2018). Non-spherical packing theories usually go around the hypothesis that their packing system can be considered similar to the spherical particle ones. (Yu et al., 1993; Yu and Standish, 1992) described an approach for a binary system where non-spherical particles are related to spherical particles through an "equivalent packing diameter" and Westman equation, allowing to predict of the mixture porosity. (Goltermann et al., 1997) worked out for a multi-component aggregate the concept of Eigen packing degree and characteristic diameter.

However, evaluating an equivalent packing diameter for OS particles is tricky. Due to the OS shape, the sieving process can be inaccurate (Cuadrado-Rica, 2016) and therefore, current models of granular skeleton optimisation might not be suitable. In this work, we will propose another way to optimise the granular packing bypassing the diameter parameter.

2.2.2 Characterisation of physical properties of aggregates for concrete

The characterisation of aggregates is extremely important when designing concrete. The aggregates represents about 70 to 80% of the volume of concrete and their importance to the final properties of the material can not be negleted. For instance, in concrete, they can influence the unit weight, strength, resistance to aggressive environments and thermal properties (Alexander and Mindess, 2010). The size, mineralogical constitution, shape, texture and densities of the aggregates used should be known prior to the concrete mixing (Neville and Brooks, 2010).

In this thesis, we investigated the loose bulk and oven-dried densities, the intergranular porosity, the water absorption coefficient and the water content of the aggregates used to produce concrete. The methods used for estimating these properties are detailed below:

Loose bulk density

The loose bulk density of a material is a ratio between the loose aggregate particles volume and, a given volume. Therefore, this density takes into consideration the aggregate particles and the voids between them. The NF EN 1097-3 (1998) proposes a method to estimate the loose bulk density and the intergranular porosity or voids. The loose bulk density test is performed using a metal container of a known volume, and the aggregates are dropped on top of the container until filling it (Fig. 2-3).

The loose bulk density can be estimated by the formula 1:

$$\text{Formula 1: } \rho_b = \frac{m_2 - m_1}{V}$$

Where:

ρ_b: is the loose bulk density (kg/m^3);

m_2: is the mass of the container with the test specimen (kg);

m_1: is the mass of the empty container (kg);

V: is the volume of the container (l).

Figure 2-4 – Empty container (left), filled container with crushed oyster shells (right) used for the loose bulk density test.

Oven-dried density and Water absorption coefficient (WA_{24})

The NF EN 1097-6 (2022) proposes a common method to estimate both oven-dried density and water absorption coefficient. The main stages of the test consist of a pre-saturation of the specimen, followed by a mass measurement using the pyknometer (Fig. 2-5). After that, specimens are slightly dried until reaching the saturated surface-dried state. Once the specimen is weighed in the saturated surface-dried state, the specimens are dried in a ventilated oven until reaching constant mass.

Figure 2-5 – Saturation of test specimens prior pyknometer method for oven-dried density test.

The cone mould method was used to detect the very particular state called saturated surface-dried state (detailed below). Identifying this state can be very complicated, especially with smaller/fine particle groups (Fig. 2-6). Thus, NF EN 1097-6:2014 standard used as a reference for the test proposes in section 9.3 a method using a cone mould to assess whether this particular state was reached or not. The specimen was considered at the saturated-surface dry state when the cone collapsed when lifting the mould (Fig. 2-6_c).

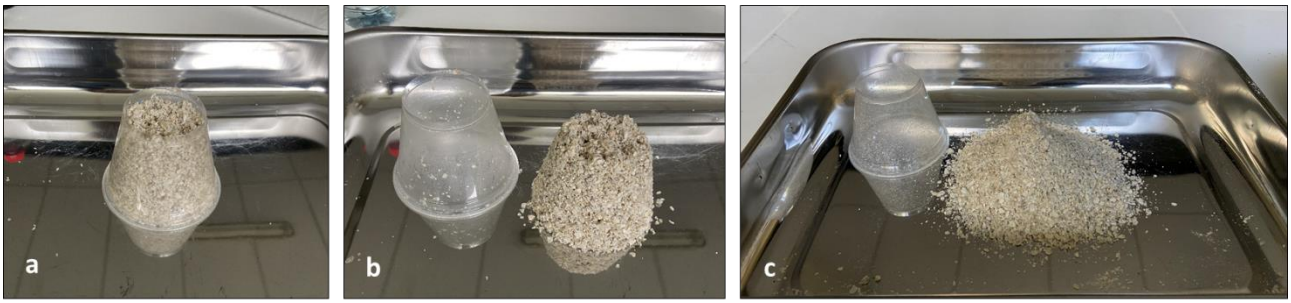

Figure 2-6 – Cone mould test for saturated surface-dried state; a) shows the cone mould filled with the specimen; b) shows a non-collapsed cone, and c) shows a collapsed cone and therefore, the saturated surface-dried state was obtained.

The oven-dried density can be estimated by the formula 2:

$$\text{Formula 2: } \rho_{od} = \rho_w \text{ x } \frac{M_4}{M_1-(M_2-M_3)}$$

Where:

ρ_{od}: is the oven-dried density (kg/m^3);

ρ_w: is the water density at the test temperature (kg/m^3);

M_1: is the specimen mass at the saturated and surface-dried state (kg);

M_2: is the mass of the pyknometer containing the saturated specimen and filled with water (kg);

M_3: is the mass of the pyknometer filled with water (kg);

M_4: is the mass of the oven-dried test portion in air (kg).

The water absorption coefficient (WA_{24} - %) can be estimated by the formula 3:

$$\text{Formula 3: } WA_{24} = \frac{100 \text{ x } (M_1 - M_4)}{M_4}$$

The water absorption coefficient is an important parameter when calculating the mixing water in concrete, so the water absorbed by the aggregates must be taken into account if the aggregates are not previously saturated.

Intergranular porosity

After estimating the loose bulk and oven-dried densities, it is possible to estimate the intergranular porosity according to a correlation proposed by the NF EN 1097-3 (1998), calculated by the formula 4:

$$\text{Formula 4: } \nu = \frac{\rho_{od} - \rho_b}{\rho_{od}} \text{ x } 100$$

Where:

ν: is the intergranular porosity or percentage of voids (%);

ρ_{od}: is the oven-dried density (kg/m^3);

ρ_b: is the loose bulk density (kg/m^3).

Water content

The water content is a important information for correcting the water on mortar and concrete formulations. This water affects the concrete mix and properties at the fresh and hardened state (Alexander and Mindess, 2010).

To estimate the water content of the aggregates, a sample of aggregates is placed to dry until reaching constant mass in a ventilated oven. The method is proposed by the NF EN 1097-5:2008.

The water content can be estimated by the formula 5:

$$\text{Formula 5: } w = \frac{M_1 - M_2}{M_2} \times 100$$

Where:

w: is the water content (%);

M_1: is the mass of test portion (g);

M_2: is the dried mass of the test portion (g).

2.2.3 Self-compacting concrete characteristics

Concrete is considered as a three granular components system at the dry state: (i) the binder and the fines, (ii) the sand, and (iii) the gravel. The active particles in the matrix are the binder and fines (if actives), which are responsible for keeping together the whole system (De Larrard, 1999).

In this thesis, we focused on developing self-compacting concrete with crushed oyster shells. Self-compacting concrete (SCC) is a type of concrete that place itself under its weight due to its high flowability and non-segregating characteristics. Differently from conventional concretes, SCC does not need vibration (extra energy) to be set and it is very suitable for situations where concrete must be placed into narrow and deep sections or congested reinforcement (Goodier, 2019; Ma et al., 2017; Shi et al., 2015a; Su et al., 2001).

To design a good quality SCC, it is important to take into consideration three main points (Goodier, 2019; Shi et al., 2015b):

- Filling ability: it means how easy the concrete flows into formworks or confined spaces and can place itself on its weight – It can be assessed with the slump-flow test for example
- Passing ability: it means how well the concrete can ingress into congested reinforcement and confined spaces without blocking or segregation – It can be assessed with the L-box test for example;
- Segregation resistance: means how well the concrete can maintain a good homogenous mixture from transportation until placing – It can be assessed with the sieve segregation test for example.

In section 4 of the French Standard NF EN 206/CN, we can find a classification for an SCC based on its fresh properties. The classifications are based on slump-flow diameter, apparent viscosity, passing ability and segregation resistance methods. The slump-flow and segregation resistance were chosen to characterise the concrete mixtures in this thesis. The slump-flow test is performed according to the method proposed by the NF EN 12350-8 (2019) and the sieve segregation by the NF EN 12350-11 (2010). The concrete mixes can be classified into three categories according to the slump-flow diameter (Table 2.1).

Table 2.1 – Slump-flow classification (NF EN 206/CN).

Class	Slump-flow diameter (mm)
SF1	550 to 650
SF2	660 to 750
SF3	760 to 850

The segregation resistance tests provide information concerning concrete segregation i.e. how well aggregate and cement paste are bonded in a homogeneous mixture. The SCC can be classified in terms of segregation resistance according to table 2.2.

Table 2.2 – Segregation resistance classification (NF EN 206/CN)

Class	Segregation portion (%)
SR1	≤ 20
SR2	≤ 15

There are several mixture design methods for creating a self-compacting concrete formulation as summarised in the sequence (Shi et al., 2015b):

- Empirical models rely on aggregates, water and cementitious materials specifications to design a mixture;
- A model based on compressive strength requirements for establishing the formulation content;

- The close aggregate packing model based on first optimising the aggregate with packing models and then filling the voids between the aggregates with cement paste (Sebaibi et al., 2013);
- The statistical factorial model based on assessing how key parameters like the volume of aggregates, cement admixtures, water/cement ratio can affect workability and strength;
- A model based on the paste rheology and measured by the fresh properties based on flowability.

According to (Su et al., 2001), they developed a method that aimed to fill the voids of the aggregate framework piled loosely with a paste of binders. The authors highlighted that for reaching good properties in SCC, the packing factor of aggregates is highly important. The packing factor (PF) is the ratio between the mass of aggregate tightly packed to the loosely packed state, indicating how well packed they are and hence, with fewer voids between them. Therefore, it is important to improve the granular packing of aggregates to decrease the number of binders reducing costs and environmental impact. Additionally, good compactness of the granular skeleton is desirable to enhance mechanical and durability properties.

Besides that, it is important to investigate the rheology of the self-compacting concrete as well. Self-compacting concrete usually have a high content of powder materials and cement paste content must be high enough to ensure flowability and to cover all aggregates. In this sense, superplasticisers plays an important role by increasing the water film and facilitating the cover of the aggregate's particles(Benaicha et al., 2019).

Generally, we can say that for designing a concrete formulation, it is important to take into consideration the granular skeleton optimisation and to decrease the amount of binder and hence, the environmental impact. The use of bio-based materials in concrete has been challenging in terms of granular skeleton and in terms of limitations established by standards. To improve sustainability, we need to increase the use of these by-products to decrease the depletion of raw resources. However, it is also important to ensure performance and durability and it is what we will discuss in the next section.

2.3 How to validate a concrete formulation?

There are several ways of validating a concrete formulation. It can be through the fresh state properties; or mechanical or durability performance according to the intended use. In this section, we are going through these steps: how a concrete formulation is designed and how it can be validated, especially when the formulation goes beyond traditional standards prescriptions.

2.3.1 Concrete formulation context and environmental exposure classes

To design a concrete structure, it is very important to identify potential risks which the structure and material can be submitted. For example, the structural loads must be taken into consideration while designing a reinforced concrete structure and the structure must be able to withstand these loads throughout the lifecycle. The choice of materials that will be used for construction is a key parameter to ensure the structure's durability in the service life. To ensure durability through time, the concrete must withstand environmental/chemical attacks that may lead to deterioration.

Environmental exposure classes

In France, the standard NF EN 206/CN provides specifications, performance, production and conformity for concrete. To design a concrete formulation, it is important to identify potential aggressive environmental agents that can be present in the soil, air or groundwater to which the concrete will be submitted. The NF EN 206/CN established several environmental exposure classes according to the environmental conditions to which the concrete will be exposed (Table 2.3).

The environmental exposure class will have a direct influence on the concrete formulation, reflecting in a minimal requirement of cement content, water/cement ratio, type of aggregate, minimal compressive strength. When exposed to more than one aggressive agent, the concrete formulation must be designed to resist the most aggressive condition or the most restricted environmental exposure class. Therefore, the choice of the environmental exposure class impact also the choice of materials like cement type, aggregates and mineral additions (AFGC, 2018a).

Table 2.3 – Environmental exposure classes (NF EN 206/CN).

Class designation		Class description
No risk of corrosion	X0	Very dry
Corrosion induced by carbonation	XC1	Dry or permanently wet
	XC2	Wet, rarely dry
	XC3	Moderate humidity
	XC4	Cyclic wet and dry
Corrosion induced by chlorides other than from seawater	XD1	Moderate humidity
	XD2	Wet, rarely dry
	XD3	Cyclic wet and dry
Corrosion induced by chlorides from seawater	XS1	Exposed to airborne salt but not in direct contact with seawater
	XS2	Permanently submerged
	XS3	Tidal, splash and spray zones
Freeze-thaw attack	XF1	Moderate water saturation without a de-icing agent
	XF2	Moderate water saturation with a de-icing agent
	XF3	High water saturation without a de-icing agent
	XF4	High water saturation with a de-icing agent
Chemical attack	XA1	Low chemical aggression
	XA2	Moderate chemical aggression
	XA3	Strong chemical aggression

Once defined the environmental exposure class, the next step is to design the concrete formulation. The formulation can be designed according to the traditional prescriptive approach (based on the NF EN 206/CN) or beyond the standard. The formulation is beyond the standard when the formulation contents (binder content, water/cement ratio, aggregates types, minimal compressive strength) are not within the values proposed by NF EN 206/CN. Therefore, we summarise below how to validate the concrete for each of these approaches:

- The traditional prescriptive approach: the concrete is validated if the limits for certain parameters/performance are in line with those established by the standard for the given environmental exposure class;
- The performance-based approach: whether the concrete is validated or not depends on its performance results. The validation can be by comparison to absolute values of durability indicators or by equivalence performance to a reference concrete.

Therefore, in the traditional prescriptive approach, the formulation content and mechanical resistance must strictly respect those predicted in the standard to validate the concrete

formulation. On the other hand, the performance-based approach allows more flexibility when choosing formulation materials and contents as long as the new concrete provides enough mechanical and durability performance for the given user. The performance-based approach is briefly introduced in the NF EN 206/CN as well recognised but no limits for mechanical or durability indicators are provided. The French Association of Civil Works (AFGC) provided a Guide with thresholds for durability indicators for validating concrete through a Performance-based approach (AFGC, 2004). These two approaches are further developed in section 2.3.3 (traditional prescriptive approach) and 2.3.4 (performance-based approach).

2.3.2 Validation of mechanical properties

A common criterion for the traditional and performance-based approaches is mechanical resistance. Even though a material must provide to be resistant to environmental aggressive agents throughout time, it also must provide a certain mechanical performance. For the NF EN 206/CN, only the investigation of the compressive strength is mandatory. However, for research purpose, we decided to investigate other properties such as flexural strength, splitting tensile strength, and elastic modulus in the concretes studied in this thesis. The test procedures used are detailed below.

Compressive strength

The compressive test was performed according to the French standard NF EN 12390-3:2019. The compressive strength can be estimated by the formula 6:

$$\text{Formula 6: } f_c = \frac{F}{A_c}$$

Where:

f_c: is the compressive strength (MPa or N/mm^2);

F: is the maximum load at failure (N);

A_c: is the cross-sectional area of the specimen where the load was applied (mm^2).

Figure 2-7 – Oyster shell concrete specimen placed in the machine for compressive test.

Flexural strength

The flexural test was performed according to the French standard NF EN 12390-5:2019. The flexural strength can be estimated by the formula 7:

$$\text{Formula 7: } f_{ct,fl} = \frac{3 \text{ x } F \text{ x } l}{2 \text{ x } d_1 \text{ x } {d_2}^2}$$

Where:

$f_{ct,fl}$: is the flexural strength (MPa or N/mm^2);

F: is the maximum load at failure (N);

l: is the distance between the lower rollers (mm);

d_1: is the width of the beam (mm);

d_2: is the height of the specimens minus the notch depth (mm).

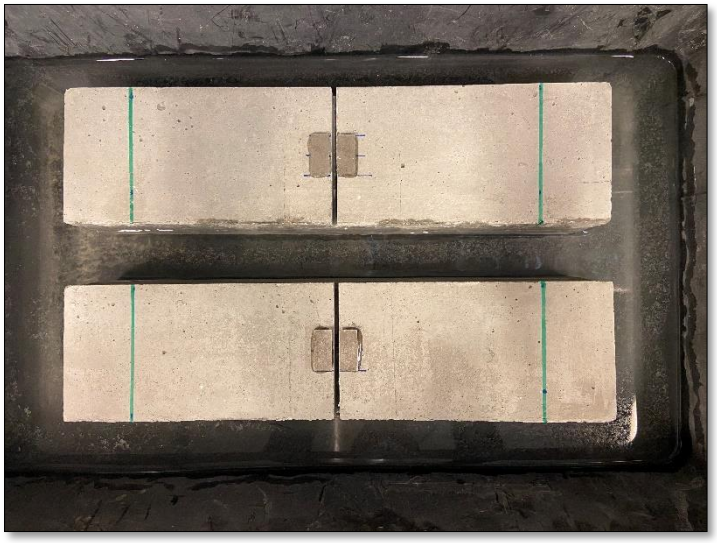

Figure 2-8 – Oyster shell concrete specimens notched (20 mm) and placed on the water until the test.

Splitting tensile strength

The splitting tensile test was performed following the recommendations of the French standard NF EN 12390-6:2012. The tensile splitting strength can be estimated by the formula 8:

$$\text{Formula 8: } f_{ct} = \frac{2 \text{ x } F}{\pi \text{ x } L \text{ x } d}$$

Where:

f_{ct}: is the tensile splitting strength (MPa or N/mm^2);

F: is the maximum load at failure (N);

L: is the length of the line of contact of the specimen (mm);

d: is the cross-sectional dimension (mm).

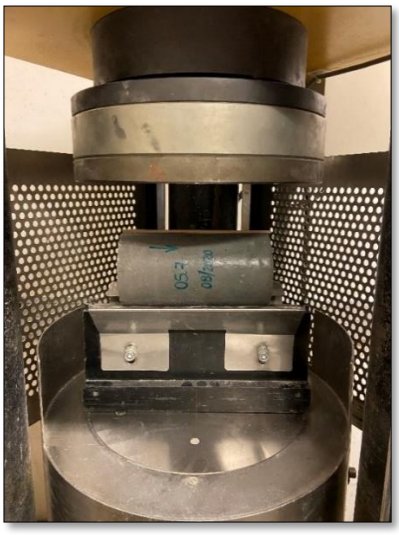

Figure 2-9 – Oyster shell concrete specimen placed for the tensile splitting test.

Elastic Modulus

The modulus of elasticity or Young's modulus was investigated to identify the resistance of the concrete to deformation under load. The test was performed according to NF EN 12390-13 (2021) with some adaptations. For this test, a special apparatus composed of two fixed aluminium rings with three screws on the bottom and top for attaching the specimen was used (Fig. 2-10). Three sensors type Linear Variable Differential Transformer (LVDT) were used to measure the vertical strain of the specimen. The LVDT were placed at an angle of 120° and can measure changes in the length of ± 1 mm.

The maximum load at failure obtained in a previous compressive test was used to calculate the characteristics of the preloading cycle. The preloading cycles were performed on load, varying from a lower limit (50 kN) to an upper limit that did not exceed 50% of the maximum load at failure. Three preloading cycles were carried out (in kN/s) to identify the displacement within these limits. Once obtained the displacement variation, ten loading cycles were performed within these limits (lower and upper), in µm/s. The test was reproduced three times for each formulation.

The modulus of elasticity is estimated by the slope of the linear regression obtained between the stress and the strain graph.

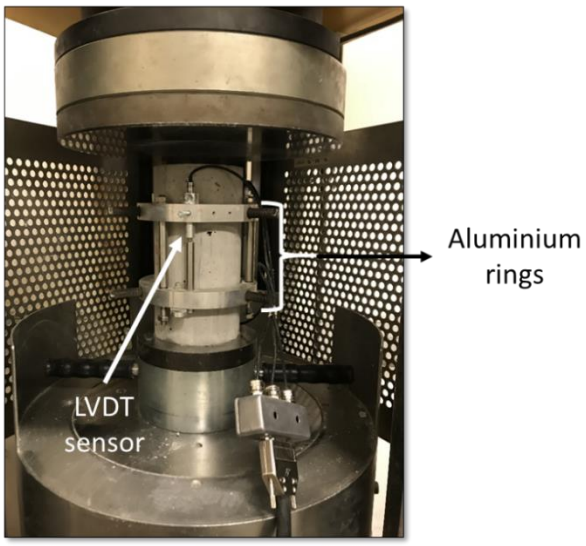

Figure 2-10 – Testing setup and apparatus for measuring uniaxial elastic modulus.

Once characterised the mechanical properties of concrete, we are going to further detail the traditional prescriptive and performance-based approaches.

2.3.3 The traditional prescriptive approach

The traditional prescriptive approach is the core of NF EN 206/CN. The base of the method is to fix limit values for concrete formulation for a given environmental exposure class and a service life of 50 years. Figure 2-11 illustrates the stages to design concrete based on the traditional prescriptive approach. As long as the prescription requirements, concrete cover, curing and maintenance conditions were kept, the durability of the concrete can be assured (NF EN 206/CN, 2014).

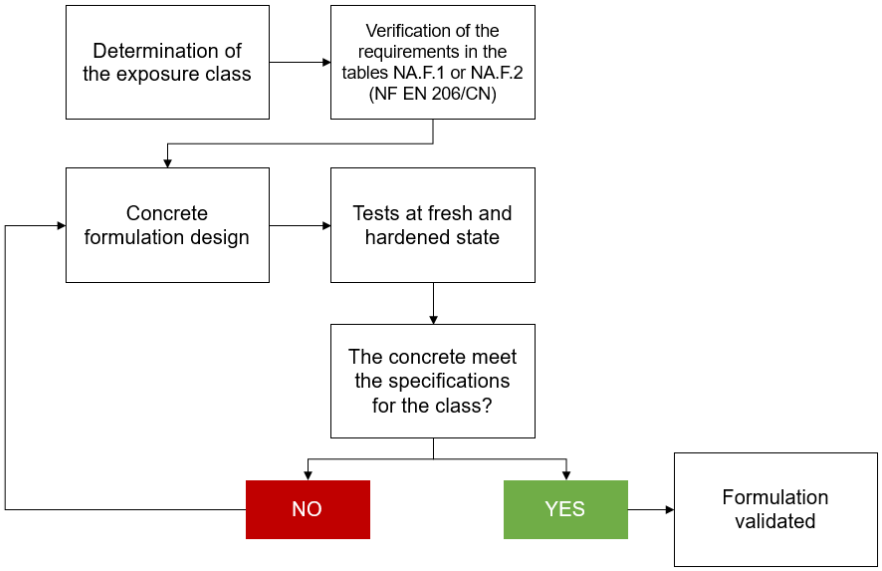

Figure 2-11 – Diagram of the steps for the traditional prescriptive approach.

In France, the limit values for the formulation content are described in the table NA.F.1 for concrete and NA.F.2 for precast concrete in the NF EN 206/CN. The advantages of this approach rely on the simplicity of the method and the credibility among the conservative people/industry once is standardised by a norm.

The NF EN 206/CN refers to the NF EN 12620 when establishing specifications for aggregate to produce concrete. This standard indicates that the shell content of coarse aggregate shall be declared when required and is acceptable when the coarse aggregate is coming from a marine source. However, the NF EN 206/CN and NF EN 12620 do not specify thresholds for replacing conventional aggregates per crushed seashells or bio-based materials. In this context, the performance-based approach becomes an important tool to validate a concrete to which the formulation content/specifications are not provided in the traditional standard for concrete formulation (NF EN 206/CN).

2.3.4 Performance-based approach

In the past years, building materials and construction methods have undoubtedly progressed towards more sustainable practices, implying the reuse and recycling of by-products from industry and agriculture to replace clinker (as supplementary cementitious materials) or

substitute conventional aggregates with bio-based ones or recycled concrete. In order to follow the progress towards more sustainable construction practices, the use of local resources and supplementary cementitious materials must be encouraged (Carcasses et al., 2015). Recently, major engineering projects are specifying not only the compressive strength to attend but also, the durability indicators based on the environmental exposure class.

Modern construction demands more flexibility in construction methods and materials, and the traditional prescriptive approach creates some obstacles. Its specifications limit the possibilities of creating innovative concrete mixes, the use of bio-based materials or other additions decreasing the opportunity of actually using sustainable materials in construction (Beushausen et al., 2019).

The performance-based approach arose from the need to validate concrete formulations that were designed beyond the traditional approach. The performance-based approach aims to validate these innovative materials through their performance (mechanical and durability) and prove that a material designed outside the traditional limits can provide an equal or better performance than the traditional one. These formulations were often composed of other types of materials than the conventional ones to replace partially or fully cement or aggregates in concrete. Some of the advantages of the performance-based approach are listed below (AFGC, 2018b):

- More flexibility for designing concrete formulations (type of concrete and constituents);
- More flexibility to incorporate by-products and valorisation of local materials to develop more sustainable materials;
- Gather together technical, economical and ecological aspects of the structure;
- Better control of the concrete structure durability allows to predict more precisely the service life as well as design structures for a life service of over 50 years;
- Decrease the environmental footprint of the structure;
- Can be used in the concept phase of a project or to estimate the residual service life of an as-built structure.

French national context

In France, large studies have been developed to consolidate performance-based approach for validating concrete durability. The French Association of Civil Works (AFGC) have extensively worked to develop a database of durability indicators based on several concrete mix designs and their constituents. The BdiduBé database (Concrete durability indicators database) was elaborated after collecting information from construction sites, concrete industries and technical and scientific literature review, and is shared by either industrial or academia (AFGC, 2018b; Carcasses et al., 2015).

In 2004, the French Association of Civil Works (AFGC) presented a guide concerning the application of the performance-based approach under the absolute concept (values for durability indicators) to control steel corrosion and alkali-aggregate reaction. The guide describes the durability concept, the conditions for using the performance-based approach, the general and substitution durability indicators, thresholds for durability indicators for the classes XC and XS, and the application to predict durability in the conception phase or the residual durability in current structures (AFGC, 2004).

In 2009, the French National Federation of Public Works (FNTP) in partnership with FFB, CERIB and FIB developed a guide with provisional recommendations for applying the comparative concept (equivalence) to validate a concrete formulation through the durability and performance parameters (FNTP, 2009).

In 2007, the GranDuBé project (quantities associated with the durability in concrete) standardised testing protocols for chloride migration, accelerated carbonation test, water porosity and gas permeability. The definition of these tests creates a common basis for setting durability indicators, making possible to build the frame of the performance-based approach. Between 2007 and 2010, the Applet project focused on developing the probabilistic aspects of the performance-based approach and the variation of the durability indicators over time (Linger, L.; Cussigh, 2017). From these two projects, many durability tests protocols were standardised in France and listed in table 2.4.

Table 2.4 – Summary of the durability test protocols standardised in France (Linger, L.; Cussigh, 2017).

Standard reference	Year	Description
XP P 18-458	2008	Test for hardened concrete – Accelerated carbonation test – Measurement of the thickness of carbonated concrete
NF P 18-459	2010	Concrete – Testing hardened concrete – testing porosity and density
XP P 18-463	2011	Concrete — Testing gas permeability on hardened concrete
XP P 18-462	2012	Testing hardened concrete — Chloride ions migration accelerated test in non-steady-state conditions — Determining the apparent chloride ions diffusion coefficient
XP P 18-461	2012	Testing hardened concrete — Chloride ions migration accelerated test in steady-state conditions—Determining the effective chloride ions diffusion coefficient

In 2010, the Laboratoire Central des Ponts et Chaussées (LCPC) presented a guide with provisional recommendations based on the initial guide of AFGC (2004) for the application of the performance-based approach based on the absolute concept to major constructions (LCPC, 2010). This LCPC guide enhanced the use of the performance-based approach extending to large structures and long service lives.

In 2015, the PERFDUB project (Approche PERFormantielle de la Durabilité des Ouvrages en Béton – Performance-based approach for justifying concrete structures durability) was launched gathering industry and academia to standardise a methodology for using the performance-based approach to complex civil engineering structures. The research topics covered in this project are divided into five different axes: 1 – durability testing; 2 – definition of eligible performance thresholds; 3 – concrete mixes selections; 4 – contractual aspects; and, 5 – dissemination.

Therefore, it can be seen that efforts have been made to develop reliable methods for durability characterisation as well to adapt to the new scenario of sustainability in construction and materials.

According to (Beushausen et al., 2019), different levels of performance-based approach evaluation can be used to assess concrete durability. These levels are the definition of durability

indicators to which the concrete must meet the requirements; the use of analytical deterioration models or the use of full probabilistic approaches.

According to the (AFGC, 2004), the performance-based approach based on durability indicators is divided into two methods:

- Absolute values: fixed thresholds for durability indicators (given for service life and environmental exposure class) are the reference and the analysed concrete must meet these criteria to be validated (AFGC, 2004);
- Equivalence performance: the given concrete is compared to the results of a reference concrete that was made according to the traditional formulation rules or project specification. The durability indicators can also be added for a comparison between the given and reference concrete. If the results for the given concrete are better than the reference one, then the concrete is validated (AFGC, 2018b; IREX, 2014).

Therefore, we will detail the absolute and equivalence methods and how they are used to validate concrete. The durability indicators are common to both methods and they are chosen regarding the environmental aggressive agents to which the concrete will be submitted and the properties that must be investigated depending on the use and service life. In this thesis, we chose to validate the concrete using the Absolute values method – Potential durability. In the sequence, we will present some of the durability indicators used to characterise the concrete in this thesis.

2.3.4.1 Absolute values method

There are two methods to validate a concrete by the absolute approach:

1. Comparing the concrete performance results to thresholds for potential durability, or specific environments (XC and XS) and a given use and life service (AFGC, 2004);
2. Numerical simulation of concrete behaviour in given environmental conditions.

We are going to focus on the first one, developed in the AFGC guide (2014) to qualify the potential durability of concrete. The guide also provides thresholds for concrete to be used in XC or XS exposure classes, respectively for carbonation and marine environment exposure, for a given use and life service. However, as we aim to evaluate the concretes studied from a more general perspective, we will focus on the potential durability (table 2.6).

Regardless of the focus on the durability indicators in this approach, the guide still recommends that the compressive strength must be determined at 28 days for all formulations and at 90 days when necessary. Concerning the durability indicators, they are organised into two groups: the general and the substitution (Table 2.5).

The general indicators were established regarding their relevance to the steel corrosion and alkali-aggregate reaction. The specific or substitution indicators were proposed to make the approach more adaptable to the project needs and suitable for a specific problem. The selection of the durability indicators is very flexible and adaptable, so a general indicator can be replaced with a substitution one or substitutes can be added to better assess the durability performance.

Table 2.5 – Summary of the general and substitution durability indicators according to the AFGC guide (AFGC, 2004).

Durability indicators	
General	Water accessible porosity
	Chloride diffusion coefficient (apparent or effective)
	Apparent gas permeability
	Water permeability
	Portlandite content
Substitution	Mercury intrusion porosimetry
	Electrical resistivity
	Electrical Indication of Concrete's Ability to Resist Chloride Ion Penetration
	The diffusion coefficient for CO_2
	The diffusion coefficient for tritiated water
	Capillary absorption coefficient

Concerning the concrete durability assessment and performance, it is possible to include complementary parameters that may help the interpretation of results or will be used as input data for predictive models. The service life (over 120 years) or particular performances may be one of the reasons why complementary parameters must be taken into account. The complementary parameters are also suggested in section 6.1.5 of the AGFC guide (AFGC, 2004).

The potential durability of a given concrete can be assessed by analysing the experimental results of the durability indicators chosen with those values proposed in table 2.6. In this table, thresholds values are proposed for the general and substitution indicators and the classification vary from a very low to very high potential durability.

Table 2.6 – Summary of the potential durability classification based on the general (G) and substitution (S) indicators (AFGC, 2004).

		Classes and limit values				
	Potential durability of the durability indicators	**Very low**	**Low**	**Medium**	**High**	**Very High**
G	Water porosity (%) P_w	> 16	14 to 16	12 to 14	9 to 12	6 to 9
S	Porosity measured by MIP (%) P_{Hg}		13 to 16	9 to 13	6 to 9	3 to 6
S	Resistivity (Ω.m) ρ	< 50	50 to 100	100 to 250	250 to 100	> 100
G	Effective chloride coefficient (migration test) (10^{-12} $m^2.s^{-1}$) D_{eff}	> 8	2 to 8	1 to 2	0.1 to 1	< 0.1
G	Apparent chloride coefficient (migration test) (10^{-12} $m^2.s^{-1}$) $D_{app\ (mig)}$	> 50	10 to 50	5 to 10	1 to 5	< 1
G	Apparent chloride coefficient (diffusion test) (10^{-12} $m^2.s^{-1}$) $D_{app\ (dif)}$				< 5	
G	Gas permeability (P_i = 0.2 MPa) (10^{-18} $m^2.s^{-1}$) K_{gaz}	> 1000	300 to 10000	100 to 300	10 to 100	< 10
G	Water permeability K_{liq}	> 10	1 to 10	0.1 to 1	0.01 to 0.1	< 0.01
	Concrete class (indicative and for ordinary mixes)	-	C25 to C40	C30 to C60	C55 to C80	> C80

2.3.4.2 Durability indicators

The durability indicators are key parameters selected to evaluate and predict the service life or durability of a material or structure under certain conditions. These indicators are measured parameters obtained after testing the material under standard protocols and control conditions in the laboratory.

One of the most important parameters when assessing durability is the penetrability and the pore structure of concrete. The aggressive species will ingress in concrete through the pore structure, and the penetrability is going to drive how easily they can ingress, causing the deterioration of the structure. The aggressive agents can be present in liquid (aggressive ions or dissolved species in the poral water) or gas phases. The transport properties measurement helps to predict the durability of the material, and they include permeation, sorption, diffusion and migration concepts (Beushausen et al., 2019; Neville and Brooks, 2010).

The concrete porous structure is very important and impacts directly the transport properties. Different types of concrete can present different values for permeability and diffusivity whereas the same porosity and vice-versa. Indeed, the total porosity is composed of the sum of porosity of different ranges (hydrate pores, capillary pores, ITZ, air bubbles in the paste and microcracks). Depending on the basic transport phenomenon, the properties can be conditioned by the average size of the capillary pores (gas permeability), or the pore connectivity and tortuosity (diffusivity) (Ilgar, 2015; Neville and Brooks, 2010; Perlot, 2005).

The pore interconnectivity can be categorised into three families (Metha, P. K.; Monteiro, 2001):

1. Interconnected pores: high impact on the transport properties and creates a continuous space in the porous media;
2. Isolated pores: it is the closed pores that are not connected to others;
3. Blind pores: it is pores that have only one entrance/exit.

Considering the importance of investigating porosity and transport properties to predict durability, we chose the following durability indicators to assess the durability of the concretes studied in this thesis: porosity accessible to water, gas permeability, chloride diffusion, capillary water absorption and carbonation and we will briefly describe below the procedures used.

Porosity accessible to water

The water porosity is a global parameter and is related to the open porosity in the material. The water porosity is often correlated to the compressive strength since the last one tends to increase with a more compact matrix which is characterised by less porosity. The porosity tends to decrease with time as the cement hydration progress. The material's porosity will directly impact other transport properties (AFGC, 2004).

The water porosity can be characterised through the method proposed by AFPC-AFREM (AFPC - AFREM a, 1997). The hydrostatic weighing device used in this thesis is shown in Figure 2-12.

The porosity accessible to water (ε) can be calculated by the formula 9:

$$\text{Formula 9: } \varepsilon = \frac{M_a - M_d}{M_a - M_w} \, x \, 100$$

Where:

ε: is the porosity accessible to water (%v);

M_d: is the dried mass (g);

M_a: is the mass on air (g);

M_w: is the mass in water (g).

Figure 2-12 - Hydrostatic weighing device.

Gas permeability

Gas permeability is a test to measure the transport properties related to the capacity of the material to allow fluid to go through it under a pressure gradient. The permeability rate indicates how fast the flow goes into the porous media of the material (Metha, P. K.; Monteiro, 2001).

The nitrogen gas was used in the test as it is a neutral percolating gas. The device setup used for the test is shown in Figure 2-13. The apparent coefficient of permeability (ka - m^2) can be calculated for different pressures (formula 10) (Saiyouri et al., 2007):

Formula 10: $$\mathrm{ka} = \frac{\mathrm{Q}}{\mathrm{A}} \mathrm{x} \frac{2\mu \mathrm{LP_{atm}}}{(\mathrm{Pi^2} - \mathrm{Patm^2})}$$

Where:

ka: is the apparent coefficient of permeability (m^2);

Q: is the gas flow (m^3/s);

A: is the cross-sectional area (m^2);

μ: is the viscosity of the fluid ($1.76x10^{-5}$ Pa.s for nitrogen gas at 20ºC);

L: is the thickness of the specimen tested;

P_{atm}: is the atmospheric pressure (Pa);

P_i: is the inlet pressure (Pa).

Additionally, the intrinsic permeability can be obtained by the relationship proposed by Klinkenberg (formula 11):

Formula 11: $$\mathrm{ka} = \mathrm{ki}\ (1 + \frac{\mathrm{b}}{\mathrm{Pm}})$$

Where:

ka: is the apparent coefficient of permeability (m^2);

ki: is the intrinsic coefficient of permeability (m^2);

b: is the Klinkenberg coefficient (Pa);

P_m: is the mean pressure gas – $P_m = (P_i + P_{atm})/2$ (Pa).

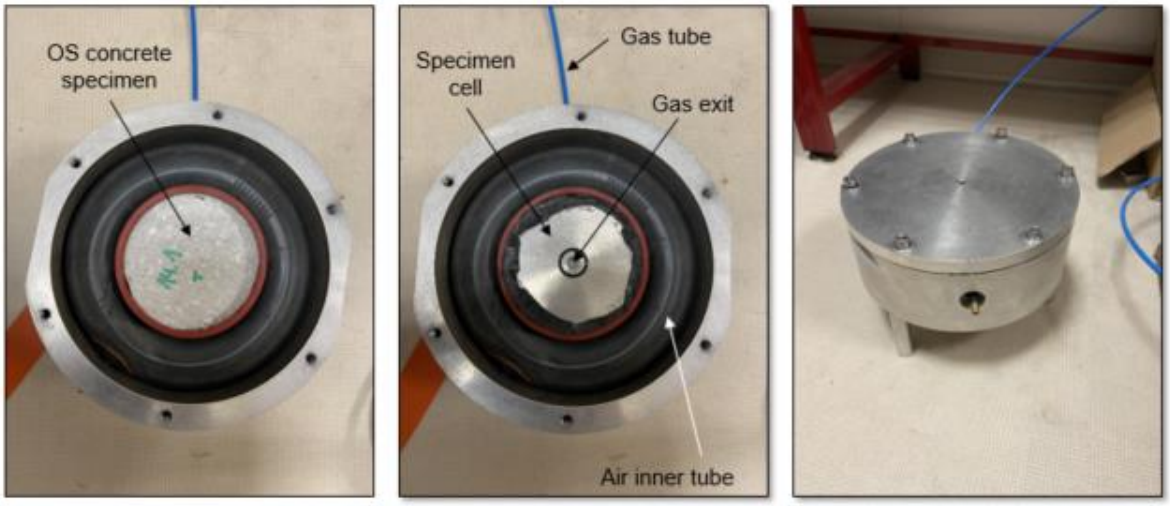

Figure 2-13 – Gas permeability setup.

Chloride migration

The chloride migration is a test to measure the transport properties related to the capacity of the material to allow ionic species (like chlorides) to go through it under a concentration gradient. It is very important to quantify the chloride diffusion once the chloride has a high potential to cause steel corrosion, decreasing the durability of the material (AFGC, 2004).

The method used for testing the chloride migration was proposed by (Truc et al., 2000). Under steady-state conditions and accelerated conditions, the effective chloride diffusion coefficient can be estimated by formula 12. The chloride migration apparatus used for the test is shown in Figure 2-14.

Formula 12: $$D_{e,up} = \frac{R \times T \times J_{up}}{C_{up} \times F \times E}$$

Where:

$D_{e,up}$: is the effective diffusion coefficient ($m^2.s^{-1}$);

C_{up}: is the average concentration in the upstream cell (mol/m^3);

R: is the perfect gas constant (8.32 J/mol.K)

T: is the temperature (K);

F: is the Faraday's constant (96487 C/mol or 2717.9 C/g)

J_{up}: is the chloride ion flux through the upstream side of the sample ($mol/m^2/s$)

E: is the electric field (V/m)

With J_{up} (formula 13):

Formula 13: $$J_{up=} \frac{C_{up,1} \times V - C_{up,2} \times V}{S \times t}$$

Where:

J_{up}: is the flux of chlorides leaving the upstream compartment ($mol/m^2.s$);

$C_{up,1}$: is the concentration of chlorides upstream at the start of the test (mol/m^3);

$C_{up,2}$: is the concentration of chlorides upstream at the end of the test (mol/m^3);

V: is the volume of upstream solution (m^3);

S: is the surface area of the specimen exposed to the chloride solution (m^2);

T: is the test duration (s).

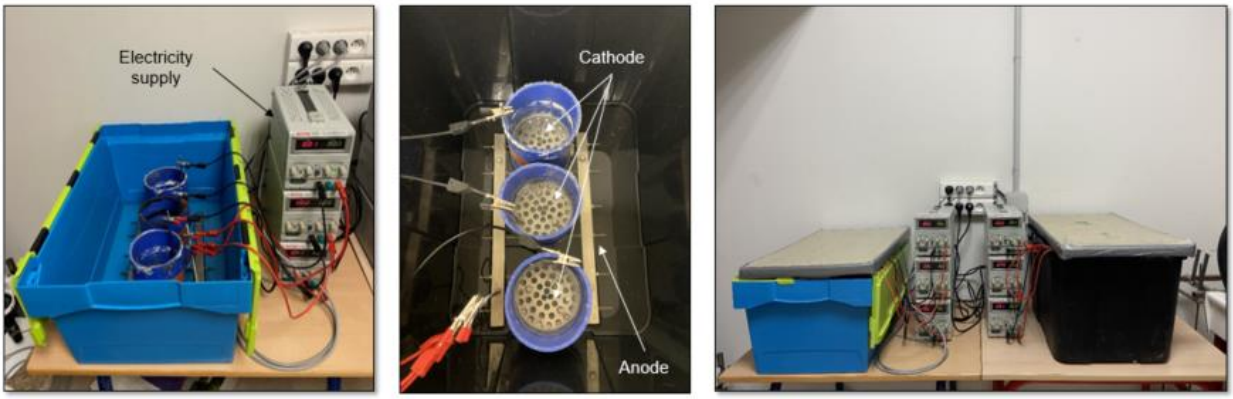

Figure 2-14 – Chloride migration apparatus.

(AFGC, 2004) proposes a correlation between the effective and apparent chloride diffusion coefficient using the formula 14:

Formula 14: $$D_{app} = \frac{D_{eff}}{\varepsilon + \rho \times \frac{\partial m_b}{\partial c_f}}$$

Where:

D_{app}: is the apparent chloride diffusion coefficient (m^2/s);

ε: is the materials accessible porosity to chloride (m^3/m^{-3});

m_b: is the mass of bound chlorides per unit mass of dry solid (kg/kg^{-1});

c_f: is the free chloride concentration of the interstitial solution (kg/m^{-3});

ρ: is the apparent density of the dry material (kg/m^{-3}).

Capillary water absorption

The capillary water absorption is based on the concept of sorptivity, in which the water is absorbed in the capillary pores of concrete due to surface tension action. This phenomenon is governed by Jurin's law also known as capillary rise. The capillary absorption in concrete depends mainly on the pore size (Ilgar, 2015).

The capillary water absorption can be characterised through the method proposed by AFPC-AFREM method (AFPC - AFREM b, 1997). The test consisted in placing the specimens over support of 5 mm high, inside a container with water, followed by consecutive weighing in determined time intervals. The water level was kept constant throughout the test and the container was kept covered to avoid any loss due to evaporation. The time interval of weighing was 0.25, 0.5, 1, 2, 4, 8, 24 hours and every 24 hours until the stabilisation. Figure 2-15 shows the schematic of the capillary water absorption test.

The capillary water absorption coefficient can be estimated by the formula 15.

Formula 15: $$C_a = \frac{M_t - M_0}{A}$$

Where:

C_a: is the water absorption coefficient (kg/m^2);

M_t: is the specimen mass in a certain time (kg);

M_0: is the specimen mass before the start of the test (kg);

A: is the contact area between the specimen and the water in (m^2).

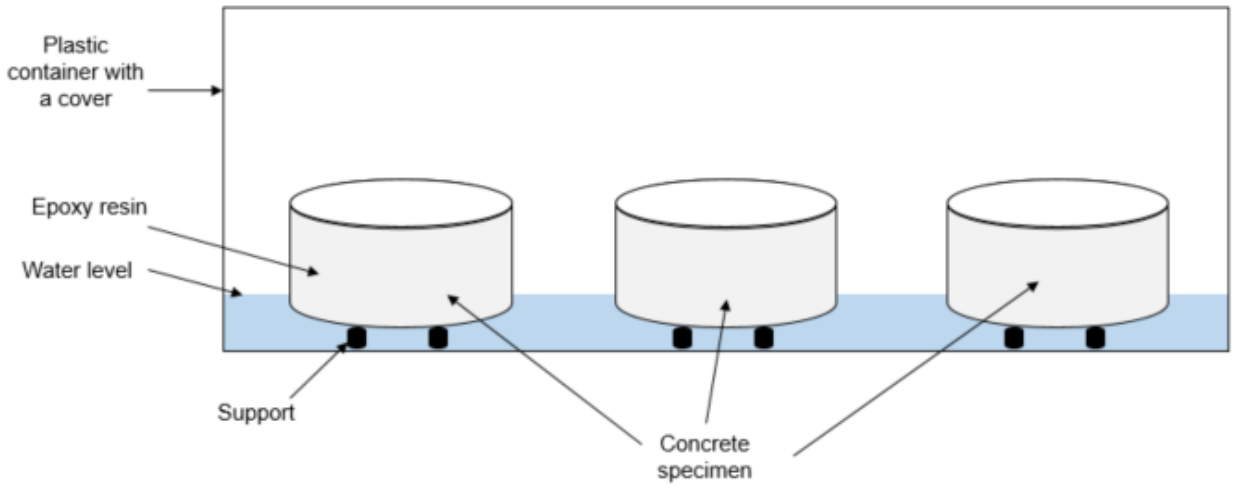

Figure 2-15 – Principe of capillary water absorption test.

Carbonation

The carbonation in concrete is a process that occurs due to the carbon dioxide gas (CO_2) that ingress into the material through the pores and cracks and dissolves into the poral solution of concrete.

The carbon dioxide will react with cement hydrates constituents to produce the carbonation in concrete. The main hydrates concerned are portlandite ($Ca(OH)_2$), hydrated calcium silicates (C-S-H), and other constituents on a lower proportions (ettringite, hydrated calcium aluminates and others) (Chabil, 2009).

The global reaction occurs with the portlandite (equation 1). In the presence of water (usually in tiny pores), the CO_2 reacts with portlandite $Ca(OH)_2$ producing calcium carbonate, an insoluble salt. The consumption of portlandite decreases the pH in the area from 13 to below 9 (Chaussadent, 1999).

Equation 1: $Ca(OH)_2 + CO_2.H_2O \longleftrightarrow CaCO_3 + 2H_2O$

For blended cement with high amounts of pozzolanic additions, almost all portlandite has reacted during pozzolanic reactions and formed secondary C-S-H. These compounds could also react with dissolved CO_2.

(Thiery, 2005) suggests that the carbonation of portlandite is faster, although the hydrated calcium silicates might also happen at the same time but in a slower rate.

The carbonation has antagonistic effects on concrete. At the same time, the carbonation could be good for concrete when the calcium carbonate formed fills the pores, increases strength and decreases permeability. Contrary, it could be harmful to reinforced concrete since the reaction of portlandite and C-S-H with carbonates decreases the pH of the poral solution, which would prevent reinforcement passivation which could induces steel corrosion (Chabil, 2009; Ilgar, 2015).

The temperature and humidity play an important role in the carbonation reaction. According to (Chaussadent, 1999), the solubility of carbon dioxide gas at atmospheric pressure decreases with temperature (formula 16) and hence, the carbonation rate is higher in winter than in summer. For optimal carbonation, the relative humidity should be between 50 and 65%.

Formula 16: $S = 5.283.10^{-6} e^{(\frac{2608.2}{T})}$

Where:

S: is the CO_2 solubility ($mol.l^{-1}$);

T: is the absolute temperature (K).

The natural carbonation is very slow and to observe the evolution of carbonation depth with time, carbonation tests at laboratory scale, can be performed under accelerated conditions. It was found a great variety of CO_2 concentrations for accelerating carbonation tests, varying from 3% to 50% (Auroy et al., 2015; Chabil, 2009; Ilgar, 2015; Rozière et al., 2009) and this variety was due to the standard method used to specific goals of the studies.

The carbonation depth in a sample is identified using a colour indicator. The most common indicator used is phenolphthalein due to the pH range covered : the color variation occurs between 8,2 and 9,9 (9 ± 1 unit pH). The pink coloration in the sample indicates the non-carbonated zone (pH ≥ 9 ± 1) whereas the colourless zone (pH ≤ 9 ± 1) indicates the carbonated zone (Drouet, 2010).

In this thesis, we built an accelerated carbonation chamber setup for performing carbonation tests in our concrete specimens. A drying process and humidity and temperature equilibrium in a climate chamber phases were carried out before starting the test. The tests conditions are detailed in Table 2.7 and the design is detailed in section 5.4.1.

Table 2.7 – Carbonation test conditions

Drying process	**Climate chamber**	**Carbonation chamber conditions throughout the test**
14 days at (45 ± 5)°C	7 days at: (65 ± 5)% relative humidity (20 ± 3)°C of temperature	(65 ± 5)% relative humidity (20 ± 3)°C of temperature (3 ± 0.5)% CO_2 concentration

The specimens were tested before being placed in the carbonation chamber to ensure there was no carbonation on them before the start of the test. Then, they were placed in the

carbonation chamber and were tested at 7, 28, 42 and 76 days. The specimens were sawn (Fig. 2-16) and phenolphthalein solution (1% in alcohol) was sprayed in the specimens to identify the carbonated zone and measure the carbonation depth. It was taken about four depth measures at the bottom and top of each side of the sawn specimen (when possible and respecting the measurement devices – a distance of 1 cm of each point and excluding the extremes), making a maximum total of 16 measures per total of 2 halves. The average of these measures was used as the result for the given specimen analysed. This procedure was done in three cylinders per formulation per day of the test. The average of them was noted as the carbonation depth in mm.

The carbonation rate (mm/day$^{1/2}$) can be estimated by the slope of the regression line obtained from the four average carbonation depths taken at four different times of testing.

Figure 2-16 – Lengthwise sawn diagram on the cylinder 110x50 mm.

2.3.4.3 Equivalence performance method

The validation of a given concrete by the equivalence performance method is based on the comparison of performances (FNTP, 2009). The relevant durability indicators are chosen according to the environmental exposure class and the given concrete performance is compared to a reference one. The reference concrete must be formulated according to the prescriptive approach (NF EN 206/CN) to the given environmental exposure class and the reference concrete formulation must provide:

- A ratio $W_{eff}/Binder_{eq} \leq [(Max\ W_{eff}/Binder_{eq}) - 0.05]$;
- $Binder_{eq}$ content higher than 5% of the minimum $Binder_{eq}$ content specified for the class in NF EN 206/CN – table NA.F.1, or water absorption < 0.5% of the maximum water absorption accepted for the class. The binder equivalent is the mass of cement + additions when applicable.

Both concrete must be done under the same conditions and procedures. Generally, the comparison is done by verifying the results by inequalities. For example, the carbonation depth of a given concrete must be less than the reference concrete for the same conditions to be validated. This can be used to compare mechanical performances as well.

$$\text{Given concrete durability indicator} < \text{Reference concrete durability indicator}$$

(San Nicolas et al., 2014) used the performance-based approach through the equivalence method to validate the use of flash-calcined metakaolin as cement replacement to produce concrete. The authors compared the index for reactivity, water porosity, chloride ion migration, gas permeability and carbonation. The index was obtained from the ratio between the durability indicator result of the given concrete per that one of the reference concrete and the reverse ratio in some other cases. Depending on the durability indicator, the index expected must be above or below 1 to indicate that the given concrete has a better performance. With this approach, the authors could validate the given concrete for all durability indicators except for carbonation.

$$\text{Index of durability indicator} = \frac{\text{Durability indicator result for the given concrete}}{\text{durability indicator result for the reference concrete}}$$

2.4 How can we assess the environmental impacts of processes and products?

Concrete is one of the most consumed materials in the world and is responsible for several environmental impacts related to the extraction of raw materials and clinker production. To develop more sustainable materials in construction, studies have been conducted to replace partially clinker in cement to reduce CO_2 emissions, or aggregates to limit natural resource depletion (Van Den Heede and De Belie, 2012). These substitutions can decrease the environmental impact of concrete and should be assessed qualitatively and quantitatively.

The importance of assessing the environmental impact of a material is to identify the processes that are responsible for the higher impacts and therefore, opportunities to improve processes reducing the impacts and potentially cost as well. The main methodology to assess environmental impacts is the Life Cycle Assessment (LCA). The LCA is a methodology standardised by NF EN ISO 14040 (principles and framework) and 14044 (requirements and guidance) (NF EN ISO 14040, 2006; NF EN ISO 14044, 2006).

The Life Cycle Assessment methodology is divided into four stages: definition of goal and scope, creation of the life cycle inventory (LCI), assessment of the life cycle environmental impacts (LCIA) and interpretation (Marinkovic, 2013). There are free and paid versions of software that the user can use to perform LCA analysis, like Simapro, GaBi, OpenLCA, others developed specifically for a type of material or structure (Betie, Ecorce, Perceval, Seve). The main types of environmental analysis are the cradle-to-gate approach (partially) or cradle-to-grave approach (full). The cradle-to-gate approach assesses the impacts from the extraction of raw materials until the gate of the industry. The cradle-to-grave approach assesses the impacts of the extraction of raw materials until the end-of-life.

There are several methods for assessing the environmental impact of processes. One of these methods is the ReCiPe model, which turns the inputs and outputs of the LCI into two types of impact categories: problem-oriented approach (midpoints) or damage-oriented approach (endpoints). There are 18 midpoint impact categories and they are focused on single environmental problems. The midpoint categories include global warming, water use, mineral resources, land use/transformation and others. The 3 endpoint indicators translate the single environmental impacts into the effect on human health, biodiversity and resource scarcity (Marinkovic, 2013).

In literature, only one study about LCA of oyster shells was found. (Alvarenga et al., 2012) studied the recycling process of oyster shells using life cycle assessment methodology. The authors investigated the environmental impacts related to 1 kg of oyster production in a cradle-to-grave approach. Two scenarios were analysed, landfill disposal or shells recycling (shells were processed to become raw material – source of $CaCO_3$). Authors found that a recycling scenario decreased the environmental impacts when compared to a landfill disposal scenario. However, the authors suggested that the recycling scenario is feasible within a limited distance otherwise the impacts turn to increase due to transportation.

In this thesis, we provided a preliminary environmental analysis of the impacts related to the aggregates (conventional and crushed oyster shells) production process inspired by the LCA idea, although it was not a proper LCA analysis (see chapter 6).

2.5 Concluding remarks

Prior studies were carried out using seashells in cementitious materials. A large number of studies have been trying to demonstrate the feasibility of using seashells as an aggregate replacement for mortar and concrete and their fresh and hardened properties. Main conclusions are:

- A large number of aggregate replacement rates were tested with different types of seashells. In general, it was found that as the replacement rate increases, the mechanical performance of mortar and concrete decreases. It was not found studies that investigated the 100% of replacement rate of coarse and fine conventional aggregate for crushed seashells, and more specifically oyster shells, at the same time;
- The use of seashells as aggregate replacement is subject to some particularities. The seashells also have higher water absorption than conventional aggregates, potentially affecting concrete properties and the interfacial transition zone as well;
- The seashells have different shape, and texture that tends to affect the fresh properties of concrete and the adhesion of the cement matrix to the seashell. Additionally, due to the shape, the conventional process of sieving tends to be inaccurate;
- Because of the flaky and elongated shape, the granular packing is a key point to improve when working with seashells as aggregate replacement for cementitious materials. Traditional methods have their limitations when optimising particles that are not spherical and when working with non-spherical particles, methods should be adapted;
- Traditional standard approach is not flexible and did not follow the progress toward innovative and sustainable materials. To compensate for that, the performance-based approach arose as an important tool when designing concrete beyond the traditional prescriptive approach. To follow this, durability indicators have to been determined;
- Besides material performance, it is important to assess the environmental impacts related to it. The environmental impacts can be carbon footprint, resource depletion and others and can be chosen more specifically according to the process of production. This

type of analysis is crucial to promote sustainable development since the project's environmental impact can be tracked and opportunities for process improvement identified.

After this brief overview of the project context, we are going to start presenting the study carried out in this thesis, using crushed oyster shells as aggregate replacement in concrete. In the next chapter, the reader will find the granular skeleton optimisation methodology used and applied to the crushed oyster shells.

CHAPTER 3 - A UNIVERSAL METHODOLOGY FOR GRANULAR SKELETON OPTIMISATION

In this chapter we present the universal methodology for granular skeleton optimisation developed during this thesis. Then, we apply this methodology to optimise the granular skeleton of a bio-based material, the crushed oyster shells.

3.1 Key strategy points for a universal methodology of optimisation

As developed in chapter 2 (state of the art), classical particle packing is not suitable when particles highly deviate from the spherical geometry. Consequently, a new approach was developed in this study to optimise the granular skeleton of non-spherical materials.

Relying on the fact that an aggregate skeleton is an assembly of particles of different sizes, we can relate this concept to the one of mixture design. A mixture is composed of constituents, and when the constituents are in the right proportions, we obtain an optimised product. However, when the proportions are unbalanced the result is normally unsatisfying. If we apply this approach to a granular skeleton distribution, we can expect that by mixing the right proportion of particle groups we will obtain a performing granular skeleton distribution of the mix. In this case, by performing granular skeleton distribution, we mean an aggregate where the particle is well organised and the voids between them are limited. Hence, the granular packing increase and the intergranular porosity decrease.

So, we present below the key points of the strategy:

- We optimised separately the fine and coarse granular skeletons. To obtain the global granular skeleton for concrete we optimised only the proportion of the previous optimise granular skeletons (fine and coarse);
- The optimisation method for the fine and coarse granular skeletons consisted in mixing particle groups 3 by 3 (ternary mixtures), always starting from the coarsest to the finest particle groups (a particle group comprises a range of particles d/D mm);
- The optimisation of the proportion between fine and coarse for the global granular skeleton for concrete was a binary mixture (2 particle groups – fine a coarse optimised granular skeletons)

- The optimisation target was the intergranular porosity and the mixtures were assessed based on this target. The intergranular porosity was estimated based on the loose bulk and oven-dried densities;
- The statistic software Minitab 17® was used for designing the experimental plan and treating the results, but any other statistical software can be used instead;
- The type of mixture design used was the simplex centroid and for statistical significance, replicates were done for vertex, double blends and centre point.

In the sequence, we present the methodology that we developed during this thesis to optimise the granular skeleton based on experimental mixture design and using the intergranular porosity as the key optimisation target.

Method

Figure 3-1 displays the summary of the main steps followed for the optimisation method proposed. Firstly, the particle groups to be combined are chosen (process variables). Then, we choose the type of mixture design (simplex centroid for example), the number of replicates and in which points of the design (vertex and centre for example). In our case, we used the software Minitab 17® to insert these parameters and create the mixture experimental plan to be run at the laboratory, but any other statistical software can be used instead. The mixture experimental plan is carried out in the laboratory and the intergranular porosity is estimated for each mixture tested. The mixture's intergranular porosity is the response parameter inputted in the software for performing the optimisation. After analysis of it, the response optimiser tool is used to identify the optimal proportion between the particle groups tested based on the target chosen (decrease the intergranular porosity) to obtain a final mixture.

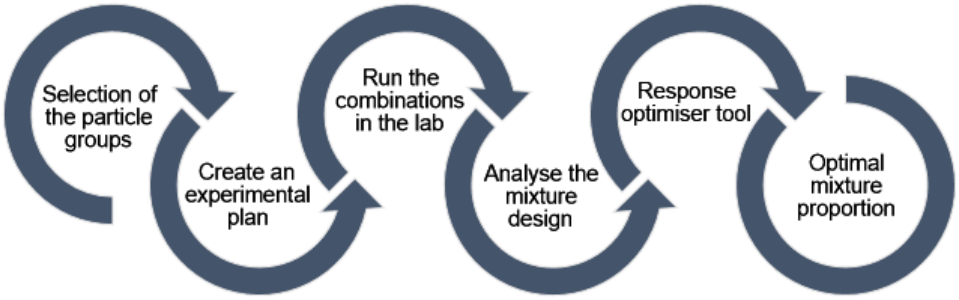

Figure 3-1 – Steps followed for the optimisation method.

To simplify the optimisation and reduce the number of experimental measurements of intergranular porosity, we chose to combine particle groups three by three in ternary mixtures.. Figure 3-2 illustrates the generic simplex centroid plot used on the optimisation for the particle groups A, B and C, obtained using the statistical software Minitab® 17.

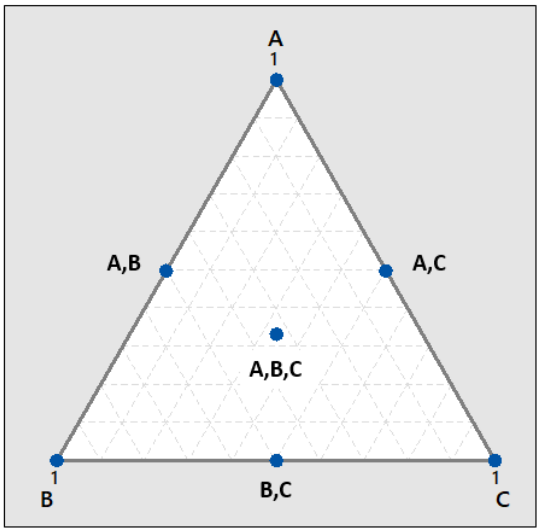

Figure 3-2 – Generic simplex centroid plot used on the optimisation method to combine three particle groups (A, B and C).

Table 3.1 is presenting the generic mixture design experimental plan created to assess the particle group combinations (three by three). The response for each of the 15 combinations was the intergranular porosity. Thus, it was necessary to estimate the loose bulk density and oven-dried density of each combination tested. Although table 3.1 shows the standard order

(StdOrder) of the mixtures, the tests were carried out in a random order. The numbers indicated for each particle group represents their proportion for the combination. For example, (1,0,0) means that it is a single combination of only particle group A – same for (0,1,0) for particle group B and (0,0,1) for particle group C. Combinations type (0.5,0.5,0) and their variations (0,0.5,0.5) or (0.5,0,0.5) represents binary combinations (two particle groups) and they were combined in equal proportions. Combinations type (0.33,0.33,0.33) represents the centre point of the triangle. This is a ternary combination (combination of three particle groups). For this type of combination, the particle groups were equaly proportion mixed, for example, 1/3 of particle group A + 1/3 of particle group B + 1/3 of particle group C.

Table 3.1 – Generic mixture design experimental plan used.

StdOrder	Particle group A (d/D)	Particle group B (d/D)	Particle group C (d/D)
1	1	0	0
2	0	1	0
3	0	0	1
4	0.5	0.5	0
5	0.5	0	0.5
6	0	0.5	0.5
7	0.33	0.33	0.33
8	1	0	0
9	0	1	0
10	0	0	1
11	0.5	0.5	0
12	0.5	0	0.5
13	0	0.5	0.5
14	0.33	0.33	0.33
15	0.33	0.33	0.33

The loose bulk density was experimentally obtained for each particle group and for the combinations tested during the mixture design. Although the oven-dried density of a material does not change when crushed into smaller particles, we preferred to characterise each particle group of the oyster shell material due to some impurities found on the crushed OS bags. Although the hand-collecting and cleaning process in the supplier is quite satisfactory, it is inevitable to find some impurities when it comes to a by-product. The impurities found

represented less than 1% of the total amount and were like plastics fishing nets, wood pieces, cigarette butts and even smaller pieces of mussel shells. Therefore, the oven-dried density was also estimated for each particle group/mixture to obtain a more accurate value to calculate the intergranular porosity.

Once the loose bulk and oven-dried densities were estimated for each combination, the intergranular porosity was calculated and inputted as the response parameter in the software. Then, the software processed the data inputted using a quadratic model with a confidence level of 95%. A mixture contour plot was used to evaluate the distribution of the intergranular porosity within the triangle area of the mixture.

Afterwards, the response optimiser tool was applied to identify the optimal proportion of the particle groups studied based on the target settled (decrease the intergranular porosity). If necessary, a sensitivity analysis can be performed by moving the red line for one or more components to evaluate the effect of changing proportion on the predicted intergranular porosity.

3.2 Application and particularity of crushed oyster shell skeleton optimisation

To optimise the granular distribution curve of crushed oyster shells, we found a series of constraints along the process that are detailed below. Therefore, some adaptations were necessary when carrying out the optimisation with this bio-based material.

First of all, due to the irregular and non-spherical shape of crushed oyster shells, the sieving method seems not to be as accurate as for conventional aggregates (sand and gravel). Usually, when we sieve a sample, we expect that for a certain sieve size the particles that are smaller than the aperture size will pass, and the bigger ones will be retained. However, we observed a different pattern for the crushed oyster shells. When sieving a sample of OS, we observed that due to elongated and flat shape, when the automatic sieving stops, some particles that seemed to be bigger than the previous aperture size passed and were found retained in the subsequent sieve. Because of this, we could see that crushed oyster shells particle groups could have higher variability in terms of particle size than conventional aggregates.

Another important observation that is related to the aforementioned point was checked in the laboratory. After sieving two big bags of 25 kg of crushed oyster shells 0/10 mm, we could see that in fact, the higher particle size was 8 mm instead of 10 mm (the lack of accuracy in sieving

crushed seashells is discussed in chapter 2). Due to this, it was necessary to adjust when designing and creating the OS coarse aggregate by adding the particle group of 10/12 mm to guarantee the presence of particles 8/10 mm.

Last but not least, it seems to be acceptable a certain percentage of particles with a diameter slightly higher than the last diameter said for the aggregate composition. For instance, it was analysed the granulometric curve of sand (0/4 mm) and gravel (4/10 mm) used in this thesis, and it was found that sand has 5.4% of 4/5.6 mm particles whereas gravel has 5.2% of 10/14 mm particles retained at these sizes.

Once point out the constraints, we are going to apply the granular skeleton optimisation methodology proposed to obtain a fine and a coarse aggregate composed of crushed oyster shells.

3.2.1 Oyster shell material and preparation

The oyster shells used in this project were grown in Arcachon Bay, France. The cleaning process of the farming area is the main source of these shells on top of food consumption. These shells are transported to Ovive facilities in La Rochelle, France. At Ovive facilities, the oyster shells pass through an industrial process consisting of phases of hand-collection of impurities, drying, crushing, sieving to finally be stored in sealed bags of several particle groups. The crushed oyster shells were transported from Ovive to the laboratory at UPPA in sealed bags (Fig. 3-3) and identified by the particle group (d/D). The particle groups of crushed oyster shell used were: 10/12 mm, 8/10 mm, 6/8 mm, 5/6 mm, 4/5 mm, 2.5/4 mm, 1.25/2.5 mm, 0.500/1.25 mm, 0.250/0.500 mm, 0.200/0.250 mm, 0.100/0.200 mm and 0/0.100 mm.

Figure 3-3 – Storage of crushed OS by particle groups in the laboratory.

To characterise the physical properties of the crushed oyster shells and their combinations, we used the loose bulk and oven-dried densities. Then, these parameters were used to estimate the intergranular porosity (also known as the percentage of voids or just voids) of each combination. The densities and the intergranular porosity were key parameters for assessing the granular skeleton optimisation.

3.2.3 Practical method for the optimisation of fine, coarse and global concrete granular skeleton

Optimisation of fine granular skeleton

It was used seven particle groups within the range of 0/4 mm to obtain the OS fine granular skeleton. The particle groups used were: 2.5/4 mm, 1.25/2.5 mm, 0.500/1.25 mm, 0.250/0.500 mm, 0.200/0.250 mm, 0.100/0.200 mm and 0/0.100 mm, and were obtained according to the sieving availability of the supplier (Ovive S.A). Based on the approach described in section 3.1, we combined the particle groups three by three starting from the largest and towards the smallest particles sizes. Figure 3-4 illustrates the schematic of combining the seven particle groups in three rounds of optimisation to obtain the oyster shell fine granular skeleton.

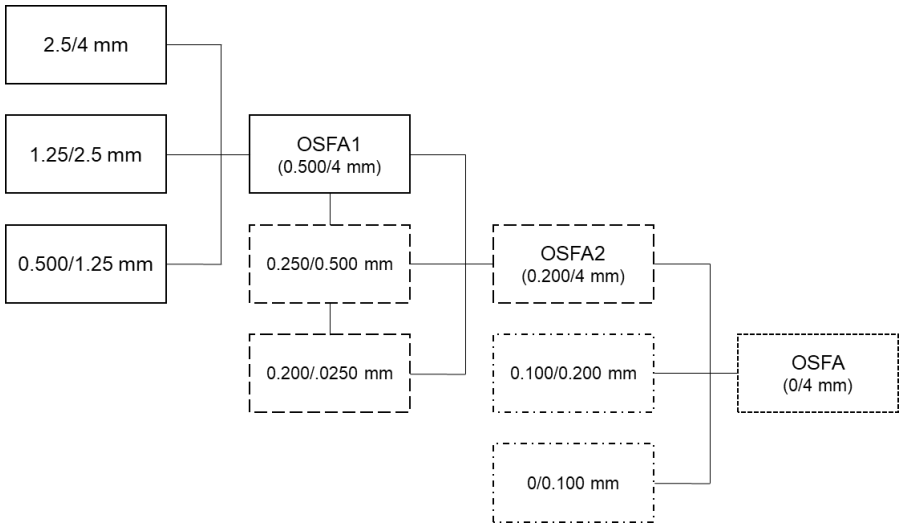

Figure 3-4 – OS fine aggregate optimisation schematic.

Based on the experimental planning designed (section 3.1) and relying in the filling effect were voids left by coarser particles will be filled by smaller particles and so on, we started the first round of optimisation combining 2.5/4 mm, 1.25/1.5 mm and 0.500/1.25 mm particle groups. The optimised mixture obtained from this combination was identified as OSFA1 (Oyster Shell Fine Aggregate 1).

The optimised mixture obtained in the first round (OSFA1) was used in the next round. Two other particle groups (0.250/0.500 mm and 0.200/0.250 mm) were added to the mixture design. From this round, we obtained the OSFA2 (Oyster Shell Fine Aggregate 2), composed of 0.200/4 mm and to be used in the next and final round of optimisation. Finally, the last round of optimisation was carried out by combining the OSFA2 with the 0.100/0.200 mm and 0/0.100 mm particle groups. The optimisation procedure was the same and the mixture obtained from the last round (Oyster Shell Fine Aggregate) corresponds to the final oyster shell granular skeleton OSFA 0/4 mm.

The results of each round of optimisation and the oyster shell fine granular skeleton (OSFA) are presented in section 3.3.1.

Optimisation of coarse granular skeleton

It was used five particle groups to obtain the Oyster Shell Coarse Aggregate (OSCA). The particle groups used were: 10/12 mm, 8/10 mm, 6/8 mm, 5/6 mm, 4/5 mm, and were obtained according to the sieving availability of the supplier (Ovive S.A). Figure 3-5 illustrates the schematic of combining the five particle groups in two rounds of optimisation to obtain the oyster shell coarse aggregate (OSCA).

Based on the approach described in section 3.1, we combined the particle groups three by three starting from the largest and towards the smallest particles sizes relying on the filling effect. We started the first round of optimisation combining the 10/12 mm, 8/10 mm and 6/8 mm particle groups. The optimised mixture obtained from this combination was identified as OSCA1 (Oyster Shell Coarse Aggregate 1). The optimised mixture obtained in the first round (OSCA1) was used in the next round. Two other particle groups (5/6 mm and 4/5 mm) were added to the mixture design and combined with OSCA1. From this round, we obtained the OSCA (Oyster Shell Coarse Aggregate), which corresponds to the final oyster shell coarse aggregate OSCA 4/10 mm.

The results of each round of optimisation and the oyster shell coarse granular skeleton (OSCA) are presented in section 3.3.2.

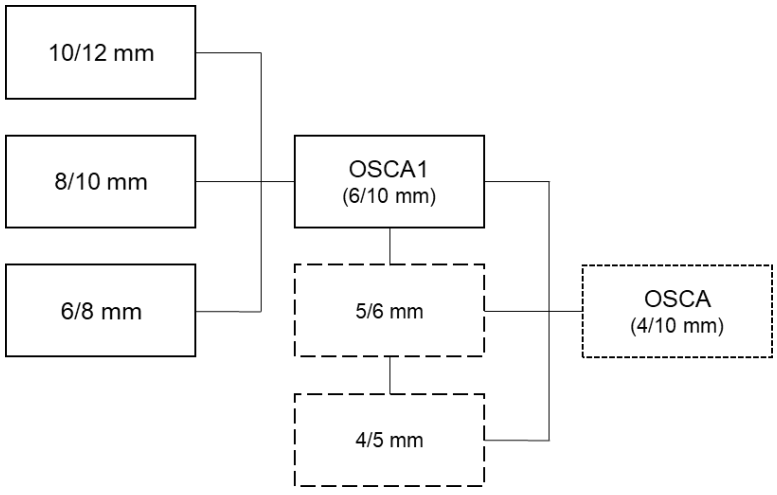

Figure 3-5 - OS coarse aggregate optimisation schematic.

Global concrete granular skeleton (OSCA + OSFA)

So far, we obtained separately the fine and coarse oyster shell granular skeletons. We aimed to replace 100% of the conventional aggregates (sand and gravel) with the crushed oyster shell in concrete. However, probably keeping the same proportion of gravel/sand as from the conventional concrete would not be suitable as the aggregate's shapes or compactness are not similar. Therefore, it was necessary to find the best mixture proportion for the OS aggregates. To do this, we keep the same approach; we created an experimental plan of the binary mixture of OSFA and OSCA using the design of experiments to find the best mixture proportion of OSFA and OSCA for the lowest intergranular porosity possible.

The result of the optimisation of OSFA and OSCA is presented in section 3.3.3.

3.3 Experimental results

3.3.1 Oyster shell fine aggregate skeleton optimisation

As described before, the optimisation of the fine aggregate skeleton was developed in three rounds. So, the experimental results of each round will be present in the sequence.

The first round of optimisation – OSFA1

In the first round, we sought to analyse the combination of the particle groups of 2.5/4 mm, 1.25/2.5 mm and 0.500/1.25 mm. Table 3.2 shows the experimental results for the mixture design performed and the values of intergranular porosity, loose bulk and oven-dried density for each combination. The intergranular porosity of each mixture was used as the response parameter in the software to assess the mixture design.

Table 3.2 – Results of the mixture design of the first round of optimisation used as input data on Minitab 17® for analysing the particle group combinations.

Mixture Design - OSFA1				Response	Loose Bulk density (kg/m³)	Oven-dried density (kg/m³)
StdOrder	2.5/4 mm	1.25/2.5 mm	0.500/1.25 mm	Intergranular porosity (%)		
1	1	0	0	64.4	770	2164
2	0	1	0	63.0	767	2073
3	0	0	1	69.8	771	2556
4	0.5	0.5	0	60.4	839	2117
5	0.5	0	0.5	61.7	898	2343
6	0	0.5	0.5	64.6	810	2289
7	0.33	0.33	0.33	61.6	863	2246
8	1	0	0	64.8	763	2164
9	0	1	0	62.5	777	2073
10	0	0	1	69.8	771	2556
11	0.5	0.5	0	60.8	830	2117
12	0.5	0	0.5	61.5	903	2343
13	0	0.5	0.5	64.9	804	2289
14	0.33	0.33	0.33	61.5	866	2246
15	0.33	0.33	0.33	61.2	871	2246

It can be seen from Figure 3-6 that the central region of the triangle (dark blue) is a combination of the three-particle groups where the intergranular porosity tends to be less than 62%. The regions on the top and right corner are the ones where the intergranular porosity tends to increase (green). This means that single mixtures of 2.5/4 mm or 0.500/1.25 mm are not suitable and should be avoided. In addition to that, mixtures with a higher proportion of 0.500/1.25 mm seem not to be favourable, with a clear tendency to increase the intergranular porosity when its proportion in the mixture grow.

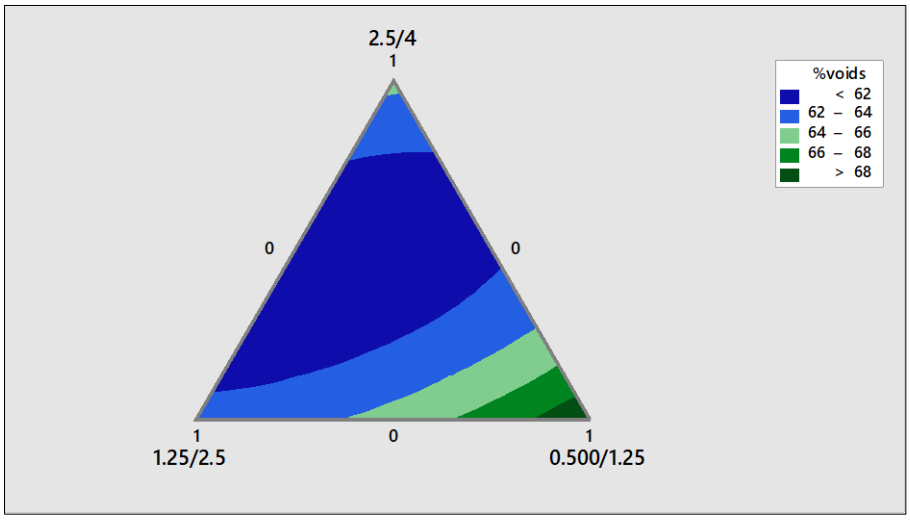

Figure 3-6 – Mixture contour plot analysis of the first round of optimisation which the response analysed is the intergranular porosity (%).

In sequence, the response optimiser tool is used to obtain a mixture proportion for a target of 60% of intergranular porosity. In the response optimiser tool, we select the particle groups that we want to analyse and the target that in this case is the intergranular porosity value (%). Then, the sotfware suggests the mixture proportion that corresponds to the target chosen. In the figure 3-7, the red line represents the current factor settings; the blue line represents the current response values, and the grey region corresponds to the response that is outside of the desirability target.

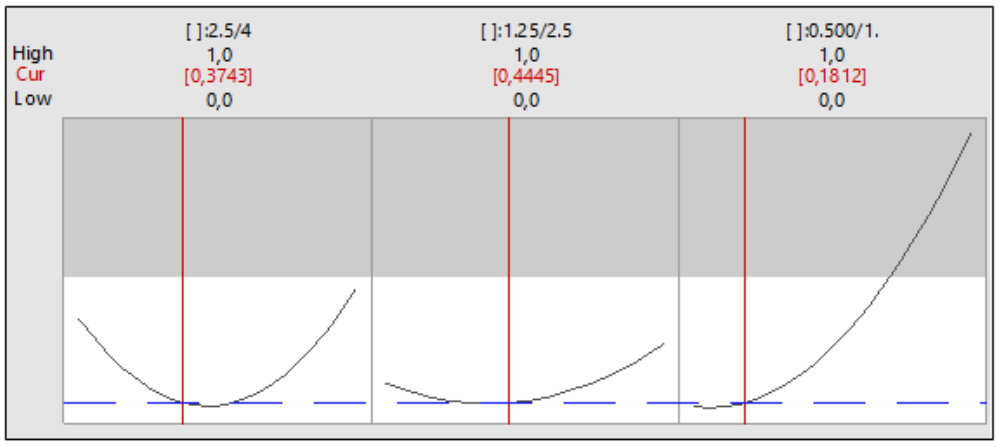

Figure 3-7 – Optimal mixture suggested by the software for the first round considering a target of 60% of intergranular porosity.

Figure 3-7 shows a higher proportion of the groups 2.5/4 mm (37.4%) and 1.25/2.5 mm (44.5%) and lower of 0.500/1.25 mm (18.1%) is proposed as the optimal combination. The software predicted an intergranular porosity of 60.8% for this combination that was confirmed by the experimental measure of 60.7% (Table 3.3). The experimental measurement was carried out in the laboratory for confirmation of the predicted value on the software. For this, we created the combination of particle groups with the proportion suggested and we measured the densities to estimate the intergranular porosity.

So, the OSFA1 (Oyster Shell Fine Aggregate 1) mixture proportion suggested by the software was kept and used for the next round.

Table 3.3 – Experimental results for the OSFA1 mixture.

	Loose bulk density (kg/m³)	**Oven-dried density (kg/m³)**	**Intergranular porosity (%)**
OSFA1	857	2182	60.7

The second round of optimisation – OSFA2

In the second round, the particle groups of 0.250/0.500 mm and 0.200/0.250 mm were tested together with OSFA1. Table 3.4 shows the experimental results for the mixture design performed and the physical properties of the mixtures. The intergranular porosity of each mixture was inputted in the software to assess the mixture design.

It is worth noting from Figure 3-8 that the central region of the triangle (dark blue) provides an intergranular porosity between 56 and 58%. This optimum proportion is obtained when combining the three-particle groups. However, as the proportion of 0.250/0.500 mm and 0.200/0.250 increases in the mixture, so does the intergranular porosity. This is evidenced by the darker green colour at the lowest third of the triangle, where the intergranular porosity tends to increase gradually towards the base of it (over 62% of voids).

Table 3.4 – Results of the mixture design of the second round used as input data on Minitab 17® for analysing the particle group combinations.

Mixture Design - OSFA2				Response	Loose Bulk density (kg/m³)	Oven-dried density (kg/m³)
StdOrder	OSFA1	0.250/0.500 mm	0.200/0.250 mm	Intergranular porosity (%)		
1	1	0	0	60.8	855	2182
2	0	1	0	64.7	826	2341
3	0	0	1	65.1	811	2323
4	0.5	0.5	0	57.4	962	2259
5	0.5	0	0.5	55.8	994	2250
6	0	0.5	0.5	64.7	823	2332
7	0.33	0.33	0.33	58.8	940	2280
8	1	0	0	60.5	861	2182
9	0	1	0	64.8	825	2341
10	0	0	1	65.3	806	2323
11	0.5	0.5	0	57.2	967	2259
12	0.5	0	0.5	55.9	992	2250
13	0	0.5	0.5	64.6	827	2332
14	0.33	0.33	0.33	58.5	946	2280
15	0.33	0.33	0.33	58.6	943	2280

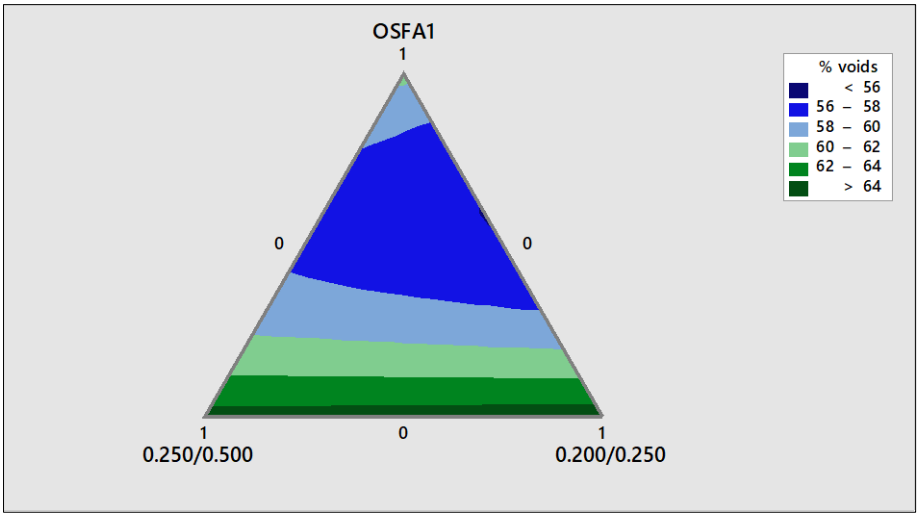

Figure 3-8 – Mixture contour plot analysis of the second round of optimisation which the response analysed is the intergranular porosity (%).

After that, the response optimiser tool is used to obtain the optimal combination for an intergranular porosity target of 55%. As predicted by the previous analysis, the proportion of the particle groups 0.250/0.500 mm and 0.200/0.250 mm should be limited to decrease the intergranular porosity. Thus, the optimal mixture proportion proposed by the software is composed of 58.6% of OSFA1, 20.7% of 0.250/0.500 mm and 20.7% of 0.200/0.250 mm (Fig. 3-9).

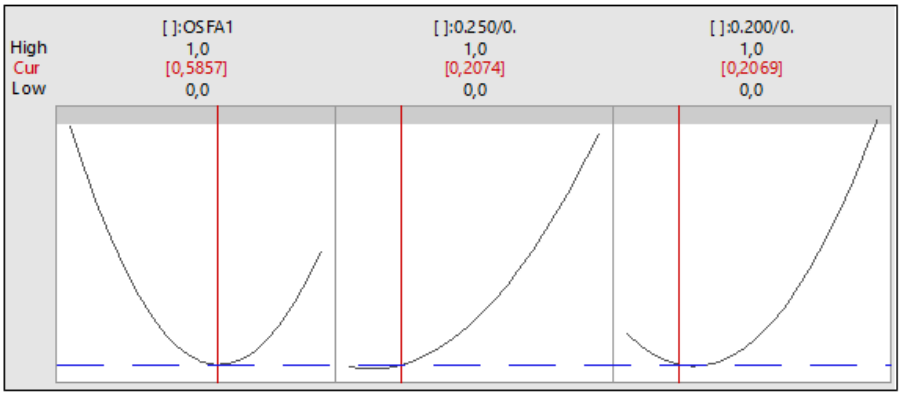

Figure 3-9 – Optimal mixture suggested by the software for the second round considering a target of 55% of intergranular porosity.

It is expected an intergranular porosity of 56,7% for this mixture whereas the experimental measure showed 56.3% (Table 3.5). So, the OSFA2 (0.200/4 mm) mixture proportion suggested by the software is kept and used for the next round.

Table 3.5 – Experimental results for the OSFA2 mixture.

	Loose bulk density (kg/m³)	**Oven-dried density (kg/m³)**	**Intergranular porosity (%)**
OSFA2	980	2242	56.3

The third round of optimisation – OSFA

Finally, the particle groups of 0.100/0.200 mm and 0/0.100 mm were tested with OSFA2 for the third round of optimisation. Table 3.6 shows the experimental results for the mixture design performed and the physical properties of the mixtures. The intergranular porosity of each mixture was used in the software to assess the mixture design.

It can be seen from Figure 3-10 that, unlike the previous rounds, the addition of the finer particle groups seems to disturb the granular packing. The intergranular porosity tends to increase over 62% as the proportion of the finer particle groups increases in the mixture. Nevertheless, the addition of these finer particle groups could disturb the granular arrangement, it was necessary to keep them to obtain an aggregate within the range of 0/4 mm to replace sand 0/4 mm. As a consequence, the proportion of these two finer particle groups was limited to avoid further losses on the optimisation done so far.

Table 3.6 – Results of the mixture design of the third round used as input data on Minitab 17® for analysing the particle group combinations.

Mixture Design - OSFA				**Response**	**Loose Bulk density (kg/m³)**	**Oven-dried density (kg/m³)**
StdOrder	**OSFA2**	**0.100/0.200 mm**	**0/0.100 mm**	**Intergranular porosity (%)**		
1	1	0	0	55.8	991	2242
2	0	1	0	68.0	698	2181
3	0	0	1	68.4	728	2305
4	0.5	0.5	0	60.9	865	2211
5	0.5	0	0.5	60.3	901	2273
6	0	0.5	0.5	67.7	725	2241
7	0.33	0.33	0.33	62.4	843	2241
8	1	0	0	55.8	990	2242
9	0	1	0	67.6	707	2181
10	0	0	1	68.8	719	2305
11	0.5	0.5	0	60.9	865	2211
12	0.5	0	0.5	60.9	889	2273
13	0	0.5	0.5	67.4	731	2241
14	0.33	0.33	0.33	62.3	844	2241
15	0.33	0.33	0.33	62.3	845	2241

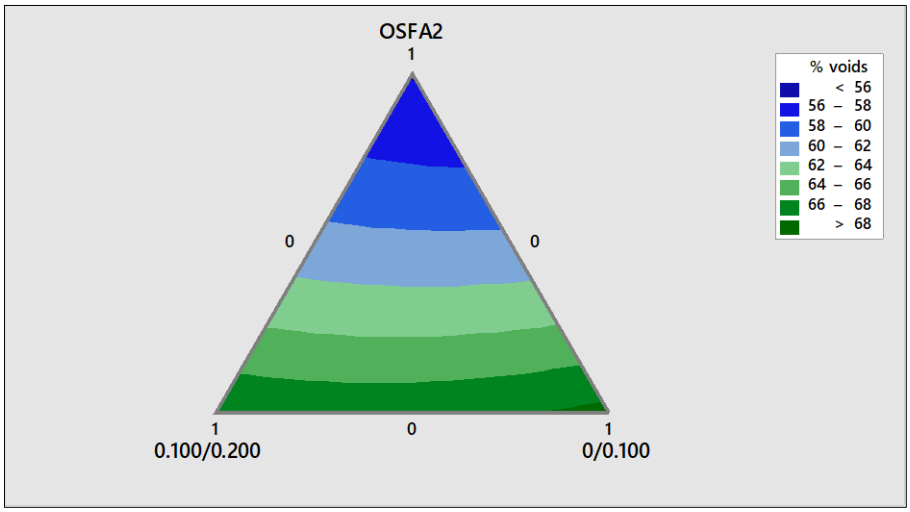

Figure 3-10 – Mixture contour plot analysis of the third round of optimisation which the response analysed is the intergranular porosity (%).

The response optimiser tool was used to assess the best proportion between the classes. The mix proportion of 83.5% of OSFA2, 8.25% of 0.100/0.200 mm and 8.25% of 0/0.100 mm was suggested for OSFA (Fig. 3-11).

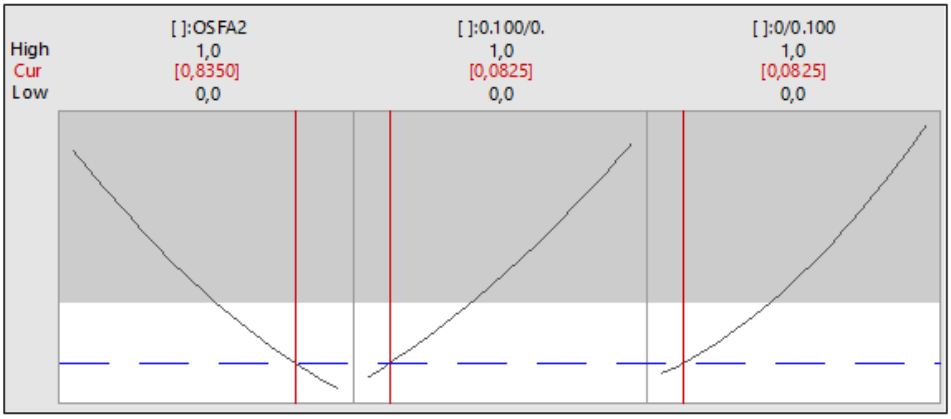

Figure 3-11 – Optimal mixture suggested by the software for the third round considering a target of 57% of intergranular porosity.

The software predicted 57% of intergranular porosity whereas the experimental measure was 54.1% (Table 3.7).

Table 3.7 – Experimental results for the OSFA mixture.

	Loose bulk density (kg/m³)	Oven-dried density (kg/m³)	Intergranular porosity (%)
OSFA	974	2123	54.1

Oyster shell fine aggregate skeleton - OSFA

The OSFA3 corresponds to the oyster shell fine aggregate within the range of 0/4 mm. Although every round of optimisation sums 100% individually, for building the aggregate skeleton is important to pay attention to the proportion backwards. Figure 3.12 shows the proportion per particle group and figure 3.13 displays the granulometric curve of the OSFA. It can be seen from figure 3.13 that the granulometric curve demonstrates a smooth and continuous shape with a small increase between the sizes of 0.200 and 1 mm.

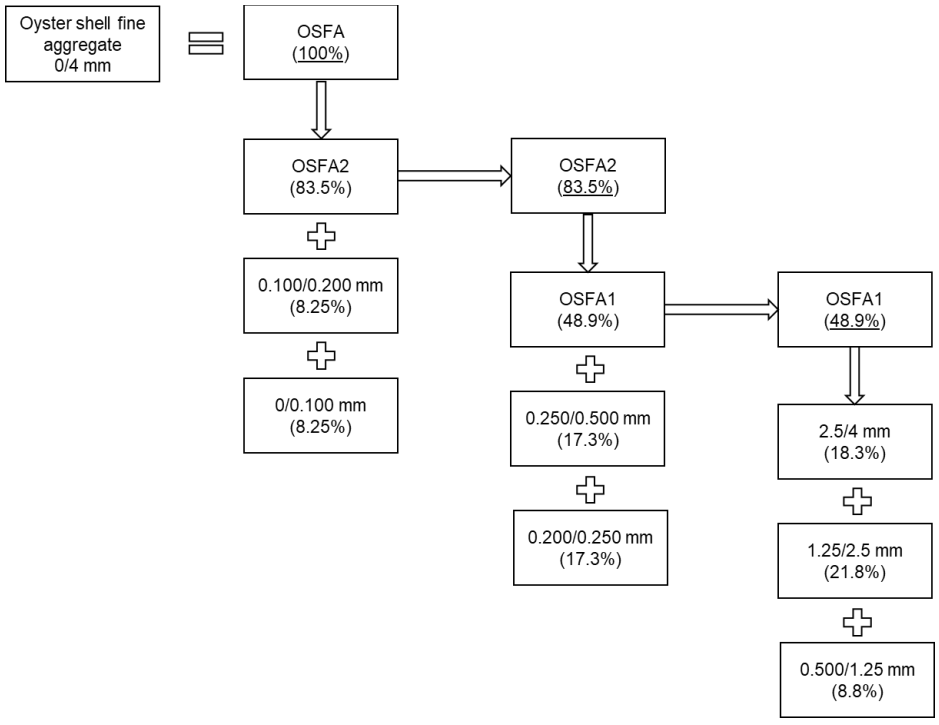

Figure 3-12 – Oyster shell fine aggregate composition, with proportion per particle group.

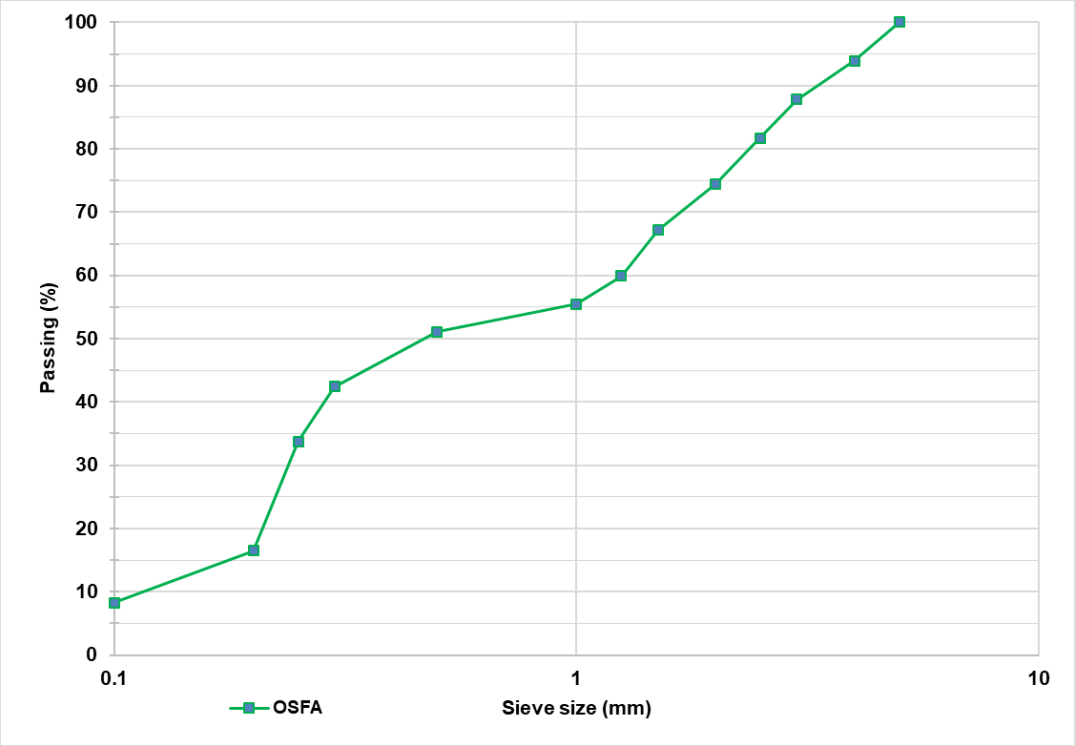

Figure 3-13 – Granulometric curve of the OSFA 0/4 mm.

3.3.2 Oyster shell coarse aggregate skeleton optimisation

As described before, the optimisation was developed in two rounds. So, the experimental results of each round will be present in the sequence.

The first round of optimisation – OSCA1

In the first round, we sought to analyse the combination of the 10/12 mm, 8/10 mm and 6/8 mm particle groups. Table 3.8 shows the experimental results for the mixture design performed and the physical properties of the mixtures. The intergranular porosity of each mixture was inputted in the software to assess the mixture design.

Table 3.8 – Results of the mixture design of the first round used as input data on Minitab 17® for analysing the particle group combinations.

Mixture Design - OSCA1				Response	Loose Bulk density (kg/m³)	Oven-dried density (kg/m³)
StdOrder	10/12 mm	8/10 mm	6/8 mm	Intergranular porosity (%)		
1	1	0	0	72.3	623	2248
2	0	1	0	70.7	680	2321
3	0	0	1	66.6	758	2269
4	0.5	0.5	0	71.3	655	2284
5	0.5	0	0.5	67.6	733	2259
6	0	0.5	0.5	66.7	764	2295
7	0.33	0.33	0.33	68.2	725	2279
8	1	0	0	72.9	610	2248
9	0	1	0	70.0	696	2321
10	0	0	1	67.0	749	2269
11	0.5	0.5	0	71.2	659	2284
12	0.5	0	0.5	67.3	738	2259
13	0	0.5	0.5	66.8	762	2295
14	0.33	0.33	0.33	68.4	720	2279
15	0.33	0.33	0.33	68.3	722	2279

It can be seen from Figure 3-14 that the intergranular porosity tends to grow (over 72%) when the proportion of the 10/12 mm increases. An intermedium phase is shown by the shades of blue (light and medium especially) where the proportion of the three particle groups are more equally distributed to decrease the intergranular porosity. Then, the darker blue towards a higher proportion of the 6/8 mm indicates an intergranular porosity below 68%.

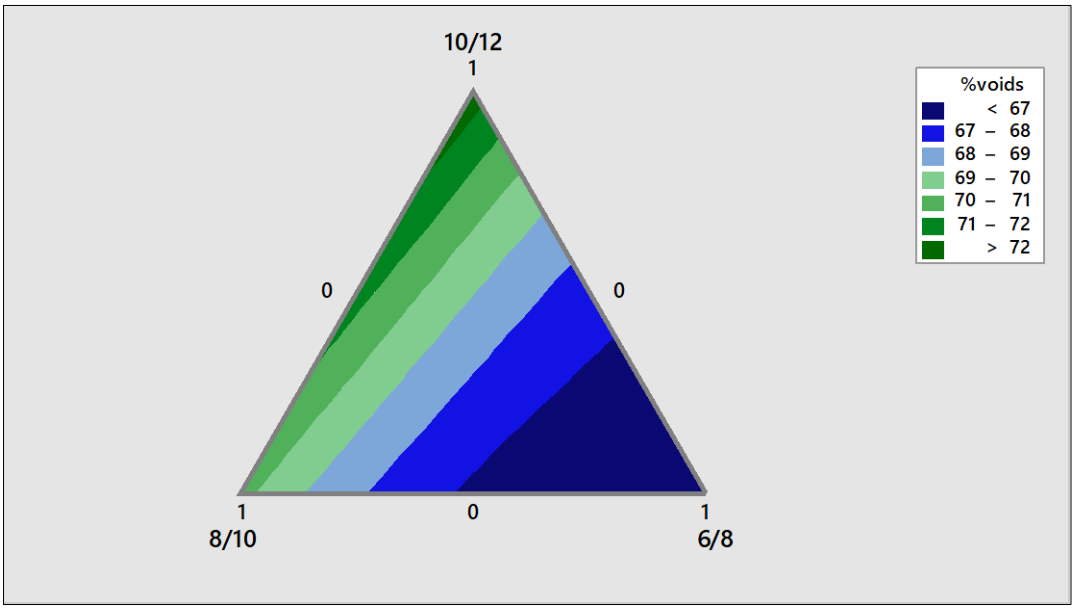

Figure 3-14 – Mixture contour plot analysis of the first round of optimisation of OSCA1 which the response analysed is the intergranular porosity (%).

The response optimiser was used to assess the best combination of the three particle groups. In this case, the target aimed was 68%, which provided quite balanced mixture proportions (Fig. 3-15). The optimal proportion combination for the target settled was composed of 10/12 mm (33.3%), 8/10 mm (30.6%) and 6/8 mm (36,1%). Table 3.9 shows the experimental results found for OSCA1 (Oyster Shell Coarse Aggregate 1).

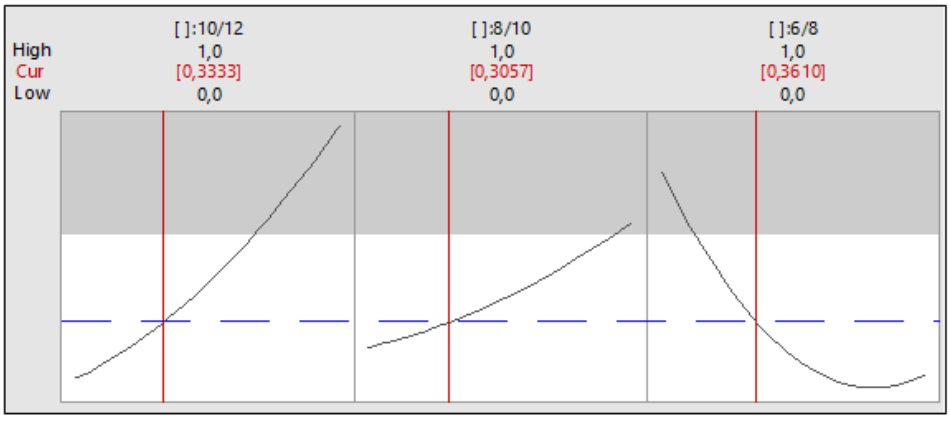

Figure 3-15 – Optimal mixture suggested by the software for the first round considering a target of 68% of intergranular porosity.

Table 3.9 – Experimental results for the OSCA1 mixture.

	Loose bulk density (kg/m³)	Oven-dried density (kg/m³)	Intergranular porosity (%)
OSCA1	695	2278	69.5

In this case, we observed that the optimisation could have been improved by a sensitivity analysis. The target could have been changed to 66% and hence, the proportion of the components. Nevertheless, we preferred to keep the first suggestion of the response optimiser tool which was still acceptable. So, the mixture proportion suggested in Figure 3-15 was identified as OSCA1 and used on the second round.

The second round of optimisation – OSCA2

In the second round, the particle groups of 5/6 mm and 4/5 mm were tested together with OSCA1. Table 3.10 shows the experimental results for the mixture design performed and the physical properties of the mixtures. The intergranular porosity of each mixture was inputted in the software to assess the mixture design.

Table 3.10 – Results of the mixture design of the second round used as input data on Minitab 17® for analysing the particle group combinations.

Mixture Design - OSCA2				Response	Loose Bulk density (kg/m³)	Oven-dried density (kg/m³)
StdOrder	OSCA1 mm	5/6 mm	4/5 mm	Intergranular porosity (%)		
1	1	0	0	69.8	689	2278
2	0	1	0	66.0	765	2250
3	0	0	1	64.9	771	2197
4	0.5	0.5	0	65.9	773	2264
5	0.5	0	0.5	66.0	760	2237
6	0	0.5	0.5	65.2	774	2223
7	0.33	0.33	0.33	65.8	767	2241
8	1	0	0	70.3	677	2278
9	0	1	0	65.3	780	2250
10	0	0	1	65.1	767	2197
11	0.5	0.5	0	66.4	760	2264
12	0.5	0	0.5	65.4	774	2237
13	0	0.5	0.5	65.3	772	2223
14	0.33	0.33	0.33	65.4	775	2241
15	0.33	0.33	0.33	64.9	786	2241

It can be seen from Fig. 3-16 that the intergranular porosity tends to grow (over 70%) when the proportion of the OSCA1 increases. In addition to that, about half of the triangle plot shows a zone where the combination of the three particle groups provides an intergranular porosity between 65 and 66%. Finally, a dark blue zone where the intergranular porosity tends to decrease (less than 65%) is found closer to the 4/5 mm particle group.

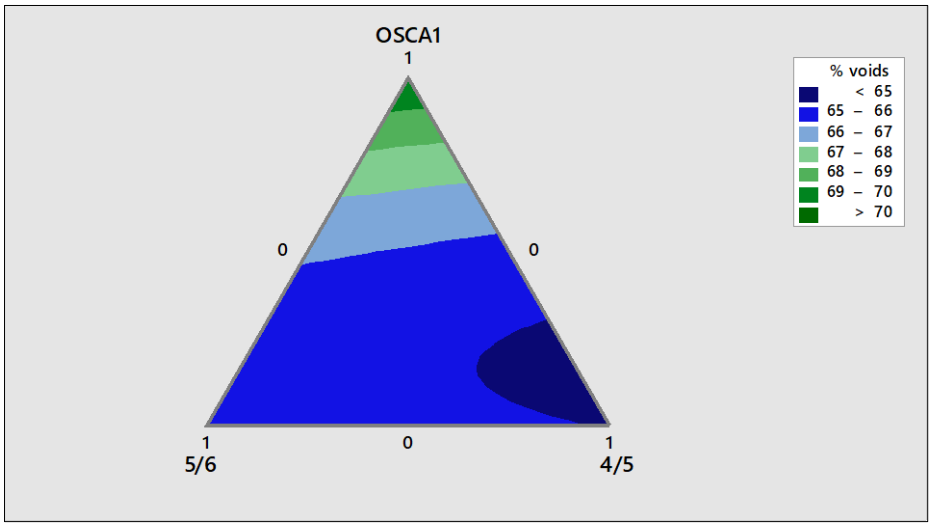

Figure 3-16 – Mixture contour plot analysis of the second round of optimisation which the response analysed is the intergranular porosity (%).

The response optimiser tool was used to assess the best combination of the three particle groups. The optimal mixture proposed was composed of OSCA1 mm (23.2%), 5/6 mm (53,7%) and 4/5 mm (23,1%) with an intergranular porosity expected of 66% (Fig. 3-17).

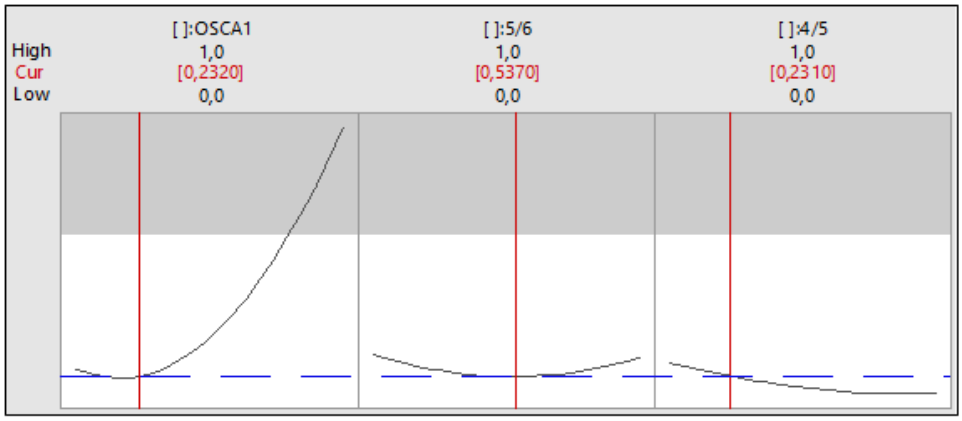

Figure 3-17 – Optimal mixture suggested by the software for the second round considering a target of 65.3% of intergranular porosity.

Table 3-11 shows the experimental results of the OSCA and an intergranular porosity of 64,6%, lower than predicted on the software. Therefore, this mixture was kept and corresponds to the OSCA (Oyster Shell Coarse Aggregate).

Table 3.11 – Experimental results for the OSCA mixture.

	Loose bulk density (kg/m³)	**Oven-dried density (kg/m³)**	**Intergranular porosity (%)**
OSCA	777	2194	64.6

Oyster shell coarse aggregate skeleton - OSCA

The OSCA corresponds to the oyster shell coarse aggregate (OSCA) within the range of 4/10 mm. Although every round of optimisation sums 100% individually, for building the aggregate mixture is important to pay attention to the proportion backwards. Figure 3-18 shows the proportion per particle group and figure 3-19 displays the granulometric curve of the OSCA. It can be seen from figure 3-19 that the granulometric curve demonstrates a continuous shape with a small peak on the size of 6 mm. This is confirmed by the proportion of the group 5/6 mm (53,7%), as demonstrated on the fig. 3-18.

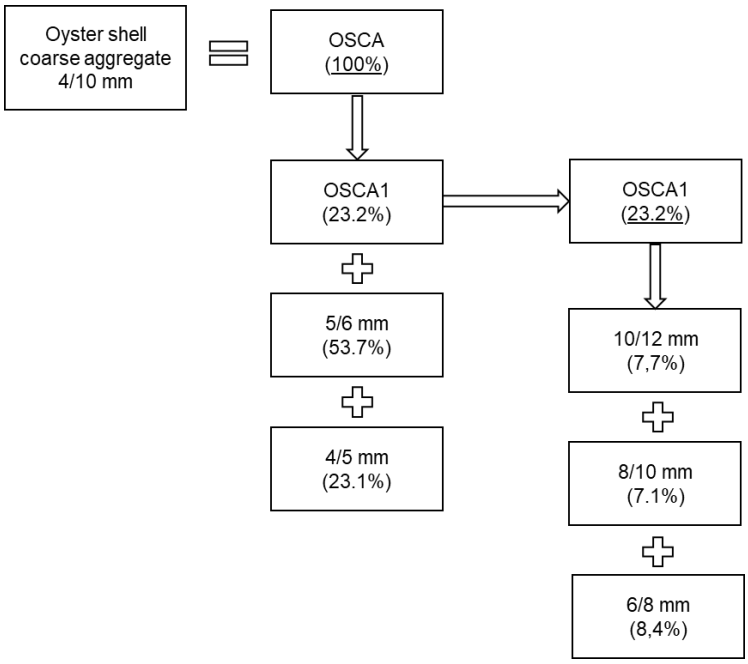

Figure 3-18 – Oyster shell coarse aggregate 4/10 mm composition, with proportion per particle group.

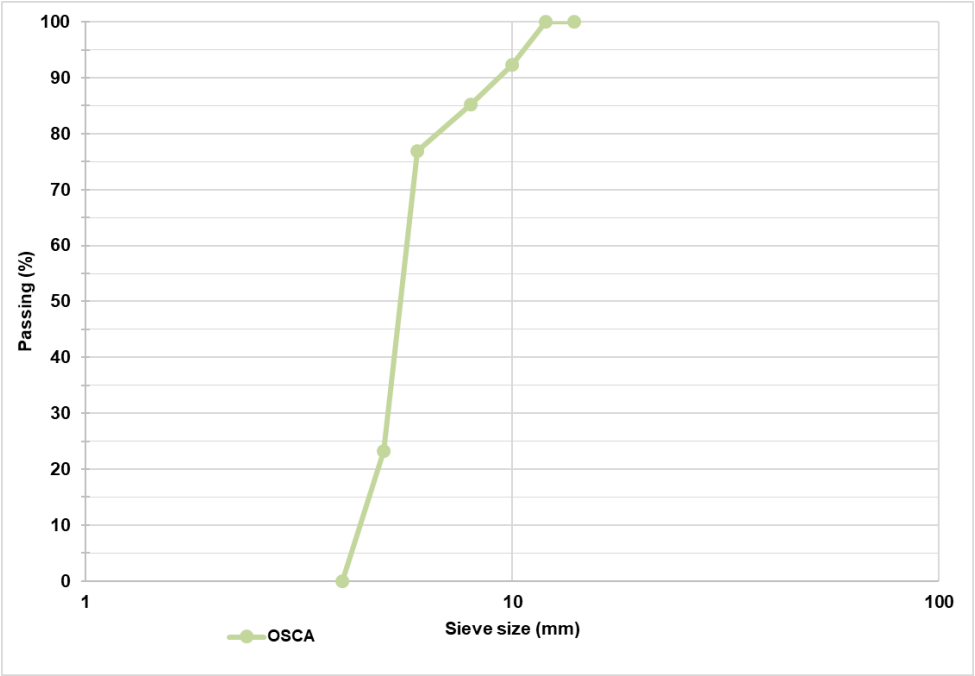

Figure 3-19 – Oyster shell coarse aggregate granulometric curve.

3.3.3 Oyster shell fine and coarse aggregate mixing for global concrete skeleton optimisation

As described before, the global concrete aggregate skeleton was composed of the fine and coarse aggregate skeleton previously optimised. To find the global concrete skeleton, we designed an experimental plan for combining OSFA and OSCA and finding the best proportion for decreasing the intergranular porosity. Table 3-12 shows the experimental plan used and the experimental results for each combination.

The results were processed in the software Minitab 17® and the response optimiser tool was used to find the best proportion between OSFA and OSCA. The optimal proportion suggested was approximately 61.9% of OSFA and 38.1% of OSCA, with an intergranular porosity of 53% (Fig. 3-20).

Table 3.12 – Experimental plan and physical properties of the mixture OSFA and OSCA.

Mixture Design - OSFA + OSCA			**Response**	**Loose bulk density (kg/m³)**	**Oven-dried density (kg/m³)**
StdOrder	**OSFA**	**OSCA**	**Intergranular porosity (%)**		
1	1	0	64.9	771	2194
2	0	1	54.6	965	2123
3	0.5	0.5	53.6	1000	2158
4	0.75	0.25	59.5	880	2176
5	0.25	0.75	52.1	1025	2140
6	1	0	64.8	772	2194
7	0.00	1.00	54.5	967	2123
8	0.5	0.5	53.8	996	2158
9	0.75	0.25	58.8	896	2176
10	0.25	0.75	52.0	1028	2140

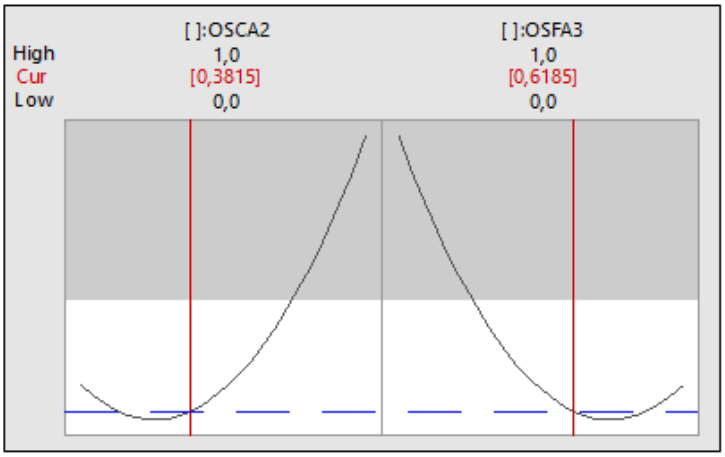

Figure 3-20 – Response optimiser graph with the proportion of OSFA and OSCA for concrete considering a target of 53% of intergranular porosity.

Table 3.13 shows the experimental results of intergranular porosity, loose bulk and oven-dried densities obtained of the mixture proportion of 61.9% OSFA and 38.1% of OSCA. It is worth noting that the predicted intergranular porosity on the software was the same found at the laboratory test, confirming the method's accuracy. Therefore, this mixture proportion was considered satisfactory and used for producing the 100% oyster shell concrete.

Table 3.13 – Physical properties of the optimal aggregate mixture of 61.9% OSFA + 38.1% OSCA.

Loose bulk density (kg/m^3)	**Oven-dried density (kg/m^3)**	**Intergranular porosity (%)**
1020	2150	53

Figure 3-21 shows the granulometric curve of the mixture composed of 61.9% of OSFA and 38.1% of OSCA. It can be seen a smooth curve with a small peak on the size of 6 mm of the OSCA and a slight increase between 0.200/1 mm of the OSFA.

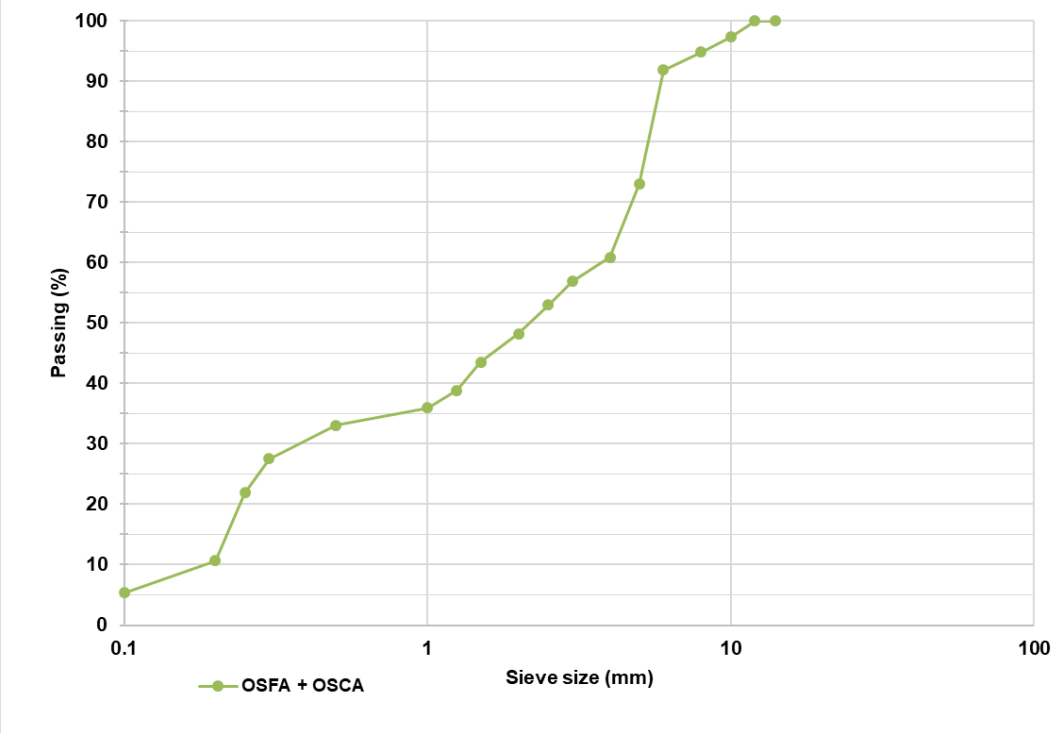

Figure 3-21 – Granulometric curve of the oyster shell aggregates for concrete (61.9% of OSFA 0/4 mm and 38.1% of OSCA 4/10 mm).

Figure 3-22 shows the fine, coarse and global granular skeletons of crushed oyster shells.

Figure 3-22 – OSFA (Oyster shell fine aggregate), OSCA (Oyster shell coarse aggregate) and Oyster shell global aggregate (mixture of OSFA + OSCA).

3.4 Concluding remarks

We proposed a way to optimise the particle packing of non-spherical material, applying this methodology to crushed oyster shells. Using the knowledge of the mixture design of the experiment, we could assess the combination of different particle groups of crushed oyster shells to obtain a granular skeleton mixture with limited intergranular porosity. Therefore, some conclusions obtained from the study presented in this chapter are summarised as follows:

- Our strategy of optimisation is based on optimising separately the fine and coarse granular skeletons. For each of them, the particle groups are mixed 3 by 3 starting from the coarsest to the finest particle group. The target is to decrease the intergranular porosity. To design the practical experimental plan we used Minitab 17® (statistical software) but any other statistical software can be used;
- The intergranular porosity was estimated by measuring the loose bulk and oven-dried densities of the particle groups;
- The optimisation method proposed relies on the densities of the material and is independent of the particle geometry. Hence, this approach might be useful and applicable for other types of seashells and bio-based materials;
- As previously discussed in chapter 2, the crushed seashells have a very particular geometry, which makes the normal sieving process not very adaptable. This leads to a certain inaccuracy of the particle size distribution and hence, greater variability of the granular skeleton;
- Either fine and coarse oyster shell granular skeletons had their intergranular porosity decreased round after round of optimisation probably associated with the filling rule (voids left by coarser particles are filled by smaller particles and so on). This corroborates the strategy chosen of mixing particles 3 by 3 from the coarsest to the smallest.

Once we obtained the oyster shell fine, coarse and global granular skeletons, we will move to the next step that is using this bio-based material to replace conventional aggregate in cementitious materials. In chapter 4, we will evaluate the effect of the optimisation method by comparing the intergranular porosity of other oyster shell granular skeletons and use them to replace sand in mortar.

CHAPTER 4 - OYSTER SHELL MORTAR OPTIMISATION AND FORMULATION

In this chapter we present a validation of the optimised oyster shell fine granular skeleton through a comparison with other types of fine oyster shell granular skeletons. After that, we will study the mechanical properties of mortars made with oyster shell granular skeletons and sand, testing two different strategies of formulations.

4.1 Oyster shell mortar skeleton optimisation: validation and comparison

To validate the optimisation method proposed, we compared the OSFA with three other types of oyster shell granular skeletons and conventional sand, from the same range of 0/4 mm. To simplify, the OS skeletons were named from OS 1 to OS 4. The OS 1 corresponds to the OSFA, the OS granular skeleton obtained from our optimisation method detailled in the chapter 3. The OS 2 is designed to contain a high amount of coarse particles. The OS 3 is designed to mimic the grading curve of the reference sand. The OS 4 is designed to contain a high amount of fine particles. The comparison parameter is the intergranular porosity as this is the key parameter of our granular skeleton optimisation strategy.

Figure 4-1 shows the particle size distribution of each granular skeleton studied (sand and OS 1-4). OS 3 has the same gradation curve of sand. OS 2 and OS 4 were designed to the two extremes, with a higher amount of coarse and fine particles respectively. In between these curves, the optimised aggregate OS 1 curve presents an inverted "S" shape if compared to the sand curve, with curves crossing around the particle group of 0.500/1 mm.

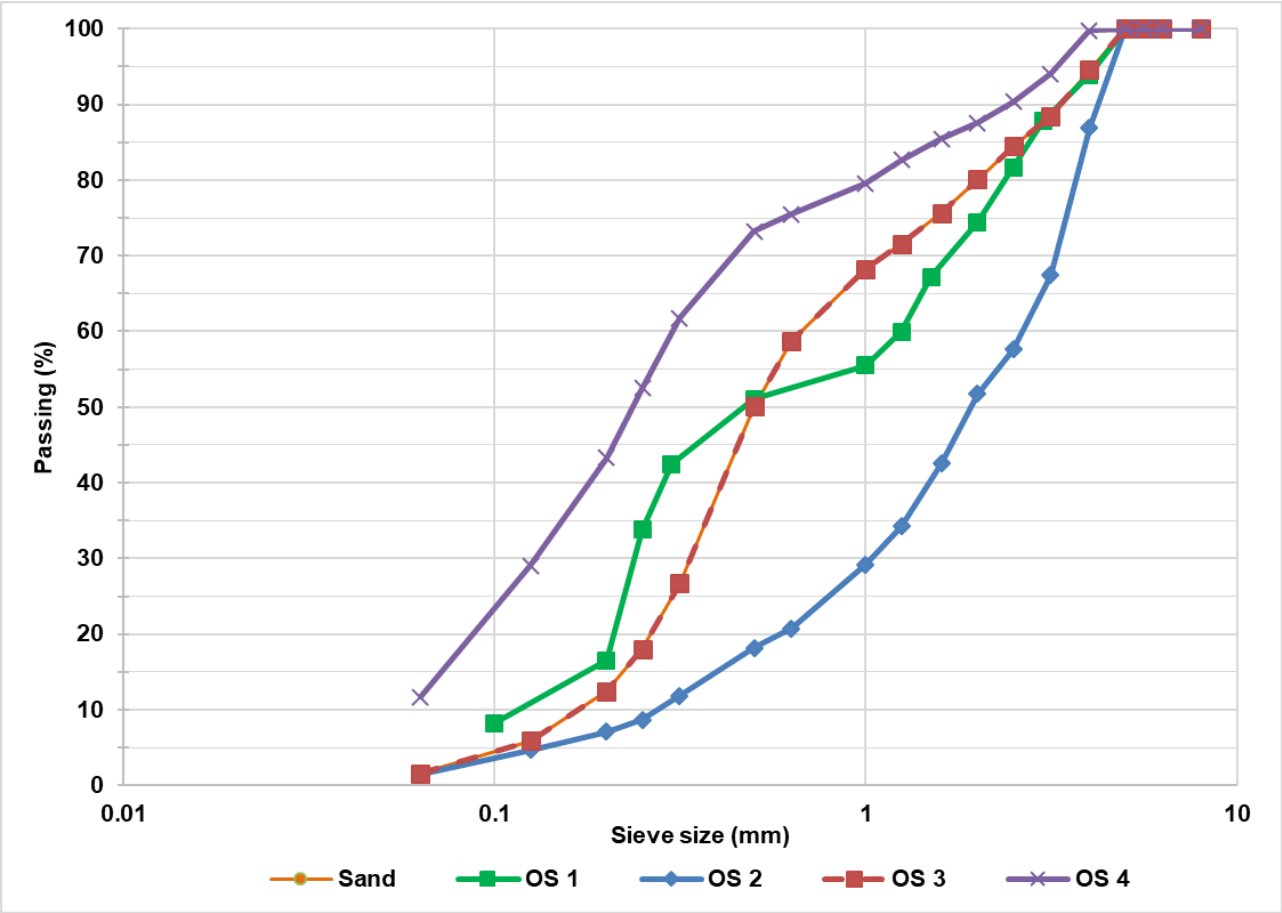

Figure 4-1 – Grading curves of the different aggregate skeletons (S - Sand; OS 1 – Optimised mixture (OSFA); OS 2: a higher amount of coarse particles; OS 3 – mimicking sand; OS 4 – higher amount of fine particles).

Table 4.1 shows the loose bulk and oven-dried densities and the intergranular porosity of sand and OS 1-4 aggregates skeletons. In terms of loose bulk and oven-dried densities, all OS skeletons are lighter than sand as their specific gravity is no higher than the sand (Yoon et al., 2003). The literature reference mentioned that oven-dried density for OS can vary between 1850 and 2480 kg/m^3, which are in line with the results found in this work (Eo and Yi, 2015; Kuo et al., 2013; Yang et al., 2010, 2005). The flaky and elongated shape affect directly the packing process, providing gaps in between the particles disturbing the granular arrangement (Mo et al., 2018).

Table 4.1 – Physical properties of the sand and the oyster shell granular skeletons (OS 1-4)

Material	Specification	Loose bulk density (kg/m^3)	Oven-dried density (kg/m^3)	Intergranular porosity (%)
S 0/4 mm	Sand	1462	2690	45.6
OS 1 0/4 mm	Optimised oyster shells granular skeleton (OSFA)	974	2123	54.1
OS 2 0/4 mm	Oyster shell granular skeleton with high amount of coarse particles	852	2160	60.6
OS 3 0/4 mm	Oyster shell granular skeleton mimicking sand grading curve	903	2463	63.6
OS 4 0/4 mm	Oyster shell granular skeleton with high amount of fine particles	840	2583	67.5

Sand skeleton presents the lowest intergranular porosity, which is expected because of its spherical particles shape that allows a better granular packing. Regarding the OS skeletons, the optimised OS 1 skeleton has the lowest intergranular porosity if compared to all of the other OS skeletons, which demonstrates the efficiency of the method proposed.

It is worth noting that OS 3, which simply mimics the sand grading, provides very poor performances in terms of intergranular porosity, even worse than the one obtained with OS 2, which was designed only for illustrative purposes. Therefore, careful attention should be taken in the transfer of grading curves from spherical particles to non-spherical particles and an optimisation scheme, as the one we propose in this thesis, should be preferred. OS 4 is also designed for illustrative purposes and shows the worse performances in terms of intergranular porosity. This is expected because it consists of an assembly of too many small particles that cannot respect the filling rule, which is the voids left by coarser particles will be filled by smaller particles and so on.

4.2 Oyster shell mortar formulation optimisation: methodology and validation

4.2.1 Key strategy points

To validate the potential replacement of sand per oyster shell granular skeleton, we decided to investigate the mechanical properties of mortars made with the OS aggregates (OS 1-4) and sand (for control). For this, we studied two types of formulation design strategies:

- The first formulation design strategy consists in investigating the effect of different granular skeletons and consequently, intergranular porosity, in a constant formulation. We considered as a constant formulation when the aggregate and cement paste volumes were kept the same in all formulations;
- The second formulation design strategy considers that a formulation can be optimised by increasing the cement paste content to fill the intergranular porosity of the granular skeleton. In this strategy, we also kept constant the aggregate volume. For this second strategy, only sand (S) and OSFA (OS 1) were used since they present the lower intergranular porosity among the granular skeletons studied. Different filling rates of the intergranular porosity were tested and the effect of this parameter on mortar's mechanical properties was investigated. The filing rate is the percentage of the intergranular porosity of the granular skeleton that is filled with cement paste.

In both strategies, the aggregate was replaced by volume, and the quantity of granular skeleton was obtained by multiplying the volume (that was constant) per the loose bulk density of each granular skeleton used.

4.2.2 Materials

The materials used in the mortar formulations are detailed in table 4.2. The sand was used to produce control samples and the four different types of oyster shell aggregates OS 1-4 to produce the four different OS mortars. The other granular skeletons were designed based in other types of composition like mimicking a conventional aggregate gradation curve (sand) and testing the extremes (with a higher amount of coarser/finer particle sizes).

Ordinary Portland cement, refers CEM I according to the standard NF EN 197-1, was chosen. We wanted to rapidly perform this initial investigation phase, which focuses on the comparison of aggregates and not the cement matrix. Therefore, cement with a higher clinker content that provides a final strength on 28 days was selected for the mortar formulations, although the goal

of this thesis is to produce a more environmentally-friendly material. The full performance study will be conducted on concrete using low clinker cement.

Table 4.2 – Physical properties of the materials used for mortars.

Material	Specification	Loose bulk density (kg/m^3)	Oven-dried density (kg/m^3)	Intergranular porosity (%)	WA_{24} (%)
Cement	CEM I 52.5 N - PM-CP2	-	3180	-	-
Sand 0/4 mm	Alluvial siliceous, washed and semi-crushed, S	1462	2690	45.6	1.2
OS 1 0/4 mm	Optimised oyster shells granular skeleton (OSFA)	974	2123	54.1	9.4
OS 2 0/4 mm	Oyster shell granular skeleton with high amount of coarse particles (OS 2)	852	2160	60.3	12.9
OS 3 0/4 mm	Oyster shell granular skeleton mimicking sand grading curve (OS 3)	903	2463	63.6	9.5
OS 4 0/4 mm	Oyster shell granular skeleton with high amount of fine particles (OS 4)	840	2583	67.5	6.2

4.2.3 First strategy: constant formulation (cement paste content and aggregate volume)

To design the constant formulation, we started with a reference formulation. The reference formulation was made with sand and followed the proportions of water, cement and aggregate (water/cement ratio of 0.5), suggested on the French Standard NF EN 196-1 – section 6.1. The aggregate volume and cement paste content of the sand formulation was used as the reference because the formulation was originally designed for that type of aggregate. Thus, when replacing the sand with the oyster shells, these volumes were kept constant and the aggregate replacement was done by volume.

The aggregate volume in the reference formulation (sand) is 0.923 l and the cement paste volume (cement + water) is 0.40 l. The aggregate volume was obtained by dividing its mass by the loose bulk density. It was chosen the loose bulk density because we need to consider the granular skeleton and the intergranular porosity, where the cement paste is going to ingress and fill it.

The cement paste volume was calculated by adding the (mass of water x density) with (mass of cement x density). In this case, we used the true density because we considered it as a liquid and therefore, with no intergranular porosity. Hence, using the sand aggregate volume as the reference for the oyster shell formulations, we can obtain the oyster shell granular skeleton mass by dividing this volume (0.923 l) per the corresponding loose bulk density. For all OS mortars, the replacement rate was 100%.

The reference mortar made with sand was identified as MS and the oyster shell mortars were identified as MOS 1-4 according to the type of granular skeleton used. The mortar formulations quantities are presented in table 4.3.

Table 4.3 – Mortar formulations for the first strategy – constant fomulation (granular skeleton and cement paste content volumes constant).

Mortar	W_{eff}/C	Cement paste (l)	Mix proportions (kg/m^3)						
			W	C	S	OS 1	OS 2	OS 3	OS 4
MS	0.50	0.37	225	450	1350	-	-	-	-
MOS 1			225	450	-	899	-	-	-
MOS 2			225	450	-	-	786.3	-	-
MOS 3			225	450	-	-	-	833.5	-
MOS 4			225	450	-	-	-	-	755.3

MS: mortar cast with sand; MOS 1-4: mortar cast with skeleton OS 1-4. W: water, C: cement, S: sand, W_{eff}/C: effective water/cement ratio.

4.2.4 Second strategy: formulation optimisation (aggregate volume constant, cement paste content increased to fill the intergranular porosity)

To optimize mortar formulation, we considered three factors:

- The first one is to decrease the intergranular porosity of the granular skeleton and this can be done by optimising its granular packing;
- The second one is to increase the binder content in order to surround all the aggregate particles, creating a solid and connected matrix;
- The third one is to increase the binder content to not only surround the aggregate's particles but also, to fill the voids in between these particle (intergranular porosity).

It was found that in the previous strategy, none of the formulations had enough cement paste content to fill all the voids of the granular skeletons studied (volume of voids > volume of cement

paste). Therefore, the second strategy comes up to observe the influence of filling rates in the formulations in terms of intergranular porosity filled, allowing a better understanding between the different mortars performances, especially in term of mechanical performances comparison.

So, considering that an optimised formulation is also made of an optimised aggregate, only sand and OS 1 were used in this second campaign. The cement paste content of mortars was calculated to fill the intergranular porosity at different rates until 100%. The volume of voids in the granular skeleton is obtained by multiplying the skeleton volume per the intergranular porosity. It was supposed that intergranular porosity was not intruded by cement paste, so this porosity was not considered. For a filling rate of 100%, the cement paste volume is equal to the voids volume in the granular skeleton. For lower rates than 100%, the cement paste volume can be obtained by multiplying the desired filling rate per the voids volume in the granular skeleton.

For mortars with sand, two filling rates were tested: 87.2% (formulation MS 87.2% – start formulation based of NF EN 196-1) and 100% (formulation MS 100%). For mortar with OS1 (OSFA), three rates of filling were tested: 64.7% (formulation MOS 1 64.7%); 73.5% (formulation MOS 1 73.5% - tested in the previous campaign) and 100% (formulation MOS 1 100%). The mortars formulations are presented on the table 4.4.

Table 4.4 - Mortars formulations for the formulation optimisation strategy.

Mortar	W/C	Cement paste (l)	Mix proportions (kg/m^3)				Filling rate (%)
			W	C	S	OS 1	
MS 87.2%	0.50	0.37	225.0	450.0	1350	-	87.2
MS 100%		0.42	258.5	516.9	1350	-	100
MOS 1 64.7%		0.32	198.3	396.6	-	899	64.7
MOS 1 73.5%		0.37	225.0	450.0	-	899	73.5
MOS 1 100%		0.50	306.4	612.7	-	899	100

MS 87.2%: mortar cast with sand for a filling rate of 87.2%. MS 100%: mortar cast with sand for a filling rate of 100%. MOS 1 64.7%: mortar cast with oyster shell optimised granular skeleton for a filling rate of 64.7%. MOS 1 73.5%: mortar cast with oyster shell optimised granular skeleton for a filling rate of 73.5%. MOS 1 100%: mortar cast with oyster shell optimised granular skeleton for a filling rate of 100%. W: water, C: cement, W/C: water/cement ratio.

4.2.5 Particularity of oyster shell mortar mixing

The mortar mixing and casting procedures were performed as recommended on the French standard NF EN 196-1 (2016), sections 6.2 and 7.2 respectively.

The procedure of aggregate preparation was adapted. Due to the high water absorption coefficient of the oyster shell aggregates (about 8 times more than the siliceous sand), aggregate used for mixing were pre-saturated. To keep the same procedure for all mortars, this saturation process was also applied to the conventional aggregate (sand). For this preparation, aggregates were dried at 80ºC until constant mass, weight and stored in hermetic bags before casting. The estimated water corresponding to the aggregates absorption was calculated from the water absorption coefficient and this quantity was added to each bag 24 hours before casting (Fig. 4-2). The effective water was added at the moment of the mixing.

The mixing procedure started by placing cement and efficace water in the mortar mixer bowl and mixed at low speed for 30 seconds. After that, the aggregate was added steadily for 30 seconds. Then, the mixer was switched to high speed for additional 30 seconds. After that, the mixer is stopped for about 90 seconds and the mortar adhering to the wall was scrapped. After that, the mixer is restarted for more 60 seconds on high speed.

Prismatic samples (40 x 40 x 160 mm) were cast, covered with a plastic bag and demoulded after 24 hours (Fig. 4-3). Then, the samples were immersed in a water tank until the date of the mechanical testing for water curing.

Figure 4-2 – Saturation of aggregate in hermetic bags 24 hours before mixing.

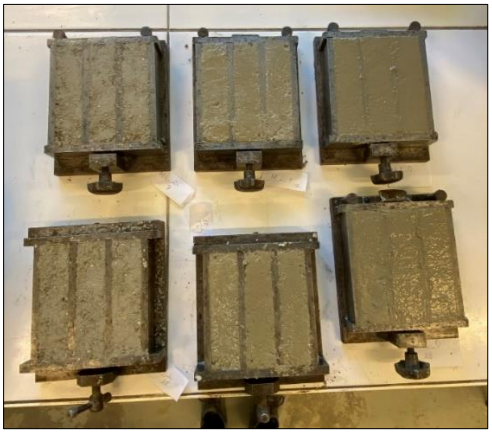

Figure 4-3 – 40 x 40 x 160 mm moulds filled with fresh mortar just after mixing.

4.3 Experimental results

4.3.1 Comparison for constant cement paste content formulation

In the first strategy, we aimed to investigate the effect of 100% replacement of sand by the oyster shell aggregates (OS 1-4) in a constant formulation, i.e a formulation with a constant paste volume). Figure 4-4 shows the compressive strength at 7 and 28 days of the tested mortars.

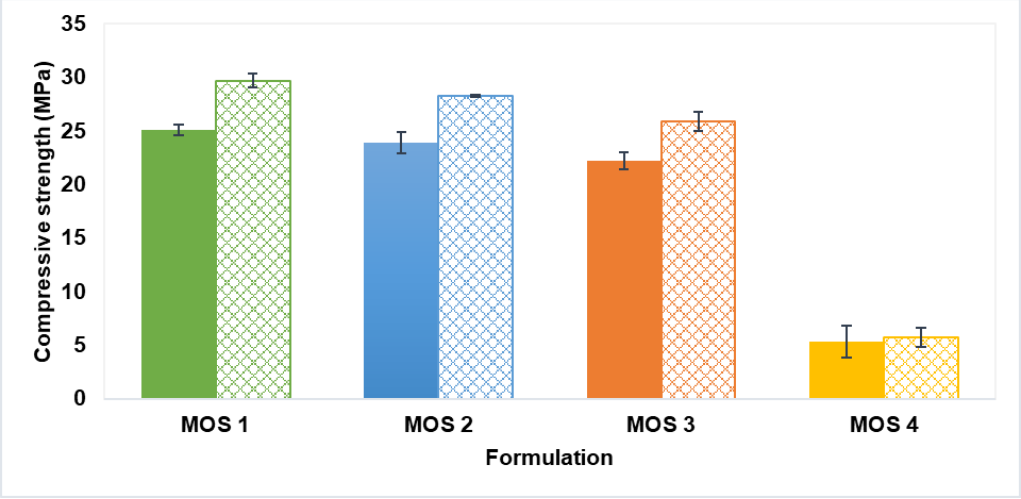

Figure 4-4 – Compressive strength (MPa) per Oyster shell mortar formulation at 7 (fully shaded) and 28 days (cross-hatch). Results for sand mortar: 45.4 ± 1 MPa for 7 days and 59.1 ± 1 MPa for 28 days.

MS is the reference formulation made with sand. MS is the most resistant formulation (45.4 ± 1 MPa at 7 days and 59.1 ± 1 MPa at 28 days) and MOS 1 is the most performing for OS aggregate mixtures. It can be seen an evolution in compressive strength from 7 to 28 days for all formulations, with a greater increase for formulations MOS 1 and MOS 2 (about 18%), then MOS 3 with an increase of about 16% and the lowest increase of about 8% for MOS 4.

It can be noticed a sharp decrease in performance for MOS 4 (about 80% at 28 days), while a slight decrease from MOS 2 to MOS 3 (about 9% at 28 days) is observed. The drop in mechanical performance of MOS 4 is related to the poor particle packing of OS 4, which lead to a higher intergranular porosity of this granular skeleton. In addition to that, the mortar formulation used was designed for spherical aggregates (sand) and due to the oyster shell shape, an adaptation to the formulation may also be necessary. This was further investigated in the second strategy studied.

4.3.2 Validation of the optimisation of the cement paste content

As previously discussed, formulation optimisation by filling intergranular porosity with cement paste was the second strategy applied. Mortars were produced with the two most performing granular skeletons in terms of intergranular porosity (sand and OS 1) and different filling rates were studied. Compressive and flexural strength were analysed at 7 and 28 days for mortars made with sand at 87.2% and 100% filling rates (MS 87.2% and MS 100%); and with OS 1 at 64.7%, 73.5% and 100% filling rates (MOS 1 64.7%, MOS 1 73.5% and MOS 1 100%).

Figure 4-5 shows the results of compressive strength at 7 and 28 days for MS mortars with 2 different filling rates, 87.2 % and 100 %. It can be seen an increase of about 30% for MS – 87.2% and 34% for MS – 100% in compressive strength from 7 to 28 days. As previously discussed, the difference between these two formulations is the filling rate. As a consequence of the filling rate, we also can see an evolution in compressive strength from MS 87.2% to MS 100%. This evolution in compressive strength is approximately 2% at 7 days and 6% at 28 days.

Figure 4-6 shows the results of compressive strength at 7 and 28 days for MOS 1 mortars with three different filling rates, 64.7%, 73.5% and 100%. It can be seen an increase in mortar compressive strength as the filling rate tends to 100%. The increase in compressive strength from MOS 1 64.7% to MOS 1 100% is about 51% at 28 days. This evolution in compressive

strength following the increase of the filling rate demonstrates the importance of this strategy to improve mechanical performance and should be further investigated.

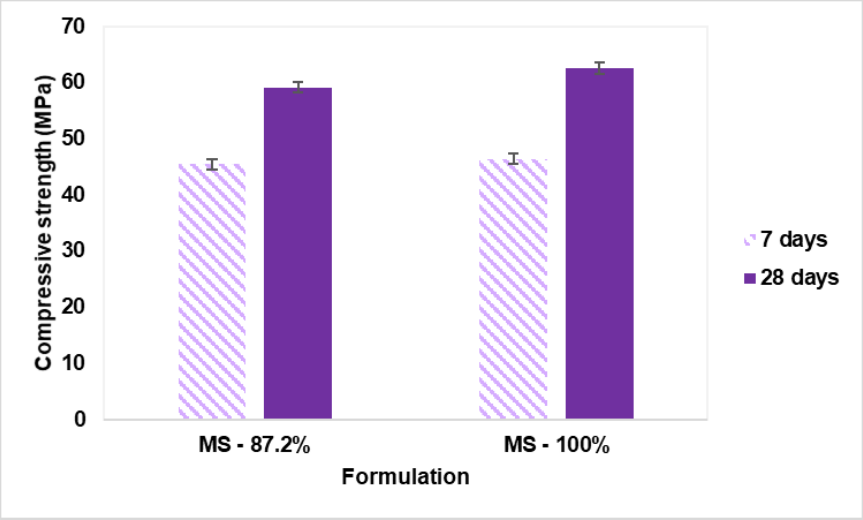

Figure 4-5 – Compressive strength (MPa) of MS – 87.2% and MS - 100% at 7 and 28 days.

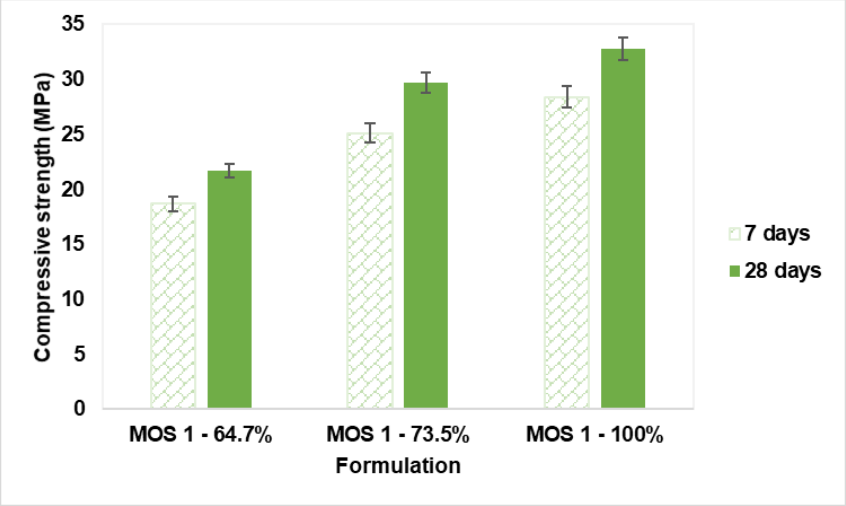

Figure 4-6 – Compressive strength (MPa) of MOS 1 – 64.7%, 73.5% and 100% at 7 and 28 days.

Figure 4-7 shows the results of flexural strength at 7 and 28 days for MS 87.2% and MS 100%. It can be seen for both formulations an evolution in flexural strength from 7 to 28 days. It can be noticed that the flexural strength increases about 5% for both 7 and 28 days results when

the filling rate pass from 87.2% to 100%. This result is also similar to those found for compressive strength.

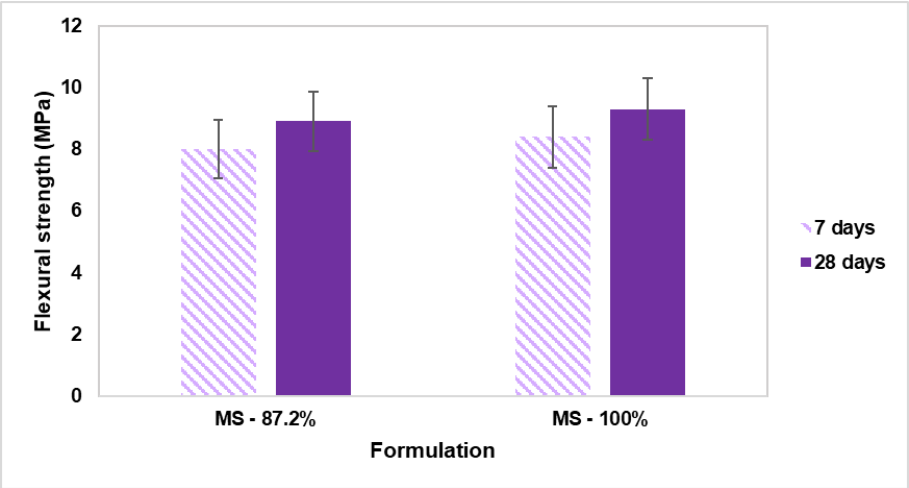

Figure 4-7 – Flexural strength (MPa) of MS – 87.2% and 100% at 7 and 28 days.

Figure 4-8 shows the results of flexural strength at 7 and 28 days for MOS 1 64.7%, MOS 1 73.5% and MOS 1 100%. The flexural strength of these mortars also increases with age (from 7 to 28 days) and also as the filling rate goes towards 100%. It can be noticed an increase of approximately 34% in flexural strength from MOS 1 64.7% to MOS 1 100%.

Note that either compressive or flexural strength, the evolution in strength from 7 to 28 days was more expressive than for mortars made with sand. This can suggest that somehow that can have an interaction between the oyster shells and the cement paste slowing down the cement reactions. (Kuo et al., 2013) suggests that due to the organic matter and the large pores of oyster shells (leading to higher water absorption coefficient), the cement hydration and the initial setting time are decreased.

Additionally, the MOS 1 100% provides similar performance in terms of flexural strength compared to the sand mortars (MS 87.2% and MS 100%). The possible reasons for that are related to the intergranular porosity filled in the MOS 1 (100%) and the shell's orientation on the mortar sample (further discussed in chapter 5).

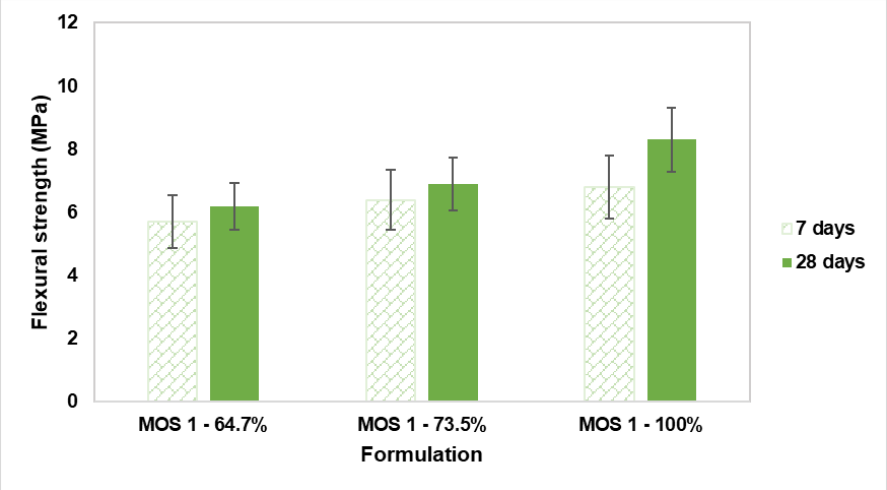

Figure 4-8 – Flexural strength (MPa) of MOS 1 – 64.7%, 73.5% and 100% at 7 and 28 days.

An evaluation of these data suggests that the mortar's mechanical performance (compressive and flexural strengths) is not related only to the aggregate characteristics but also to cement paste content in the formulation. The cement paste must be enough to coat the particles, providing the bond and cohesion of the matrix (aggregate + cement paste) and filling the intergranular porosity. As we could see in the previously discussed results, the best mechanical results are found when the intergranular porosity is 100% filled, especially in the case of the oyster shell mortars.

An interesting observation was seen while performing the compressive test on specimens of mortars made with oyster shells (Fig. 4-9). When loading the sample during the compressive test, the cracks start at the centre of the specimen progressing towards the extremities. This behaviour resulted in a deformation of the centre of the specimen being similar to a crushing action than actually a fracture like in sand mortars.

(Yoon et al., 2004) also observed a similar effect during the compressive strength test on the mortars with oyster shells studied. The fractures in these mortars started at the centre of the specimen and progressed to the outer edges before reaching failure. The authors also observed that the shear failure plane was coincident with the region where there was a high concentration of oyster shells.

This will be further investigated in the group in another PhD thesis in the group.

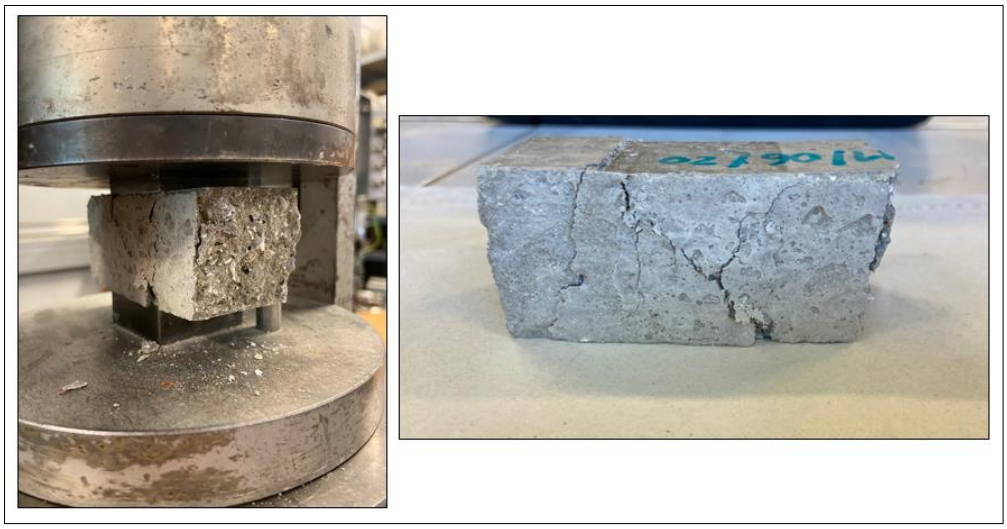

Figure 4-9 – MOS 1 specimen after compressive test. Effect on crushing the sample instead of fracturing.

4.4 Toward a new method for cementitious material design

Cement is known for its environmental impact (especially the carbon footprint) due to the clinker manufacturing process. To decrease the environmental impact of cementitious materials, cement with high clinker content should be avoided when possible, and the cement content should be optimised to the minimum necessary to obtain the desired properties. Especially for bio-based materials, we could see the importance of filling the intergranular porosity of the oyster shells mortars to increase the mechanical performance.

From the previous results in compressive strength discussed in this chapter, we could identify a possible trend between the intergranular porosity filled and the compressive strength results. Figure 4-10 gathers the results of MS and MOS 1 at the different filling rates up to 100%. The normalised compressive strength was obtained by dividing the compressive strength at different filling rates by the compressive strength at a filling rate of 100%, for MS and MOS 1 separately. Therefore, the compressive strength with 100% of voids filled for MS or MOS 1 is the maximum 1. The other filling rates studied presents values under 1.

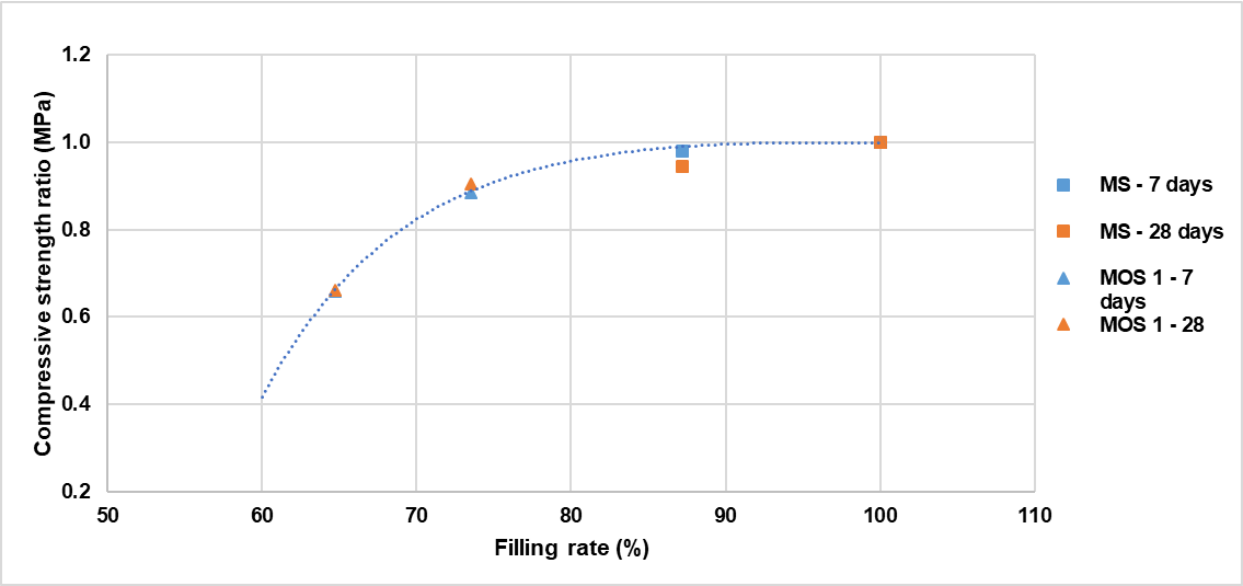

Figure 4-10 – Normalised compressive strength for mortars in function of the filling rate.

The blue dotted line in figure 4-10 suggests that the compressive strength (performance) can be predicted according to the filling rate in the formulation. This potential relationship brings an interesting discussion in terms of formulation optimisation and environmental impact. The formulation optimisation approach considered in this work is a combination of low intergranular porosity and a cement paste content enough to fill the voids between the aggregates particles. According to this approach, as the particle packing is improved, less binder is needed. Therefore, the possibility of estimating the cement content to obtain just the performance seek, neither more nor less, might reduce significantly the number of materials used and hence, the environmental impact (for instance, climate change and resource depletion). This remains an initial study and further investigation must be carried out by testing different filling rates and different type of aggregates to confirm this trend and broaden this application to other bio-based aggregates.

4.5 Concluding remarks

A prior investigation of the effect of fully replacing sand with different oyster shell fine aggregates (OS) was carried out in this chapter. Firstly, we aimed to validate the optmisation methodology presented in the chapter 3 by comparing the optimised oyster shell granular skeleton to other OS granular skeletons and sand. The oyster shells granular skeletons and

sand were used to produce mortars in different formulation strategies. The first stategy was focused on a constant formulation, just replacing the aggregate by volume. The second strategy investigated different filling rates with mortars made with sand and OS 1. From this last strategy we could observe an interesting trending correlating the compressive strength and the filling rate of formulations. Therefore, some conclusions obtained from the study presented in this chapter are summarised as follow:

- Comparing the intergranular porosity of all OS granular skeletons studied (OS 1 to OS 4), the optimised skeleton OS 1 presented the lowest intergranular porosity among them. From OS 4 to OS 1, we found a relative decrease in intergranular porosity of approximately 20%, confirming the importance of the chosen optimisation process;
- From the granulometric distribution and correlation to the intergranular porosity, a tendency of increasing intergranular porosity of OS granular skeletons when particles are not proportionally distributed is noted;
- The traditional approach of optimisation (mimicking a reference-grading curve - sand in the case) showed to not be suitable for oyster shells because it increases the intergranular porosity of the aggregate (OS 3) by approximately 18% compared to the optimised granular skeleton (OS 1);
- From the first strategy used, we could conclude that the granular skeleton optimisation impacts the mechanical performance (decrease in 80% of compressive strength from MOS 1 to MOS 4). Additionally, the type of aggregate and its particularities must be taken into account when designing a formulation;
- From the second strategy, we could conclude that the filling rate of the formulation affects directly the mechanical properties, especially in the case of the oyster shell mortars (an increase of 51% from MOS 1 64.7% to MOS 1 100%). Additionally, MOS 1 100% presented similar flexural strength to MS at 28 days (8.3 ± 1 MPa for MOS 1 100% and 9.3 ± 1 MPa for MS 100% at 28 days);
- The mechanical performances of MOS 1 demonstrate that a full substitution of conventional aggregate by oyster shell ones could be envisaged.

Once presented the validation of the oyster shell granular skeleton optimisation and its use to produce mortar, we will continue this study and present the results of a concrete made with oyster shell granular skeleton in the chapter 5.

CHAPTER 5 - CHARACTERISATION OF THE OYSTER SHELL CONCRETE PROPERTIES

Progressing in the study of the oyster shell as aggregate replacement in cementitious materials, in this chapter we are going to evaluate some mechanical and durability properties of concrete made with 100% of replacement of fine and coarse aggregates per crushed oyster shells and two other formulations made with conventional aggregates.

5.1 Designing the concrete formulations studied

In this section, we are going to detail the three concrete formulations studied, being two made with conventional aggregates (sand and gravel) and another made with 100% of oyster shells replacing conventional aggregates (fine and coarse). All formulations were designed for meeting the requirements for self-compacting concrete.

Table 5.1 shows the description of the acronym used to identify each concrete studied. The CAC – PA formulation was formulated according to the traditional prescriptive approach based on the NF EN 206/CN and using conventional aggregates (sand and gravel). The OSC was formulated with the optimised oyster shell granular skeletons to replace (by volume) 100% of fine and coarse conventional aggregates based on the formulation CAC - PA. The CAC – NPA was formulated with conventional aggregates but with a different cement content beyond the NF EN 206/CN recommendations.

Table 5.1 - Identification of the concrete formulations studied.

ID	Meaning	Sub-section
CAC - PA	**C**onventional **A**ggregate **C**oncrete - **P**rescriptive **A**pproach	5.1.1
OSC	**O**yster **S**hell **C**oncrete	5.1.2
CAC - NPA	**C**onventional **A**ggregate **C**oncrete - **N**on-**P**rescriptive **A**pproach	5.1.3

5.1.1 Conventional Aggregate Concrete – Prescriptive Approach (CAC - PA)

To design the formulation composed of conventional aggregate and following the prescriptive approach, we based on the formulation recommendations of the table NA.F.1 (limits values applicable to France) of the NF EN 206/CN. The target was a formulation to meet the criteria of the environmental exposure class XS3 (corrosion induced by chlorides from sea water – Tidal, spray and splash zones). This environmental exposure class was chosen because of the context of the project which aims to develop concrete to be used in the marine environment, more precisely in the Arcachon Bay or close region. Therefore, for XS3 class, the effective water/cement ratio (w_{eff}/c) of 0.50, resistance class of C35/45, and minimum cement content of 350 kg/m^3 plus an extra 10% due to the size of the biggest aggregate used (D ≤ 12.5 mm) were considered in the formulation.

To start the concrete formulation design, we used as reference a traditional self-compacting concrete formulation already used and tested in the laboratory of ISA BTP, UPPA. Then, we increased the cement content to meet the minimum cement content specified for XS3. Additionally, we also increased the siliceous filler content and superplasticizer in the formulation in order to reach the self-compacting concrete properties limiting the cement content. We did not use any concrete software for designing this formulation and we only carried out practical tests in the laboratory to adapt the formulation to the requirements needed.

The cement content was fixed at 385 kg/m^3 and the w_{eff}/c ratio at 0.5. The siliceous filler was used to attend fresh properties for self-compacting concrete without the need to increase even more the cement content. The coarse/fine aggregate ratio was 0.98 (49% of coarse and 51% of fine aggregate). The materials specification used to produce the CAC – PA are detailed in table 5.2 and the aggregate's physical properties are shown in table 5.3.

Table 5.2 – Materials used for producing the CAC – PA (specification and properties)

Material	Specification	Loose bulk density (kg/m^3)	Oven-dried density (kg/m^3)	Intergranular porosity (%)	Water absorption coefficient (WA_{24} - %)
Sand 0/4 mm	Alluvial siliceous, washed and semi-crushed	1462	2690	45.7	1.2
Gravel 4/10 mm	Limestone, crushed	1538	2700	43.0	0.2
Cement*	CEM V/A (S-V) 42.5 N	-	2920	-	-
Filler*	Siliceous	-	2650	-	-
Superplasticizer	MasterEase 3000	-	1070	-	-

*The cement used is CEM V/A 42.5 N, composed of 56% of clinker, 22% of slag and 22% of fly-ash. The siliceous filler used is composed of 99.1% SiO_2, average diameter d_{50} of particles is 35 µm.

Table 5.3 – Additional information of the granular skeleton of the CAC - PA (49% gravel 4/10 mm + 51% sand 0/4 mm).

Loose bulk density (kg/m^3)	Oven-dried density (kg/m^3)	Intergranular porosity (%)	Granular skeleton volume (m^3)
1858	2695	31.1	0.914

To design the next formulations, we decided to keep a constant parameter among them. This parameter was the volume of the granular skeleton and the effective water /cement ratio (w/c) of 0.5. As we started with a conventional aggregate formulation, we decided to keep the granular skeleton volume of this formulation (CAC – PA) for the next formulations. The granular skeleton volume can be calculated by the sum of the mass of the granular skeleton (sand + gravel) divided by the loose bulk density of this granular skeleton. It was used the loose bulk density because we aimed to know the total volume of aggregates + intergranular porosity (voids). Thus, we found a granular skeleton volume of 0.914 m^3, which was used as the constant parameter to design the next formulations. Therefore, the CAC – PA formulation presented in table 5.4 is for a granular skeleton volume of 0.914 m^3.

Table 5.4 – CAC– PA formulation (real quantities used in the laboratory) for a granular skeleton volume of 0.914 m^3.

Material	Quantity	Unit
Gravel 4/10 mm	840.3	kg
Sand 0/4 mm	857.5	kg
Filler	150	kg
Cement CEM V/A	385	kg
Superplasticizer	1.7	% (C+F)*
Effective water	192.5	l

* (C + F) is the sum of Cement plus Filler content

5.1.2 Oyster Shell Concrete (OSC)

To design the oyster shell concrete, it is important to point out a few things:

1) We aimed to replace 100% of fine and coarse aggregates with crushed oyster shells. However, the NF EN 206/CN does not specify any threshold for replacing conventional aggregates per crushed seashells or bio-based materials. Therefore, doing this replacement implies that the concrete is placed beyond the traditional prescriptive approach. Hence, the performance-based approach is used to evaluate the OSC properties, especially the durability;
2) As previously discussed, the constant parameter for all concretes is the granular skeleton volume and the water effective/cement ratio of 0.5. Due to the lighter density of oyster shells, the granular skeleton was replaced by volume and not mass;
3) As previously studied in the mortar study (chapter 4), the oyster shell granular skeleton has a higher intergranular porosity than the conventional aggregate granular skeletons. In order to counterbalance this, the cement paste content (cement + filler + water) was increased to achieve the desired fresh properties of self-compacting concrete and limit losses in mechanical and durability performance;
4) Still relying on the mortar study, we chose to limit the amount of cement paste content just enough to achieve the properties sought, and avoid losing the environmental benefits of using a recycled bio-based material by the high amount of cement in the concrete.

Once establish these points, we proceed with the formulation design. The OS granular skeleton mass was estimated by multiplying the granular skeleton volume (0.914 m^3) per

the loose bulk density of the optimised fine aggregate OSFA + optimised coarse aggregate OSCA, which granular skeletons were optimised in the previous chapter. The total granular skeleton mass was approximately 932.3 kg and the proportion between OSFA and OSCA is simply found by multiplying the optimal proportions obtained during the optimisation process shown in chapter 3 for each aggregate. Table 5.5 shows a summary of the OSFA and OSCA physical properties and proportions obtained on the optimisation process.

Table 5.5 – Summary of the OSFA and OSCA aggregates physical properties and proportions.

Loose bulk density (kg/m^3)	**Oven-dried density (kg/m^3)**	**Intergranular porosity (%)**	**Granular skeleton proportion (%)**	
			OSFA	**OSCA**
1020	2150	53	61.9	38.1

Table 5.6 shows the materials specifications used in the Oyster Shell Concrete. Table 5.7 presents the OSC formulation designed for a granular skeleton volume of 0.914 m^3 with the real quantities used in the laboratory for the concrete batch.

Table 5.6 – Materials used for producing the OSC (specification and properties).

Material	**Specification**	**Loose bulk density (kg/m^3)**	**Oven-dried density (kg/m^3)**	**Intergranular porosity (%)**	**Water absorption coefficient (WA_{24} - %)**
OSFA 0/4 mm	Crushed oyster shells	974	2123	54.1	9.4
OSCA 4/10 mm	Crushed oyster shells	777	2194	64.6	6.3
Cement	CEM V/A (S-V) 42.5 N	-	2920	-	-
Filler	Siliceous	-	2650	-	-
Superplasticizer	MasterEase 3000	-	1070	-	-

Table 5.7 – OSC formulation (real quantities used in the laboratory) for a granular skeleton volume of 0.914 m^3.

Material	Quantity	Unit
OSCA 4/10 mm	355.7	Kg
OSFA 0/4 mm	576.6	Kg
Filler	178.4	Kg
Cement CEM V/A	457.8	Kg
Superplasticizer	1.8	% (C+F)*
Effective water	228.9	l

* (C + F) is the sum of Cement plus Filler content

5.1.3 Conventional Aggregate Concrete – Non-Prescriptive Approach (CAC – NPA)

As the OSC goes beyond the prescriptive approach in terms of formulation content, we decided to investigate another concrete with conventional aggregates (sand and gravel) that also does not meet completely the requirements of the traditional prescriptive approach.

To design this concrete, we kept the same granular skeleton volume (0.914 m^3) and the effective water /cement ratio of 0.5, but we decreased the cement paste content. The granular skeleton used was the same as the CAC – PA, as well as the coarse/fine aggregate ratio of 0.98. As this new formulation does not fit in any environmental class proposed in the table NA.F.1 of NF EN 206/CN, we named it as Conventional Aggregate Concrete – Non-Prescriptive Approach (CAC – NPA).

The materials specification used for this concrete are the same as the CAC – PA and were presented in table 5.2 and 5.3. The CAC – NPA formulation for a granular skeleton of 0.914 m^3 is presented in table 5.8.

Table 5.8 - CAC – NPA formulation (real quantities used in the laboratory) for a granular skeleton volume of 0.914 m^3.

Material	Quantity	Unit
Gravel 4/10 mm	840.3	kg
Sand 0/4 mm	857.5	kg
Filler	119.3	kg
Cement CEM V/A	306.2	kg
Superplasticizer	1.9	% (C+F)
Effective water	153.1	l

* (C + F) is the sum of Cement plus Filler content

5.1.4 Concrete mixing protocol

A concrete mixer machine hydraulic of 100 l capacity was used to mix the concrete formulations. The materials were introduced in the concrete mixer in the following order: coarse aggregate, filler, cement and fine aggregate. The water content and water absorption coefficient of the aggregates were taken into account to adjust the mixing water (based on the effective w/c ratio). Conversely from the procedure adopted for the mortar batching (the OS aggregate was dried and previously saturated before batching), this procedure was not kept for producing the OS concrete. The greater quantity of concrete aggregates made it unfeasible to keep this process. Hence, the water absorbed by the oyster shell granular skeleton was added during the batching. The superplasticizer was mixed with the mixing water used in the batch. Figure 5-1 shows part of the materials preparation for the oyster shell concrete batch.

The mixing protocol started by mixing the “dry” materials for 2 minutes in the concrete mixer. Then, water was introduced slowly and regularly around the mixer at a constant speed for 1 minute. After this, the mixer was stopped for a quick hand mixing with a trowel to assure there were no spots with hidden dry materials. Then, the concrete mixer restarted and the concrete was mixed for about 3 minutes. The fresh state tests were carried out straight after the end of the concrete mixing.

It was used cylindrical cardboard moulds of 110x220 mm and metallic moulds of 100x100x400 mm for casting the specimens needed for mechanical and durability tests. After casting the specimens, they were covered at room temperature and demoulded after 48 hours. The 48 hours was necessary because the OSC was not completely set for demoulding after 24 hours.

After demoulding, they were placed in a water tank to water curing until the test day (it was used tap water in the water tank).

The 110x220 mm cylindrical specimens were used for compressive strength, elasticity modulus and splitting tensile strength tests. The sawn cylindrical specimens (110x50 mm) were used for gas permeability, chloride diffusion, carbonation and capillary water absorption tests. Smaller specimens obtained from the cylindrical specimens were used on the porosity accessible to water test. The prismatic samples were used for the flexural strength test.

Figure 5-1 – Materials preparation for the OSC batch.

5.1.5 A hindsight analysis of the concrete formulations

5.1.5.1 Filling rate of the granular skeleton voids

The mortar investigation led in chapter 4 demonstrated the importance of filling the intergranular porosity to achieve better mechanical performances and hence, durability.

In the previous chapter, we could estimate the intergranular porosity filled in each formulation by calculating the cement paste volume and the intergranular porosity of the granular skeleton in volume (volume of voids). We considered that the cement paste includes the cement, filler, water and superplasticizer. The cement paste volume is estimated by a correlation between these material's quantities and their true density. The apparent volume of the granular skeleton multiplied by its intergranular porosity can estimate the volume of voids in the granular skeleton. After obtaining these two values (volume of voids and volume of cement paste), the filling rate

can be estimated for a given formulation. Table 5.9 shows the filling rate for CAC – PA, OSC and CAC – NPA.

Table 5.9 – Hindsight analysis of the concrete's intergranular porosity filling rate based on the formulations in tables 5.4, 5.7 and 5.8.

	CAC - PA	OSC	CAC - NPA
Cement paste volume (m^3)	0.390	0.464	0.311
Volume of voids in the granular skeleton (m^3)	0.284	0.484	0.284
Surplus of cement paste (m^3)	0.106	0	0.03
Voids filled by cement paste (%)	137	96	109

It can be seen that for the same granular skeleton type and volume of voids (formulations type CAC), the voids are completely filled by the cement paste and there is a surplus of cement paste. The surplus is found by doing the volume of cement paste minus the volume of voids. For the formulation CAC – PA, the voids in the granular skeleton are 100% filled, and there is a surplus of 0.106 m^3 of cement paste, resulting in a total volume filled of 137%. For the formulation CAC – NPA, the voids are also 100% filled by cement paste and there is a surplus of 0,03 m^3 of cement paste, resulting in a total volume filled of 109%. It is important to note that the cement paste volume was reduced by about 21% for the CAC – NPA and yet, fill the voids of the granular skeleton.

We can also see that the OSC formulation designed is filling 96% of the voids and not 100%. This means that the cement paste volume is not enough to completely fill the voids between the particles nor provide the surplus seen in the CAC formulations. Ideally, the cement paste volume should be increased to fill 100% of the intergranular porosity. Also, for a fair comparison of performance in the hardened state among the three concretes; they should have the same total volume of voids filled (for example: 137% for CAC - PA, OSC and CAC - NPA).

Figure 5-2 illustrates the volume of granular skeleton and cement paste (when surplus) for the CAC – PA, OSC and CAC – NPA. Firstly, it is important to highlight that all formulations were designed for the same apparent granular skeleton volume of 0.914 m^3. However, in function of a surplus of cement paste or not, the final apparent concrete volume might change. So now, we are going to analyse each concrete formulation in terms of final apparent concrete volume.

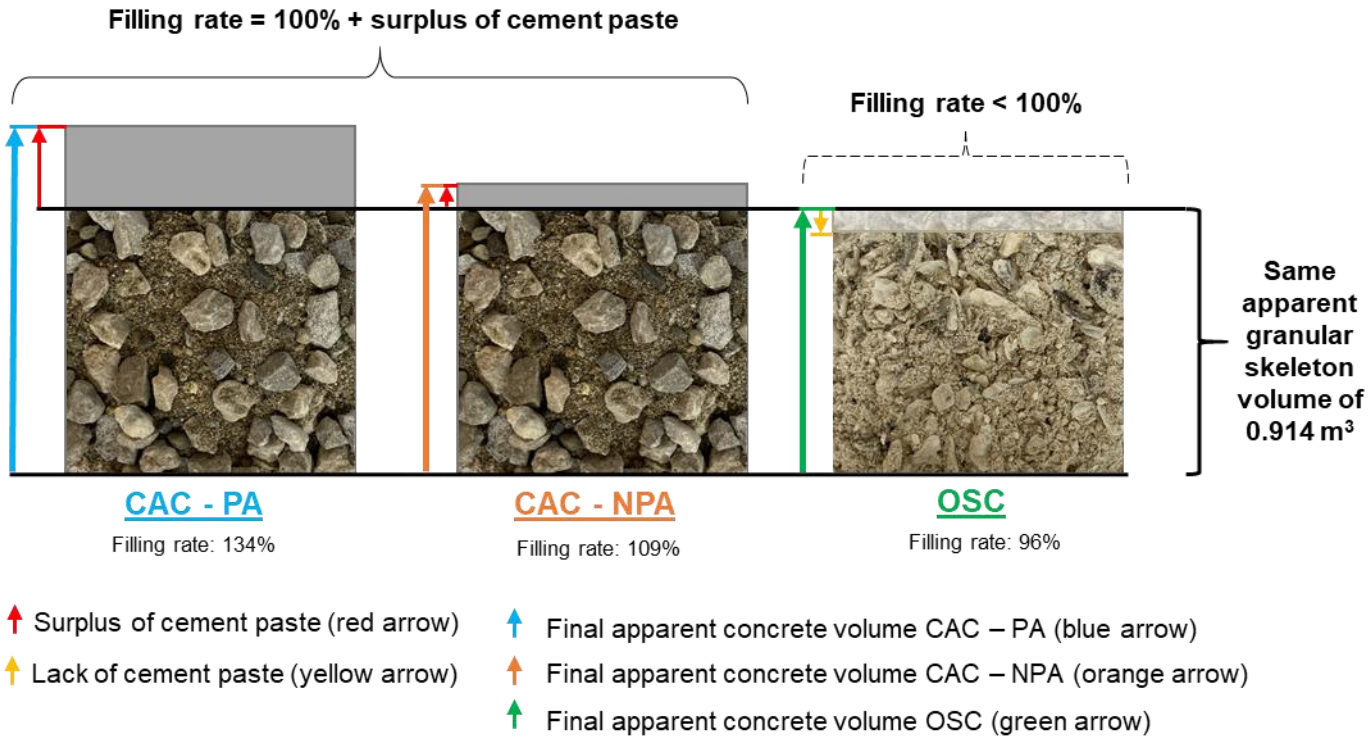

Figure 5-2 – Diagram of the repartition of granular skeleton and the cement paste for CAC – PA, CAC – NPA and OSC, by filling rate equal or less than 100%. The three concretes have the same granular skeleton volume of 0.914 m^3 and different filling rates. The arrows in blue, orange and green show the final apparent concrete volume.

CAC – PA and CAC - NPA

In the case of CAC – PA and CAC – NPA, we can see that the volume of cement paste fills all the voids in the granular skeleton and still provides a surplus. Therefore, the volume of voids is smaller than the volume of cement paste.

For didactic purposes, the surplus of cement paste is showed as the extra grey part over the top of the granular skeleton in Figure 5.2. Although the granular skeleton volume is constant in these formulations (0.914 m^3), the final volume of concrete is variable according to the surplus of cement paste that will be present.

The surplus of cement paste is estimated by substracting the volume of voids from the total volume of cement paste. Therefore, to obtain the apparent concrete volume, we add the volume of the granular skeleton (that includes the fine and coarse aggregates, and the voids filled with cement paste) plus the surplus of cement paste.

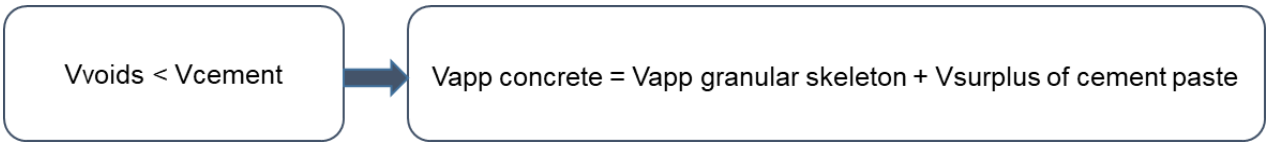

OSC

In this case, the volume of voids in the granular skeleton was not 100% filled. Therefore, all the cement paste content will fill the voids in the granular skeleton but it will not be enough, resulting in a lack of 4% of voids remaining empty in the granular skeleton. However, in this case when the voids are not 100% filled, the final apparent concrete volume is equal to the apparent volume of the granular skeleton.

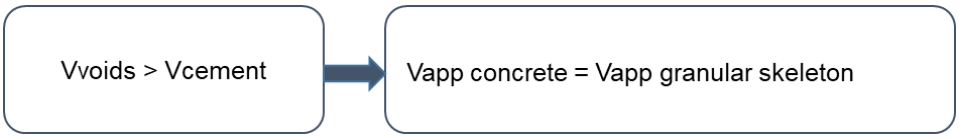

5.1.5.2 CAC – PA, OSC and CAC – NPA formulations for 1 m^3 of apparent concrete volume

As previously discussed, although CAC – PA, OSC and CAC – NPA were designed based in the same apparent granular skeleton volume, the final apparent concrete volume is variable according to the filling rate and hence, the surplus or not of cement paste. Therefore, for illustrative purpose, we recalculate the formulations in order to provide the quantities for an apparent concrete volume of 1 m^3 and quantities are shown in table 5.10. However, it is important to mention that the difference between the apparent concrete volume of the current formulations (for a granular skeleton volume of 0.914 m^3) and those ones recalculated for an apparent concrete volume of 1 m^3 are minimal. For comparison, we estimate that the previous formulations shall give an apparent concrete volume of 1.019 m^3 for CAC – PA, 0.914 m^3 for OSC, and 0.944 m^3 for CAC – NPA.

To recalculate the formulation for 1 m^3 of apparent concrete volume, we kept the same filling rates and we also kept the same proportion between granular skeleton and surplus of cement

paste when existent. The new schematic with the formulations recalculated for 1 m^3 of apparent concrete volume is shown in figure 5-3.

Table 5.10 – Concrete quantities for 1 m^3 of apparent volume of concrete (CAC – PA, OSC, CAC – NPA).

	CAC - PA	OSC	CAC - NPA	Unit
Coarse aggregate	815.7	388.6	881.3	kg
Fine aggregate	849.0	631.4	917.3	kg
Siliceous filler	146.9	195.3	127.7	kg
Cement CEM V/A	377.1	501.2	327.9	kg
Superplasticizer	8.91	12.5	8.7	kg
Effective water	188.6	250.6	163.9	l/m^3

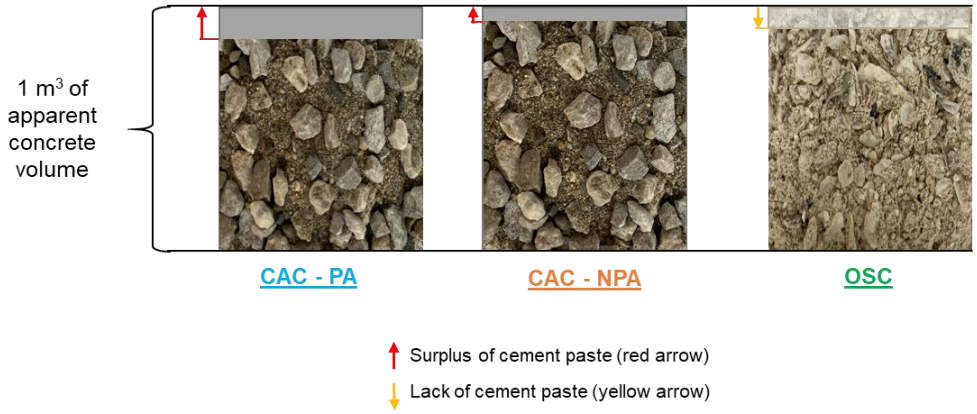

Figure 5-3 – Schematic of the new repartition of granular skeleton and cement paste for CAC – PA, CAC – NPA and OSC for 1 m^3 of apparent volume of concrete.

5.1.6 Synthesis

The knowledge acquired along a thesis is not always linear and chronological. In this work, the concrete samples were produced before the mortar study (shown in chapter 4), and the mortar study was carried out afterwards to understand the effect of granular optimisation and formulation optimisation (filling rate). As a result, we could understand better the impact of filling the voids in the concrete formulation to achieve better performances, especially in the case of the oyster shell concrete. Therefore, we carried out a hindsight analysis in the concrete

formulations based on the knowledge acquired along this work, and here we summarize a few important points:

- The constant parameter keep for the three concrete formulations (CAC – PA, OSC and CAC – NPA) was the granular skeleton volume (0.914 m^3). The conventional aggregate was replaced by the oyster shell fine and coarse aggregate in volume, and the replacement rate was 100%;
- The hindsight analysis allowed us to verify that the concretes had different filling rates (the volume of voids in the granular skeleton filled compared to the volume of cement paste). The OSC concrete does not have the intergranular porosity completely filled by cement paste whereas the CAC – PA and CAC – NPA have the intergranular porosity 100% filled and still, a surplus of cement paste;
- Although the CAC – NPA and OSC are close in terms of filling rate, the CAC – NPA does not fill the requirements of the traditional prescriptive approach for comparison. That is the reason why it was necessary to produce the CAC – PA (within the traditional prescriptive approach requirements);

That being said, we are now going to analyse the fresh and hardened properties of CAC – PA, OSC and CAC – NPA.

5.2 Fresh state properties

The fresh properties of concrete are very important to be investigated as they provide information about the workability, consistency, segregation and mobility of the concrete. Based on that, it can be verified whether the concrete meets the requirements for its final use or not. In this case, we aim to validate the concrete mixes (CAC – PA, OSC and CAC – NPA) as self-compacting concrete. Therefore, slump flow and sieve segregation tests are performed for validation of the concrete mixes. Additionally, the entrapped air and density were measured.

5.2.1 Methodology

Table 5-11 shows the tests chosen to characterise the concretes in the fresh state, the objective of each test and the method used for performing it. All tests at the fresh state were performed to the concrete just after batching the components in the concrete mixer and before casting the samples.

Table 5.11 – Tests used to chracterise the CAC – PA, OSC, CAC – NPA in the fresh state.

Test	Objective	Method used
Slump-flow	Investigate the flowability of the concrete in the abscence of obstructions	NF EN 12350-8 (2019)
Sieve segregation	Investigate the resistance of the concrete to segregation	NF EN 12350-11 (2010)
Air entrapped	Investigate the air entrapped in the concrete	NF EN 12350-7 (2019)
Density	Obtain the density of the concrete	NF EN 12350-6 (2019)

5.2.2 Experimental results of the fresh state

Figure 5-4, 5-5 and table 5.12 present the fresh properties of the three concrete mixes studied: CAC – PA, OSC and CAC – NPA. According to NF EN 206/CN, the three formulations validate the fresh state properties for self-compacting concrete. In terms of slump flow (fresh concrete consistency/workability) at time 0 minutes, the OSC and CAC – NPA are classified as SF1 class (550 – 650 mm) whereas CAC – PA is SF2 class (660 – 750 mm).

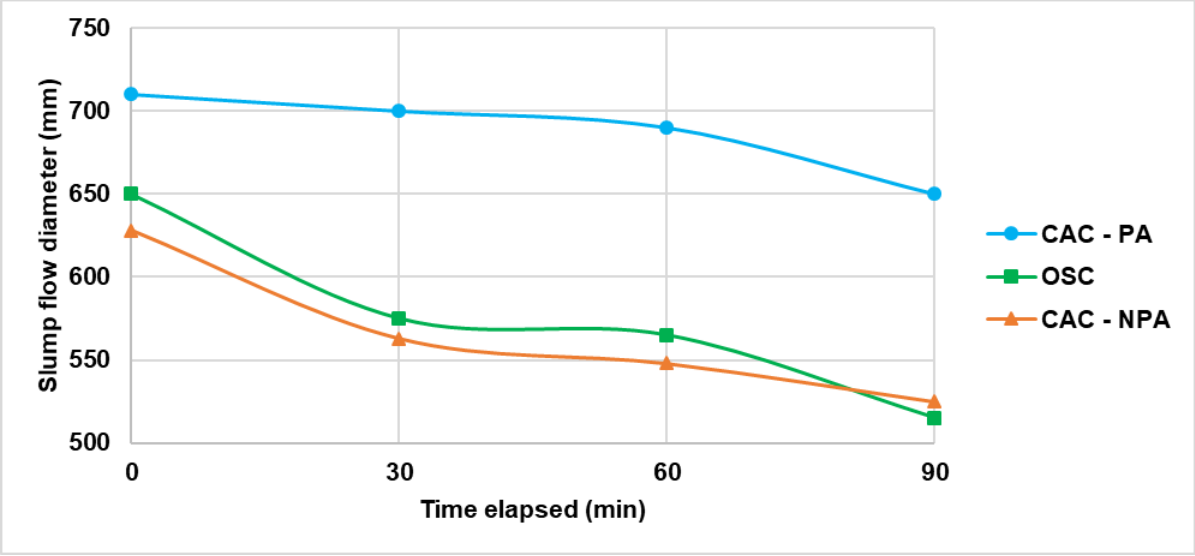

Figure 5-4 – Slump flow diameter evolution of CAC – PA, OSC CAC – NPA with time.

It is worth noting that CAC – PA has a higher slump flow diameter. The workability is steadily decreasing until 60 minutes, with a sudden fall at 90 minutes reaching a diameter of 650 mm. Despite this drop, the CAC – PA is still within the limits for an SCC after 90 minutes. Although the cement paste of OSC does not fill all the intergranular porosity, the use of superplasticizer probably increased the workability of the concrete reaching 650 mm of slump flow diameter at time 0 min. On the contrary, the cement paste does fill all the voids for CAC – NPA and still, there is a lack of fluidity in this mix seen by the diameter of 630 mm at time 0 minutes. OSC and CAC – NPA follows a similar trend, with a sharp drop in the concrete consistency after 30 minutes and then, a steadily decrease until reaching around 520 mm of diameter at time 90 minutes. It is worth noting that in our case, the OSC provided better workability than the CAC – NPA until 60 minutes after batching.

However, some authors have observed a drop in workability for high replacement rates in concrete with crushed seashells. This loss in workability was related to the seashell characteristics such as flaky, irregular, elongated or angular shape. The rough texture, higher specific surface area and higher water absorption coefficient also contribute to decreasing workability in fresh concrete when compared to conventional aggregate concrete (Cuadrado-Rica et al., 2016; Eziefula et al., 2018; Martínez-García et al., 2017).

Table 5.12 – Sieve segregation, entrapped air and density at the fresh state of CAC – PA, OSC and CAC – NPA.

	Sieve segregation (%)	**Entrapped air (%)**	**Density (kg/m^3)***
CAC - PA	8.8	1.9	2485
OSC	0.9	2.9	1787
CAC - NPA	2.6	6	2378

*The density was measured in the concrete at a fresh state in the laboratory.

In terms of resistance to segregation (sieve segregation test), all concretes are classified as SR2 class (≤ 15%) (table 5.11). Although the three mixes are within the threshold in terms of the resistance of segregation (see chapter 2), the OSC presents the better result showing a possible interesting effect of interaction between the crushed oyster shells and the cement paste. This is possibly explained because of the rough texture of the crushed shells particles, which might contribute to the cement paste adhesion.

It was no found thresholds for entrapped air. However, we can observe that the OSC has a slightly higher percentage of entrapped air than the CAC – PA (Table 5.12). Hence, in our concrete, the oyster shells did not affect significantly this property.

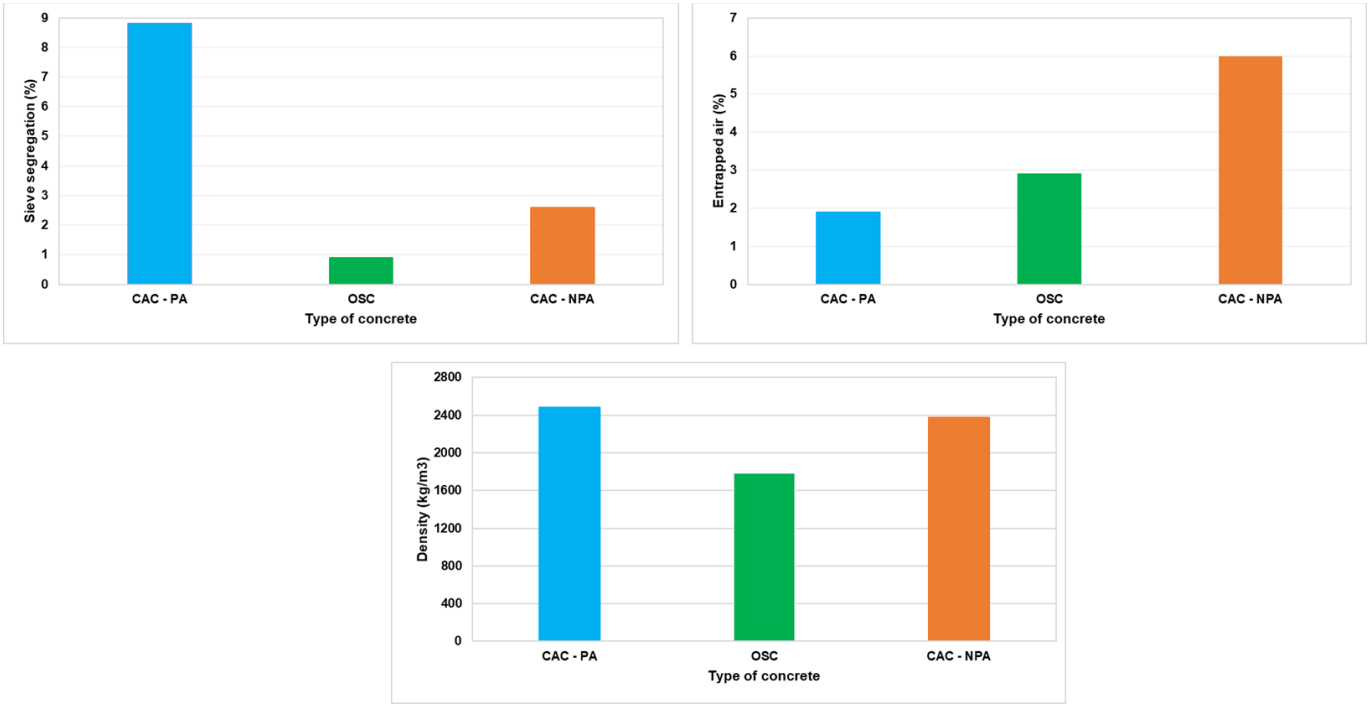

Figure 5-5 - Sieve segregation (%), entrapped air (%) and density (kg/m^3) at the fresh state of CAC – PA, OSC and CAC – NPA.

Some authors associate the increase of air entrapped in seashell concretes are related to the seashell shape (angular and irregular that can limit air drainage), the presence of organic matter trapped within the shells and the porous nature of the oyster shell (Cuadrado-Rica et al., 2016; Eo and Yi, 2015; Yang et al., 2005).

It is interesting noting that the CAC – NPA has the highest entrapped air content. We believe that this could have happened due to a mixing process problem. Figure 5-6 shows the aesthetic aspect of the CAC – NPA probably caused by the entrapped air.

Figure 5-6 - Effect of the higher air entrapped in the CAC – NPA specimen.

The OSC is the lighter concrete whereas CAC – PA and CAC – NPA have similar fresh densities (table 5.12). The lighter density of the OSC (about 26% less) can be explained because the crushed oyster shells are lighter than sand and gravel, contributing to a decrease in the material's density (Nguyen et al., 2013; Varhen et al., 2017).

5.3 Mechanical properties

The investigation of the mechanical behaviour provides a better understanding of the possible applications for construction and the material's capacity to withstand stress.

5.3.1 Methodology

Table 5.13 shows the tests chosen to characterise the mechanical properties of the concretes in the hardened state, the objective of each test and the reference method used for performing it. All of the mechanical tests were performed at 28 and 90 days. The specimens tested were at saturated state and every test was reproduced three times.

Table 5.13 - Tests used to chracterise the mechanical properties of the CAC – PA, OSC, CAC - NPA in the hardened state.

Test	Method used	Specimen dimensions
Compressive strength	NF EN 12390-3 (2019)	Cylinders 110x220 mm
Splitting tensile strength	NF EN 12390-6 (2012)	Cylinders 110x220 mm
Flexural strength	NF EN 12390-5 (2019)*	Beam 100x100x400 mm
Elastic modulus	NF EN 12390-13 (2021)**	Cylinders 110x220 mm

A few adaptations were made in two tests and are described below:

* Flexural strengh: a centre notch of 20 ± 1 mm was done in the beam. The notch was done to trigger where the crack was going to start in the specimen during the test. Rectangular aluminium boards were pasted with epoxy glue on each side of the notch (Fig. 5-7). Before starting the test, the sensor type Crack Mouth Opening Displacement (CMOD) was coupled to the aluminium board.

** Elastic modulus: The maximum load at failure obtained in a previous compressive test was used to calculate the characteristics of the preloading cycle. It was performed three preloading cycles and once obtained the displacement variation, ten loading cycles were performed within these limits (lower and upper), in µm/s.

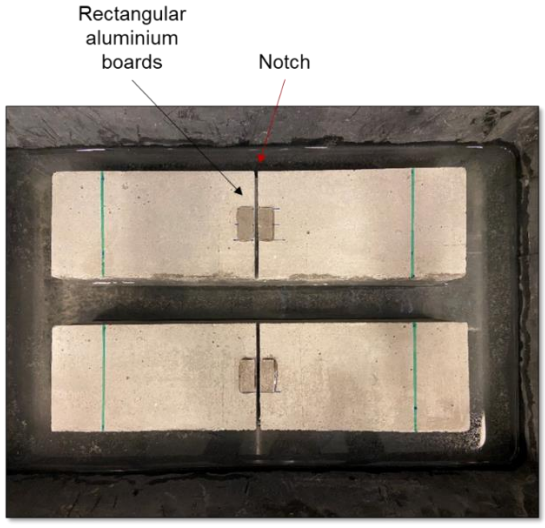

Figure 5-7 – OSC specimens notched and placed on the water until the test.

5.3.2 Experimental results

5.3.2.1 Compressive strength

Figure 5-8 and table 5.14 present the mean compressive strength at 28 and 90 days for CAC – PA, OSC and CAC – NPA. It can be noticed an increase of about 20% in strength for the concretes made with conventional aggregate and about 9% for the oyster shell concrete when passing from 28 to 90 days. The OSC shows the lowest compressive strength between the studied mixes. However, this concrete is a whole-replaced with 100% of oyster shell aggregates and the 27 MPa strength (C25/30) is still acceptable for many purposes like house slabs, concrete driveways and footpaths.

Table 5.14 – Compressive strength (MPa) at 28 and 90 days for CAC – PA, OSC and CAC – NPA.

	Compressive strength (MPa)	
	28 days	**90 days**
CAC - PA	67.4 ± 1.6	79.1 ± 3.7
OSC	25.1 ± 0.9	27.3 ± 1.2
CAC - NPA	65.4 ± 1.2	78.5 ± 1.1

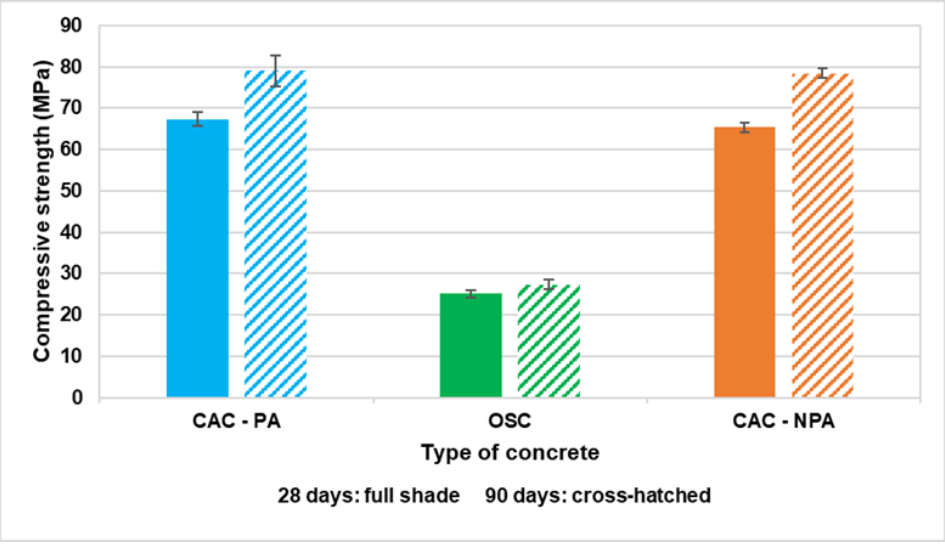

Figure 5-8 – Compressive strength (MPa) at 28 and 90 days for CAC – PA, OSC and CAC – NPA.

One of the reasons for the mechanical drop performance for OSC is the intergranular porosity that is not completely filled by the cement paste. Therefore, the aggregate type (oyster shells

are more fragile than sand and gravel), and the voids in the granular skeleton could be playing an important role in the drop in the mechanical performance. Furthermore, the mixes should be designed for the same filling rate for a more fair comparison.

It was not found in the literature specific studies performing concrete mixes made with 100% replacement of fine and coarse aggregate by oyster shells in the same mix, nor mixes using the cement CEM V/A to carry out a fair comparison. However, many studies were conducted with different types of seashells and replacement rates. We are using these studies not for a direct comparison, but for pointing out the findings in this field in relation to ours.

Some authors suggested that generally, the increase of the replacement rate of conventional aggregates per crushed seashells in concrete tends to decrease the compressive strength. Some authors attribute this strength loss to the higher water absorption coefficient of seashells, presence of organic matter and the seashell particle shape (elongated or flaky). Additionally, seashells present a higher surface area and the lack of cement paste to cover all the particles could cause a loss in the bonding strength of the matrix paste + aggregate (Eziefula et al., 2018; Mo et al., 2018; Tayeh et al., 2020).

(Cuadrado-Rica, 2016) suggests that the use of seashells in concrete increase the setting time due to the soluble organic matter present in the seashells and is proportional to the replacement rate.

Therefore, it would be interesting to test the OSC strength at different ages and longer than 90 days of curing as well as investigate the organic matter and chloride ions content (known to slow down the setting time).

5.3.2.2 Flexural strength and splitting tensile strength

Figures 5-9 and 5-10 and table 5.15 present the mean flexural strength and splitting tensile strength at 90 days for CAC – PA, OSC and CAC – NPA. It is observed a decrease in both flexural and splitting tensile strength for the OSC (about 12% for flexural strength and 24% for splitting tensile strength) compared to the concrete mixes with conventional aggregates.

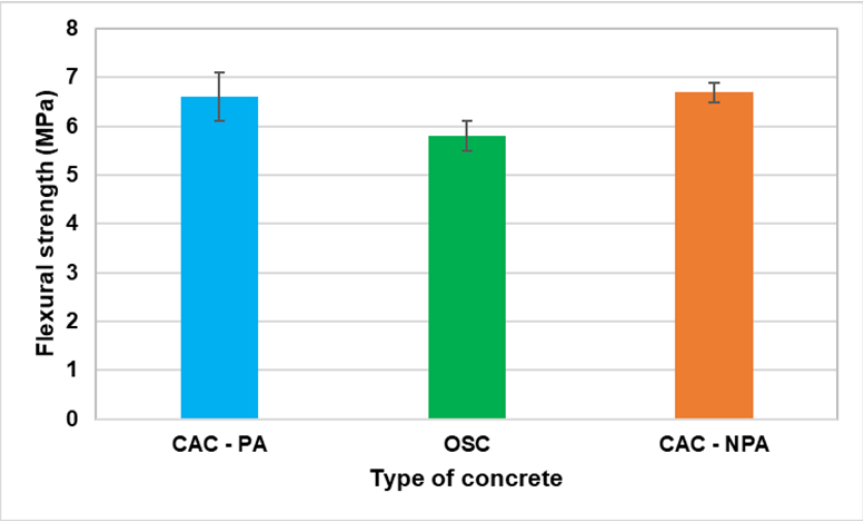

Figure 5-9 – Flexural strength (MPa) at 90 days for CAC – PA, OSC and CAC – NPA.

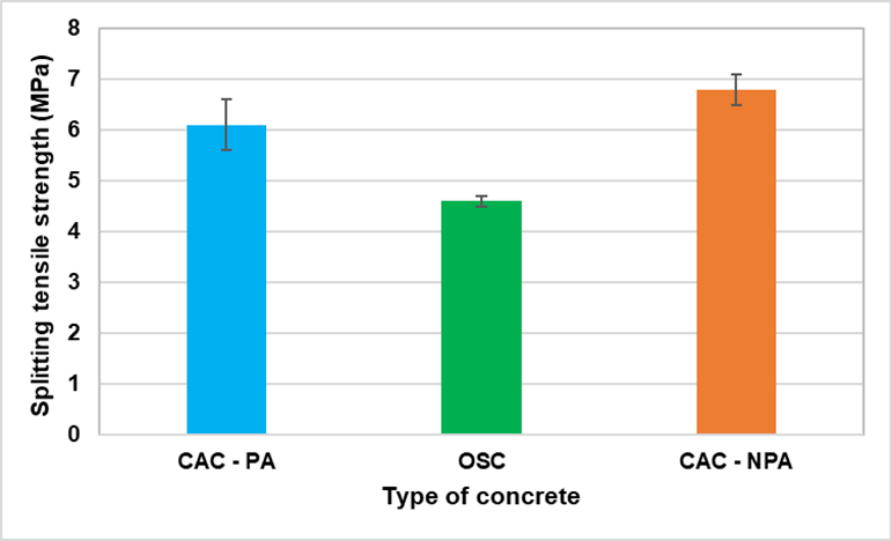

Figure 5-10 - Splitting strength (MPa) at 90 days for CAC – PA, OSC and CAC – NPA.

Table 5.15 – Flexural strength (MPa) and splitting tensile strength (MPa) at 90 days for CAC – PA, OSC and CAC – NPA.

	Flexural strength (MPa)	Splitting tensile strength (MPa)
	90 days	**90 days**
CAC - PA	6.6 ± 0.5	6.1 ± 0.5
OSC	5.8 ± 0.3	4.6 ± 0.1
CAC - NPA	6.7 ± 0.2	6.8 ± 0.3

As previously discussed and reported in the chapter 2, the effect of seashells use in concrete for flexural strength and splitting tensile strength follows a similar trend to that one observed for compressive strength. Therefore, a drop in performance is expected with authors reporting a decrease of 10 to 30% in tensile strength (Eo and Yi, 2015; Eziefula et al., 2018).

It is worth noting that the substantial downfall in compressive strength of the OSC compared to CAC – PA or CAC – NPA is not observed in flexural strength or splitting tensile strength. Fig. 5-7 shows the view of the OSC beam after being tested in flexural strength. It can be observed that the crushed oyster shells tend to place themselves forming layers (perpendicular to the sense of casting) and maybe the flexural strength is even higher for a crack propagation parallel to the casting sense. This could be an interesting property useful for products/applications where flexural strength is required. Nevertheless, further investigation must be carried out to confirm this correlation.

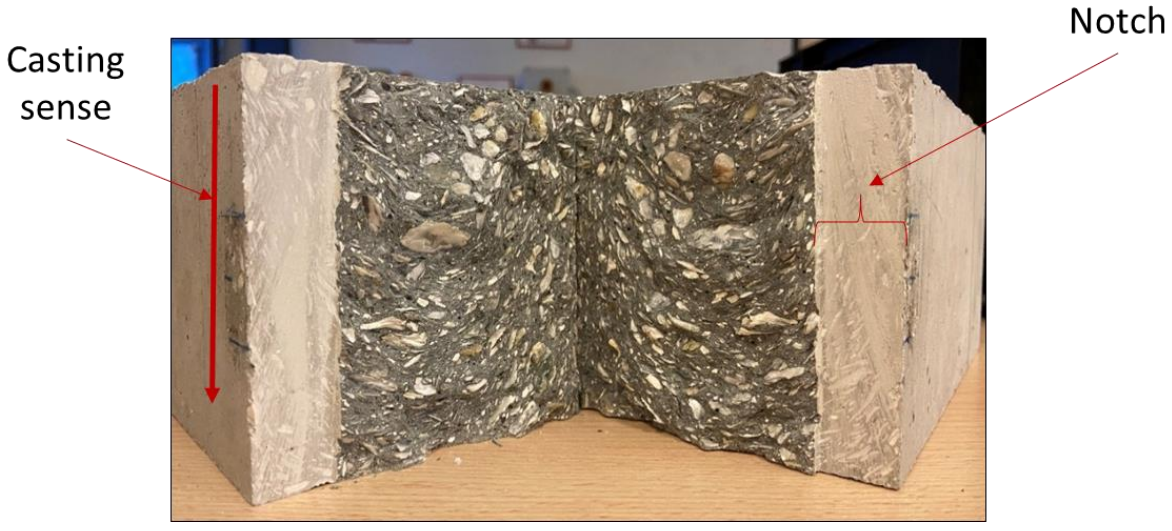

Figure 5-11 – OSC specimen after being tested for flexural strength.

5.3.2.3 Modulus of elasticity

Figure 5-12 and table 5.16 present the mean modulus of elasticity obtained at 28 and 90 days for CAC – PA, OSC and CAC – NPA. CAC – PA and CAC – NPA have similar elastic modulus at both ages, about 41 GPa at 28 days and 44 GPa at 90 days. OSC has a significant reduction of about 63% in the elastic modulus for both ages when compared to CAC – PA and CAC – NPA. This reduction is probably due to the lower elastic modulus of the seashells and the weak bond between the cement matrix and the seashells since the cement content used seems to be not enough for covering all the particles and the intergranular porosity.

(Yang et al., 2010, 2005) also mention that the loss in the elastic modulus is due to the aggregate replacement since the elastic modulus of oyster shells are smaller than those for conventional aggregates. (Olivia et al., 2015) suggests that the modulus of elasticity of seashell concrete can increase with the age of concrete since one of the main factors that influence this property is the aggregate-cement paste interfacial transition zone. The losses in mechanical properties could be minimised by limiting the replacement rate if necessary, but the focus of this work was to make a wholly-replaced concrete.

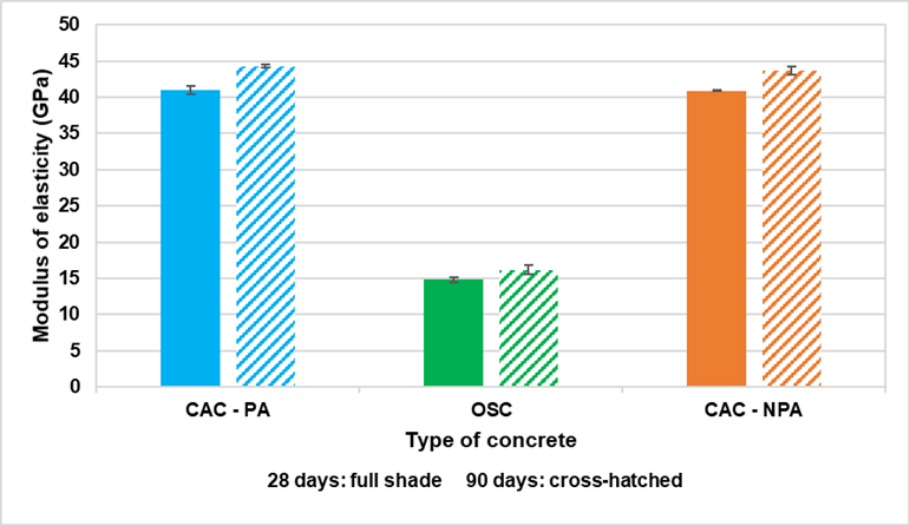

Figure 5-12 - Modulus of elasticity (GPa) at 28 and 90 days for CAC – PA, OSC and CAC – NPA.

Table 5.16 – Modulus of elasticity (GPa) at 28 and 90 days for CAC – PA, OSC and CAC – NPA.

	Modulus of elasticity (GPa)	
	28 days	**90 days**
CAC - PA	41.0 ± 0.6	44.3 ± 0.2
OSC	14.8 ± 0.4	16.2 ± 0.6
CAC - NPA	40.9 ± 0.1	43.7 ± 0.6

5.4 Durability properties

The investigation of durability properties in concrete provides a better understanding of how the material can withstand certain environments and resist aggressive agent's penetration throughout time.

5.4.1 Design, conception and development of an accelerated carbonation chamber

A material's durability depends on its characteristics to withstand environmental aggressions throughout its lifetime. Some of the external chemical attacks to which the concrete is submitted are the carbon dioxide (CO_2), a real danger to the steel in reinforced concrete. The carbon dioxide reacts to the cement compounds in the presence of water reducing the pH and weakening the steel protection. If the steel is no longer protected, corrosion of the steel reinforcements may start compromising the structure's safety and integrity. Therefore, it is very important to investigate the concrete resistance to carbonation to predict its service life and to which environmental classes the concrete can be used for (Chabil, 2009).

Therefore, we develop an experimental setup of an accelerated carbonation chamber for the laboratories LFCR (Laboratoire des Fluides Complexes et leurs Réservoirs) and SIAME (Laboratoire des sciences pour l'ingénieur appliquées à la mécanique et au génie électrique) at the University of Pau and the Adour Region.

We undertook all the steps for building this experimental setup, starting with extensive literature research of existent carbonation setups used on previous thesis, especially the one developed by (Chabil, 2009). In addition to that, we are very thankful for the advice shared by Professor Philippe Turcry from the University of La Rochelle about the carbonation chamber conception, explanations and advice for the carbonation test itself. Scientific papers were also important to understand the variability of carbonation tests, especially performed at different CO_2

concentration rates. Once completed this first stage of collecting information, we proceeded to design our carbonation chamber.

To develop the layout and dimensions, we based on the amount of concrete specimens that will be tested at the same time. The shelves were perforated so the gas mixture could circulate on the entire chamber, and fans were placed at the middle of each shelf to improve the air circulation in the chamber.

To assure a constant humidity inside the chamber, a saline solution was placed at the bottom of the chamber below the fan on the first shelf (Fig. 5.13). Thus, the fan was important to ensure the gas circulation and to spread the humidity all over the chamber. Fans speed has been adapted to ensure gas homogeneity without drying out the surface of nearby samples

Figure 5-13 – Carbonation chamber details

A gas circuit was settled in a platinum board. The setup allows a gas mixture of air and CO_2 before injection to the chamber, if necessary. Two flowmeters control the gas flow injection (the flow range for air is 0-10 sl/min and for the CO_2 is 0-50 sml/min). A regulator box controls the gas injection and the inlet flow. The CO_2 sensor inside the chamber guides the regulator box

to inject the gas in order to keep a CO_2 constant concentration of (2.5 ± 0.5)%. The CO_2 is consumed by the samples along with the test, so a constant injection of CO_2 in the chamber is needed throughout the test, even though it is at a very low rate (about 14 sml/min). The system was developed to operate at atmospheric pressure. However, in case of overpressure, the surplus of gas in the chamber can escape through a plastic pipe that will drive this gas to dip into a lime-water solution creating bubbles. This is a safety measure to avoid releasing the surplus of gas into the laboratory.

The complete setup is presented in figure 5.14. The main specifications of the carbonation chamber are detailed below:

- A transparent polyvinyl chloride box of 700 x 500 x 600 mm, with a thickness of 10 mm, 2 perforated shelves and a front watertight door;
- A CO_2 sensor to measure CO_2 concentration in percentage, placed inside the box, and connected to an analogue output transmitter (all Vaisala®). Range of measure of the sensor (0 to 5 ± 0.1)%, measurement uncertainty of ± 0.12%;
- Two fans were placed at the middle of each shelf to ensure gas homogenisation;
- A humidity and temperature sensor was placed inside the chamber to follow and record these two indicators throughout the test. Humidity measurement tolerance of ± 2.0% and ± 0.4°C for temperature;
- A saturated saline solution (1 l) of sodium nitrite ($NaNO_2$) placed in a plastic container at the bottom of the chamber to regulate the humidity in (65 ± 5)%;
- A platinum board display of gas circuit with flowmeters for CO_2 and dried air.

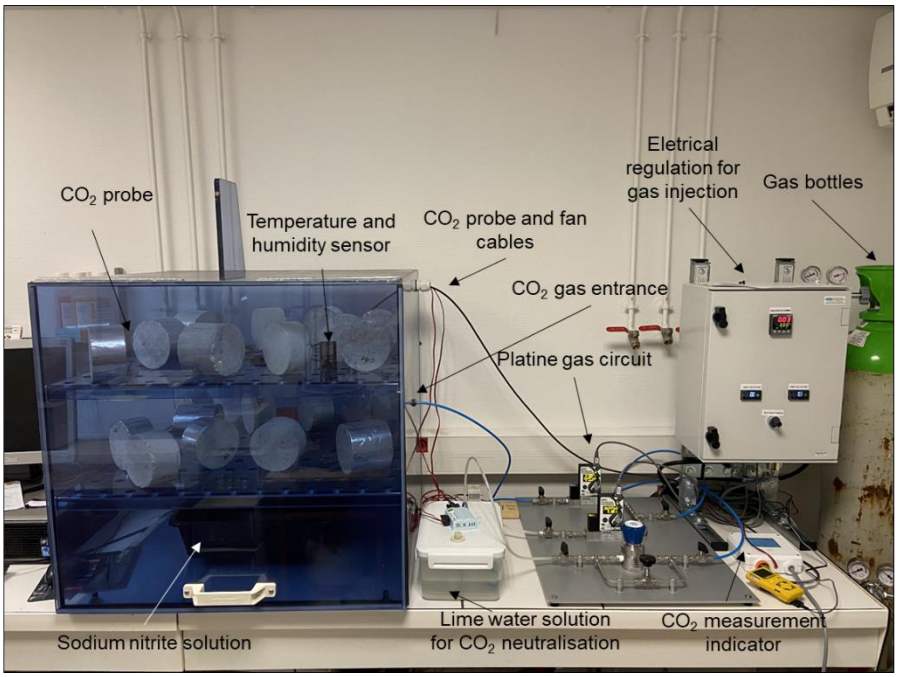

Figure 5-14 – Carbonation chamber experimental setup.

5.4.2 Methodology

Table 5.17 shows the tests chosen to characterise the durability properties of the concretes in the hardened state, the objective of each test and the reference method used for performing it. Every test was reproduced three times and all specimens tested were over 90 days age.

In this thesis, the durability indicators were selected to evaluate the ability of the concrete mixes (CAC – PA, OSC and CAC – NPA) to withstand steel-corrosion attack, using the performance-based approach for assessment (this approach is explained in chapter 2). The porosity is the main entrance of environment aggressive agents into concrete damaging the steel in reinforced concretes. Therefore, we selected the porosity accessible to water (general indicator) and capillary water absorption (substitution indicator) to assess the porosity in the concrete. The transport properties in concrete (permeability and diffusivity) play an essential role in concrete durability. Because of this, we selected the general indicators given by the tests of gas permeability and chloride migration to evaluate the concrete's resistance to the penetration of environment aggressive agents through form of gas (nitrogen) and ions (chloride). Although the carbonation in concrete can be positive in a way of filling the existent porosity, it is highly

harmful to the reinforcements in concrete. Because of this, we are investigating the carbonation under accelerated conditions in CAC – PA, OSC and CAC – NPA as well.

Table 5.17 - Tests used to chracterise the durability properties of the CAC – PA, OSC, CAC - NPA in the hardened state.

Test	Objective	Specimen dimensions	Method used	Adaptations	
Porosity accesible to water	Investigate the volume of pores in the concrete. Durability indicator used for the performance-based approach.	Irregular sizes	AFPC - AFREM a, 1997	Specimens dried at 80°C	
Gas permeability	Investigate the concrete permeability to gas (transport property). Durability indicator used for the performance-based approach.	Cylinders 110x50 mm	XP P18-463 (2011)	Specimens dried at 80°C	
Chloride migration	Investigate the concrete resistence to chloride diffusion (transport property). Durability indicator used for the performance-based approach.	Cylinders 110x50 mm	TRUC et al., 2000	Specimens dried at 80°C	
Capillary water absorption	Investigate the capillary coefficient in the concrete. Durability indicator used for the performance-based approach.	Cylinders 110x50 mm	AFPC - AFREM b, 1997	Specimens dried at 80°C	
Carbonation	Investigate the concrete resistance to carbonation. Durability indicator used for the performance-based approach.	Cylinders 110x50 mm	-	Pre-test conditions: Drying at 45ºC for 14 days Climate chamber at the same conditions of the test but without CO_2: 7 days	Test conditions: CO_2 concentration: 2.5 ± 0.5% Relative humidity: 65 ± 5% Temperature: 20 ± 3°C Samples tested at: 7, 28, 42, 76 days

Carbonation test

The conditions of the carbonation test are the topic of many studies (Auroy et al., 2015; Chabil, 2009; Chaussadent, 1999; Ilgar, 2015), where the CO_2 concentration is highly varying as discussed in chapter 2. In order to perform our test, we chose the parameters that are described in the table 5.17. Phenolphthalein indicator was been sprayed on the fresh sawn specimen surface – the pink colour indicates the non-carbonated zone and the colourless indicates the carbonated zone).

Once presented the methodology used for the durability tests, we are going to present and discuss the experimental results obtained. We are also applying the performance-based approach (detailed in chapter 2) to evaluate the potential durability of CAC – PA, OSC, and

CAC – NPA. The potential durability was assessed according to the Durability Guide provided by the French Association of Civil Engineering (AFGC, 2004).

5.4.3 Experimental results and durability analysis

5.4.3.1 Porosity accessible to water (general indicator)

Figure 5-15 shows the results of porosity accessible to water for CAC – PA, OSC and CAC – NPA (all samples tested at the age of 90 days). It can be seen from figure 5-15 that the OSC has the higher porosity accessible to water (29.8 ± 0.3 %) whereas both concrete with conventional aggregates remains below 15 % (14.5 ± 0.8% for CAC – PA and 12.7 ± 0.5% for CAC – NPA). The higher OSC porosity accessible to water result can be explained by the following reasons: the voids in the oyster shell granular skeleton are not completed filled; the OSC has a higher content of cement compared to CAC – PA and CAC – NPA; and, the shells itself that are naturally more porous than conventional aggregates (sand and gravel).

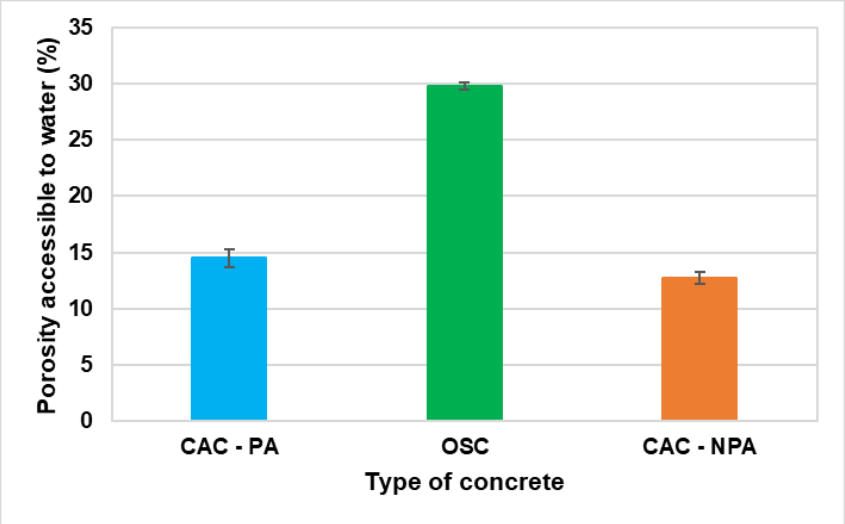

Figure 5-15 – Porosity accessible to water for CAC – PA, OSC and CAC – NPA measured ate 90 days aged specimens.

According to (Cuadrado-Rica, 2016), the total porosity of pervious concrete is composed of the macroporosity (capillary pores and ITZ) and the cement paste porosity. Thus, the use of

crushed seashells in concrete tends to modify the macroporous structure that is affected by the granular skeleton compactness and the cement paste content.

Additionally, the poorly particle packing and the higher porosity of the seashells increase the porosity accessible to water in concrete, and this value tends to rise as the replacement rate increases. (Kuo et al., 2013; Nguyen et al., 2013)

If we make an analogy to our OSC, the granular skeleton porosity was not whole-filled with cement paste. In this case, we believe that the measured porosity accessible to water can be related to a few possibilities. One of the possibilities is that part of that porosity accessible to water is related to the cement paste and the interfacial transition zone (ITZ). Another possibility to explain the result is that part of it can be related to the lack of cement paste to fill the voids and the intergranular porosity of the oyster shell granular skeleton. The compressive strength results are in line with these results since these two characteristics are strongly related. The last possibility is that the shells, naturally more porous than conventional aggregates, can store water inside of their pores. Once the oyster shell concrete specimen is dried, the water inside of the shells is dried as well, affecting the result of the porosity accessible to water.

Potential durability qualification (AFGC guide)

As previously discussed, OSC presents the higher porosity accessible to water whereas CAC – PA and CAC – NPA present similar values. In terms of porosity accessible to water, the OSC is classified as very low durability whereas CAC – PA is classified as low durability and CAC – NPA as medium durability (table 5.18)

Table 5.18 – Potential durability qualification for porosity accessible to water (general durability indicator) according to AFGC guide (AFGC, 2004).

Potential durability qualification	Very low	Low	Medium	High	Very high
Porosity accessible to water (%)	> 16	14 to 16	12 to 14	9 to 12	6 to 9
Concrete mixes qualification	OSC	CAC - PA	CAC - NPA		

5.4.3.2 Gas permeability (general indicator)

Figure 5-16 and table 5.19 shows the results obtained for the intrinsic gas permeability and the apparent gas permeability at 0.2 MPa for the CAC – PA, OSC and CAC – NPA. The specimens were tested at the age of 493 days for CAC – PA, 134 days for OSC and 220 days for CAC – NPA.

It can be seen that the OSC has an intrinsic permeability in the order of 10^{-16} m^2 whereas the CAC – PA and CAC – NPA is in the order of 10^{-17} m^2. The apparent gas permeability was measured at 0.2 MPa for further comparison based on the performance-based approach thresholds. In this case, greater variability was found for the concretes as OSC has an apparent gas permeability about 9 times greater than CAC – PA and about 4 times smaller than CAC – NPA.

Gas permeability is a transport property that will measure the material's permeation under a pressure gradient. The permeability is driven by the larger pores and a number of parameters might alter the gas permeability, like the open porosity, the moisture content, pore connectivity and tortuosity (Boel et al., 2008; Perlot, 2005).

It was not found in the literature studies about the gas permeability in concrete with seashells for comparison.

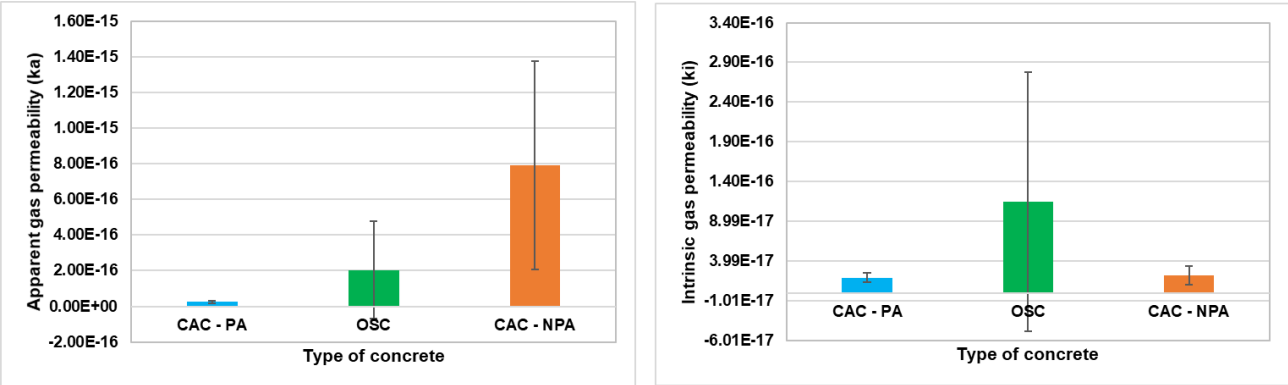

Figure 5-16 – Apparent at 0.2 MPa (ka) and intrinsic (ki) gas permeability (m^2) of CAC – PA, OSC and CAC – NPA.

Table 5.19 – Apparent at 0.2 MPa (ka) and intrinsic (ki) gas permeability (m^2) of CAC – PA, OSC and CAC – NPA.

	Gas permeability	
	ka (x 10^{-18} m^2) at 0.2 MPa	**ki** (x 10^{-18} m^2)
CAC - PA	23.8 ± 6.4	19.2 ± 5.6
OSC	202 ± 273	115 ± 163
CAC - NPA	792 ± 585*	22 ± 12

*Due to the significant standard deviation, the gas permeability test with CAC – NPA specimens must be redone.

Potential durability qualification (AFGC guide)

In terms of gas permeability, the durability guide provided by AFGC (AFGC, 2004) classify the potential durability in function of the apparent gas permeability at 0.2 MPa after drying the sample at 105ºC. We dried the concrete specimens at 80ºC in order to avoid damage to the microstructure. Nevertheless, we will use the thresholds proposed in the guide for apparent gas permeability as an indicative reference to assess our concretes in terms of potential durability (Table 5.20).

Although the three concretes present similar intrinsic gas permeability, they indeed present very different apparent gas permeability values, which will classify them in different potential durability qualification. The CAC – PA is classified as high potential durability, the OSC is classified as medium and CAC – NPA has low potential durability in terms of apparent gas permeability.

Table 5.20 – Apparent gas permeability thresholds and qualification of the potential durability (AFGC, 2004).

Potential durability qualification	Very low	Low	Medium	High	Very high
Apparent gas permeability (at 0.2 MPa, dried at 105 ºC) - K_{gas} (10^{-18} m^2)	> 1000	300 - 1000	100 - 300	10 - 100	< 10
Concrete mixes qualification		CAC - NPA	OSC	CAC - PA	

5.4.3.3 Chloride migration (general indicator)

The effective chloride diffusion coefficient D_{eff} (m^2/s) was obtained through a steady-state migration test and the results are shown in figure 5-16 and table 5.21. It can be seen that for all concretes, the effective diffusion coefficient varies between 0.20 and 0.41x10^{-12} m^2/s. Considering the standard deviation, CAC – PA, OSC and CAC - NPA have similar chloride diffusion coefficient. This is explained by the use of the cement CEM V/A, which is a blended cement with pozzolanic additions. Usually, these types of blends contribute to modifying the porous media of the cement matrix (smaller porosity, constrictivity). Additionally, the cement CEM V/A is adapted to marine environment which make the concrete made with it more resistant to the chloride penetration.

Table 5.21 – Effective chloride diffusion coefficient (m^2/s) for CAC – PA, OSC and CAC – NPA.

	Chloride effective diffusion coefficient - D_{eff} (m^2/s) x 10^{-12}
CAC - PA	0.20 ± 0.13
OSC	0.41 ± 0.24
CAC - NPA	0.27 ± 0.01

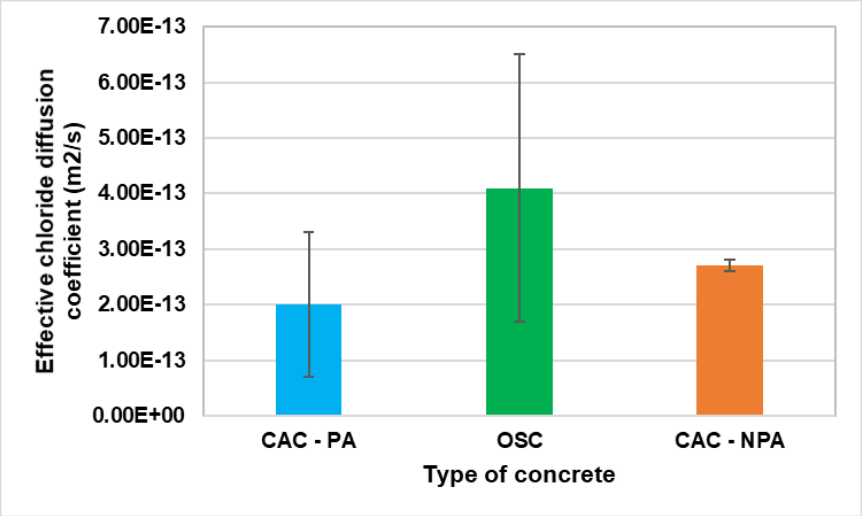

Figure 5-17 - Effective chloride diffusion coefficient (m^2/s) for CAC – PA, OSC and CAC – NPA.

(Cuadrado-Rica et al., 2016) used the chloride migration test for testing the concretes with crushed queen scallop shells (replacement rate up to 60% of fine aggregate). The effective chloride diffusion coefficient found was in the range of 3 to 6 x 10^{-12} m^2/s, and the permeability to chloride increased with the aggregate replacement.

(Georges et al., 2020) studied a few concrete formulations replacing 20% of conventional aggregates for crushed oyster shells (4/10 mm) using CEM II and CEM V/A and investigated the chloride penetration through the ion chromatography method. They found that the concretes made with CEM II are more resistant to chloride penetration than those made with CEM V/A, and the use of seashells does not change considerably the chloride penetration in natural seawater but increases in artificial seawater.

Potential durability qualification (AFGC guide)

In terms of chloride diffusivity, the durability guide provided by AFGC classify the potential durability in the function of the effective chloride diffusion coefficient. For these durability indicators, the three concretes performed similarly, being classified as very high potential durability (table 5.22). Conversely, the OSC has the higher porosity and capillary absorption, the resistance to chloride penetration was similar to CAC – PA and CAC – NPA, being all classified as high potential durability. However, if we look at the number, the effective coefficient of OSC is two times greater than the others (0.4 x 10^{-12} $m^2.s^{-1}$), showing that the chloride diffusion is slightly higher in the OSC.

Table 5.22 – Effective chloride diffusion coefficient thresholds and qualification of the potential durability (AFGC, 2004).

Potential durability qualification	Very low	Low	Medium	High	Very high
Effective chloride diffusion coefficient - Deff (10^{-12} m^2/s)	>8	2 to 8	1 to 2	0.1 to 1	< 0.1
Concrete mixes qualification				CAC - PA	
				OSC	
				CAC - NPA	

(Ilgar, 2015) mention that diffusivity depends on the microstructure, which is related to the characteristics of the mineral additions used in the concrete. Concrete containing blast furnace, fly ash and metakaolin generally improve the resistance to chloride penetration.

(Cuadrado-Rica et al., 2016) found that chloride diffusion increased with the aggregate replacement rate for concrete with crushed queen scallop shells, although found smaller diffusion coefficient and being classified as very permeable to chloride ions. The author also indicated that the chloride penetration varies along the sample height and is more evident in the concrete with scallop shells.

5.4.3.4 Capillary water absorption (substitution indicator)

Figure 5.18 shows the capillary water absorption curves of the concretes CAC – PA, OSC and CA – NPA and table 5.23 the coefficients for 24 hours and when it reaches stabilisation. It can be seen that the OSC takes the longest time to reach stabilisation and also provides the higher capillary water absorption coefficient, 3.1 ± 0.5 kg/m^2 at 24 hours and 7.3 ± 0.8 kg/m^2 at 1008 hours (at the curve stabilisation).

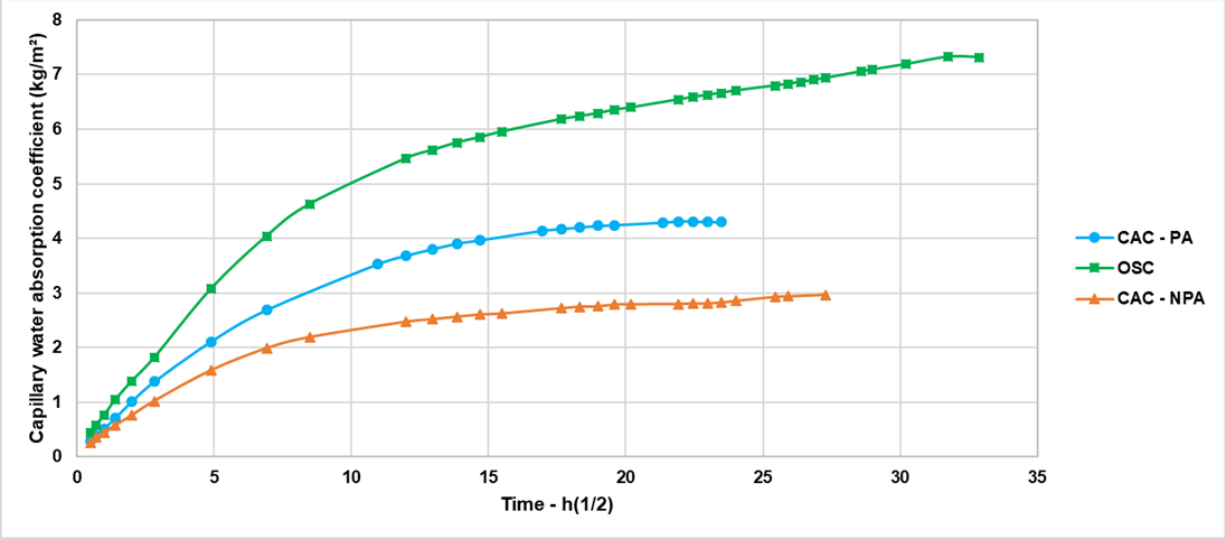

Figure 5-18 – Capillary water absorption curves of concretes CAC – PA, OSC and CAC – NPA.

It is interesting noting that the CAC – NPA provides lower capillary water absorption coefficient than CAC – PA for both 24 hours and at stabilisation. The results for conventional aggregates are in line with those found for porosity accessible to water (12.7% for CAC – NPA and 14.5% for CAC – PA). This demonstrates that for the same granular skeleton, the concrete with less cement content (CAC – NPA) provides similar or even better results than that one designed on the prescriptive approach. In terms of the time for stabilisation, CAC – PA is the concrete that reached the quickest stabilisation (after 19 days), CAC – NPA after 28 days and the OSC after 42 days (the longest time). Table 5.23 shows the capillary water absorption coefficient at 24 hours and at the stabilisation.

Table 5.23 – Capillary water absorption coefficient (kg/m^2) for CAP – PA, OSC and CAC – NPA at 24 hours and at stabilisation.

	Capillary water absorption coefficient ($kg/m^{2)}$	
	24 hours	**Stabilisation**
CAC - PA	(2.1 ± 0.1)	(4.3 ± 0.1)
OSC	(3.1 ± 0.5)	(7.3 ± 0.8)
CAC - NPA	(1.6 ± 0.1)	(2.9 ± 0.1)

The concrete porosity is provided by the surplus of water not used in the cement hydration (creating the capillary porosity), the voids in the granular skeleton and ITZ (Boel et al., 2008). The higher capillary water absorption coefficient of the OSC can be explained by two main points:

1. The oyster shells have higher intrinsic water absorption coefficient (WA_{24}) than conventional aggregates. Thus, the water to be absorbed by their own porosity was added during the concrete mixing. It is possible that this water was not absorbed immediately by the oyster shells, creating a surplus. This surplus could be “storage” as the interlayer water that evaporates after creating voids and hence, increasing porosity;
2. The second important point is that the voids in the oyster shell granular skeleton were not completely filled with cement paste in the OSC. Therefore, these voids also increase the concrete total porosity and hence, the poorer performances in terms of porosity accessible to water and capillary water absorption.

Figure 5-19 shows a correlation between the capillary water absorption and the porosity accessible to water. The OSC shows the higher porosity accessible to water and capillary water absorption. The CAC – PA and CAC – NPA show the smaller porosity and capillary absorption coefficient.

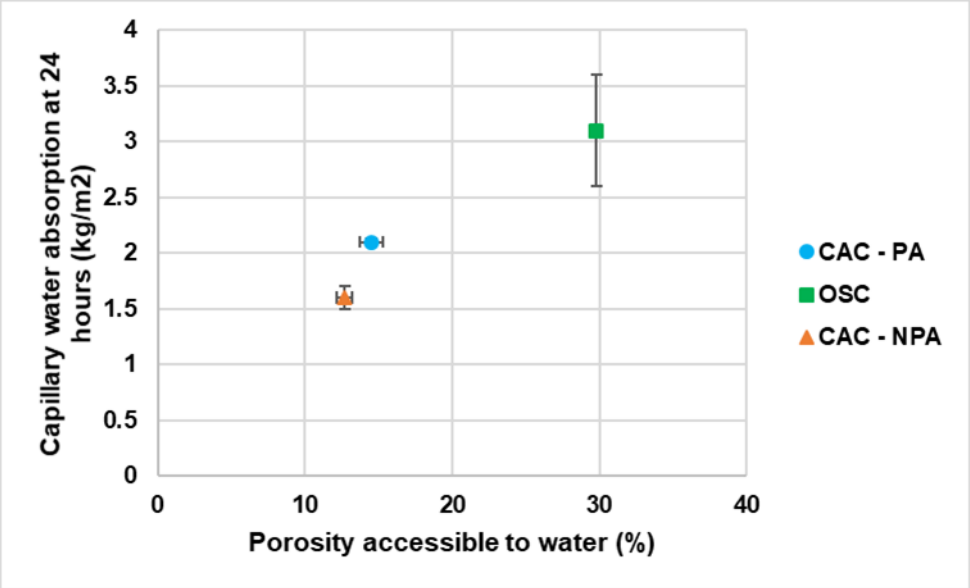

Figure 5-19 – Correlation between porosity accessible to water and capillary water absorption at 24 hours, for the concretes studied.

Potential durability qualification (AFGC guide)

The capillary water absorption is a substitution indicator and the AFGC guide does not provide a potential durability qualification specific for it. Therefore, we will make a comparison among the three concretes using the CAC – PA as the reference. The CAC – PA was chosen as a reference since its formulation meets the criteria of the prescriptive approach and therefore, can be used in the performance-based approach on the equivalence method. We will compare the water absorption coefficient at 24 hours as the method used (AFPC - AFREM b, 1997) suggests it. Therefore, comparing to CAC – PA, the OSC presents the highest capillary water absorption whereas the CAC – NPA that was formulated beyond the prescriptive approach provides better performance than the CAC – PA.

5.4.3.5 Carbonation

The temperature and relative humidity are crucial parameters for conducting the accelerated carbonation test. Therefore, we followed these parameters throughout the carbonation test with the concretes CAC – PA, OSC and CAC – NPA. Figure 5-20 shows the CO_2 concentration throughout the test. The drop in the graphic indicates when the carbonation chamber door was open to collect specimens for testing or maintenance of the saline solution. The CO_2 concentration was kept constant and close to 3% throughout the test. Figure 5-21 shows the temperature and relative humidity throughout the test. It can be noted the drop in the relative humidity coincident with the CO_2 drop for the same reason explained before. The relative humidity was kept between 60 and 70% and the temperature between 20 and 23°C (ideal conditions according to (Chaussadent, 1999)).

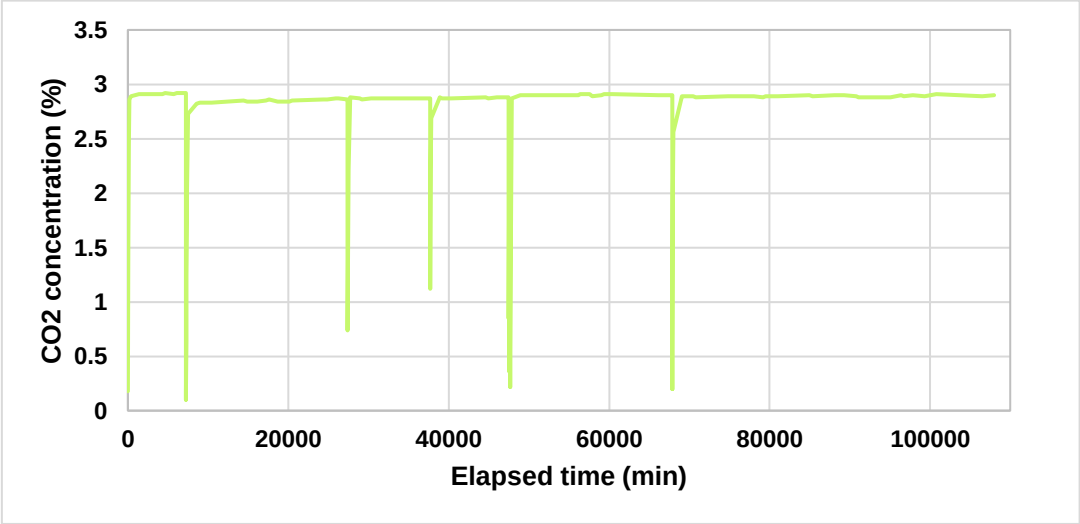

Figure 5-20 - CO_2 concentration throughout the test in the accelerated carbonation chamber.

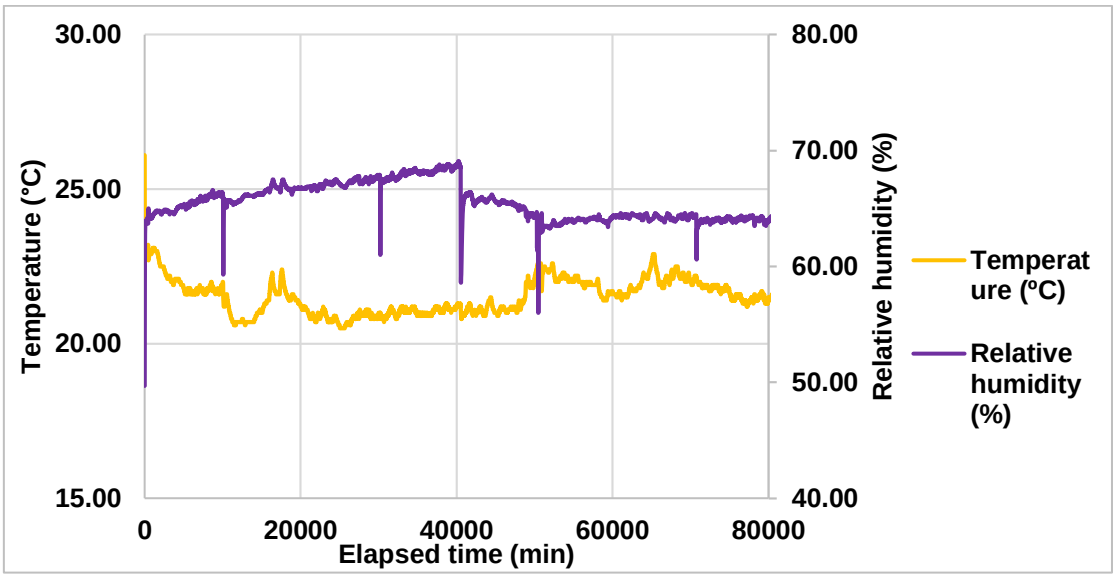

Figure 5-21 – Temperature (ºC) and relative humidity (%) conditions kept in the accelerated carbonation chamber along the carbonation test.

As previously mentioned, the specimens were tested after 7, 28, 46 and 76 days of exposure to the accelerated carbonation conditions. Figures 5-22, 5-23, 5-24 show the carbonation evolution with time (7, 28, 46 and 76 days of exposure) for CAC – PA, OSC and CAC – NPA specimens, respectively. It is more evident the carbonation progression on the OSC, especially at 76 days (Fig. 5.30), whereas for the concretes with conventional aggregates (CAC – PA and CAC – NPA) the carbonation progress is slower.

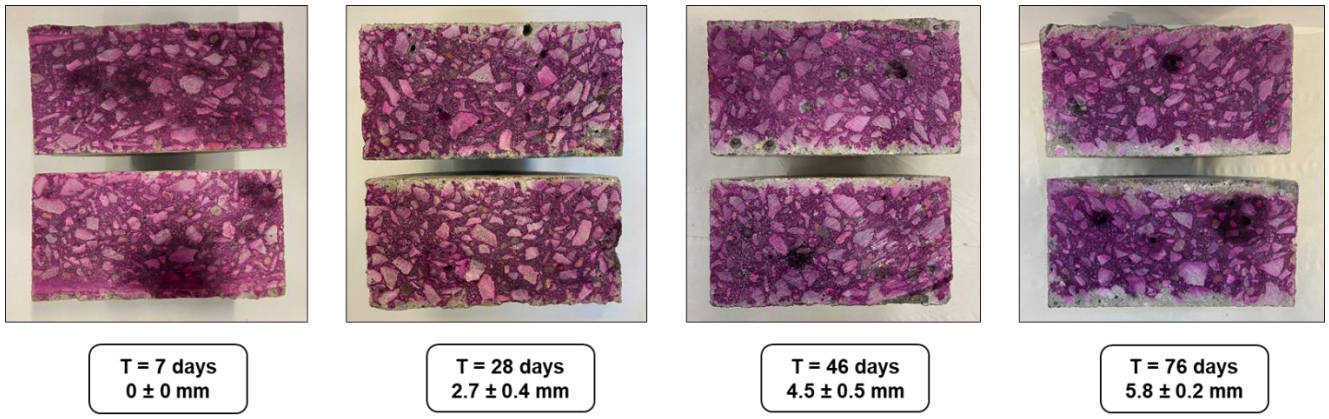

Figure 5-22 – Carbonation evolution on CAC - PA specimens at 7, 28, 42 and 76 days.

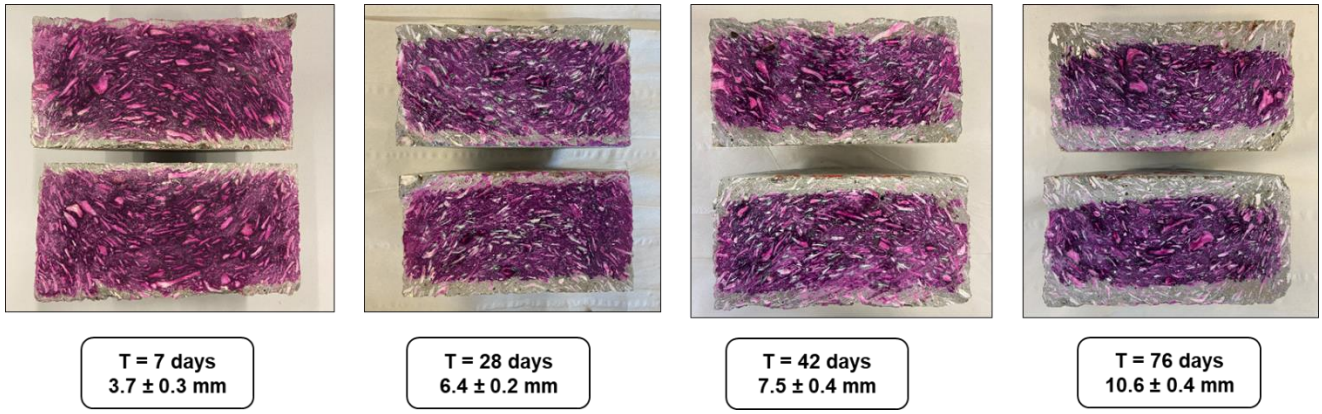

Figure 5-23 – Carbonation evolution on OSC specimens at 7, 28, 42 and 76 days.

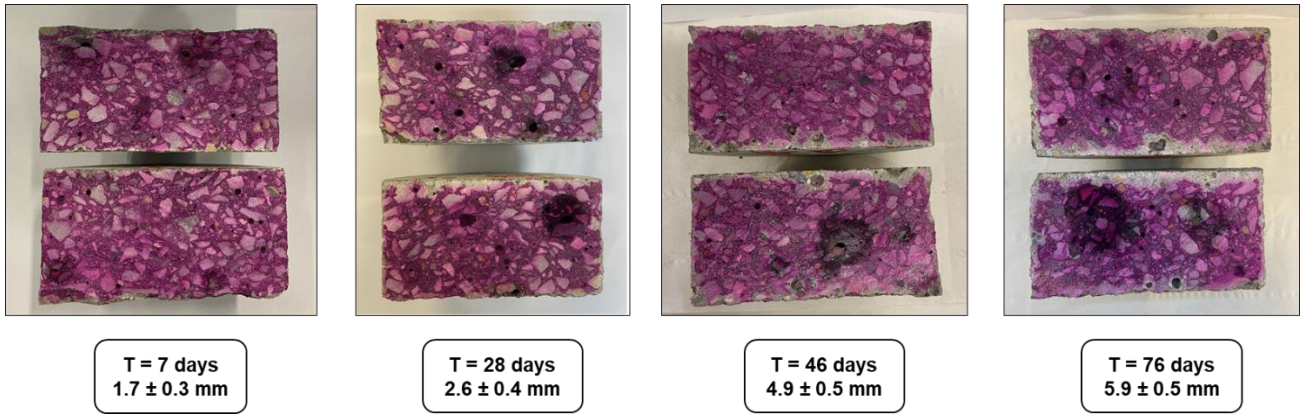

Figure 5-24 – Carbonation evolution on CAC - NPA specimens at 7, 28, 42 and 76 days.

Figure 5-25 shows the carbonation depth in the function of squared days. As previously noted in the pictures, the carbonation progress considerably faster in the OSC than on the conventional aggregate concretes (CAC – PA and CAC – NPA). Additionally, the evolution of the carbonation depth seems to follow a linear trend in the function of squared root of time for all concretes, which confirms that the same diffusive phenomenon takes place in all concrete, regardless of aggregate type. It can be seen that for 76 days, the carbonation depth of OSC is almost double of the CAC – PA or CAC – NPA (Fig. 5-22, 5-23, 5-24). We believe that the quicker progress of carbonation in the OSC specimens is due to the higher porosity in the concrete specimens caused by the lack of cement paste to cover the voids in the granular skeleton and the granular skeleton compactness itself.

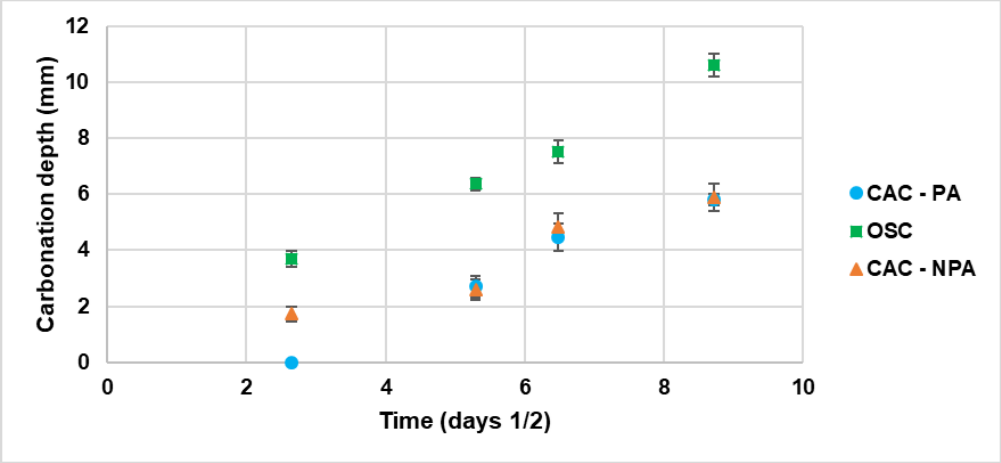

Figure 5-25 – Carbonation depth per time (days $^{1/2}$) of CAC – PA, OSC and CAC – NPA.

As expected, the carbonation rate is greater for the OSC (1.13 mm/day$^{1/2}$), followed by the CAC – PA 0.98 mm/day$^{1/2}$ and not surprisingly, slower in the CAC – NPA (0.73 mm/day$^{1/2}$). The CAC – NPA has a lower porosity, less cement paste content although still enough for covering the granular skeleton voids, and the lower intrinsic gas permeability resulting in the best performance for the concrete tested made with conventional aggregate. Conversely, the slightly higher intrinsic gas permeability value of OSC and the higher porosity are the reasons for the higher carbonation rate (Table 5.24). However, the higher carbonation rate of the OSC is not a limitation for its use as this concrete can be applied for surfaces that are not exposed directly to the environment, for instance, non-structural inside walls.

Table 5.24 – Carbonation rate (mm/day$^{1/2}$) of CAC – PA, OSC and CAC – NPA.

	Carbonation rate (mm/day $^{1/2}$)	**Coefficient of linear regression (R^2)**
CAC - PA	0.98	0.98
OSC	1.13	0.99
CAC - NPA	0.73	0.91

During the carbonation experiment, it was noted an interesting finding in the OSC specimens. After spraying the phenolphthalein solution on the freshly sawn specimen and waiting for a couple of minutes to dry, we can notice the emergence of colourless zones around the crushed oyster shells in the middle of the non-carbonated zone (see Fig. 5-26).

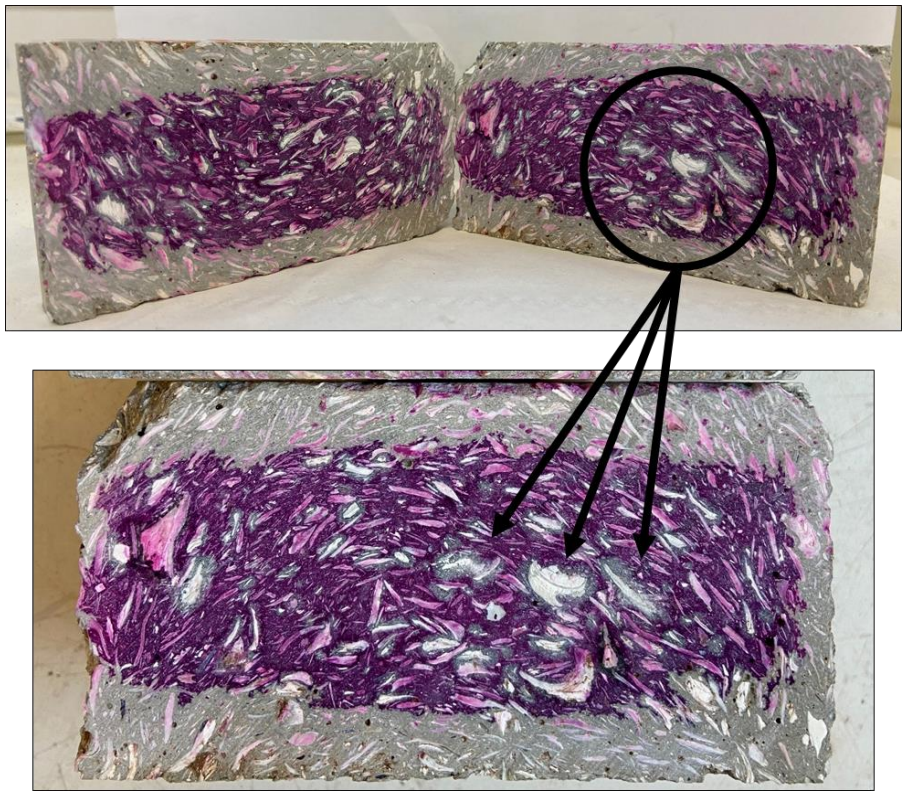

Figure 5-26 – pH ≤ 9 ± 1 zones around crushed oyster shell aggregates in the non-carbonated zone of OSC.

As the phenolphthalein is a pH indicator, that indicates that for some reason these areas have a pH ≤ 9 ± 1, which is very interesting since they are inside of non-carbonated zones (pH ≥ 9 ± 1). The concrete pH is normally between 12 and 13. The difference of pH can be due to a chemical interaction between the seashells with the cement matrix, and this interaction might develop different mineral phases modifying the pH in that specific zone. Additionally, the phenolphthalein indicator covers a range of pH 9 ± 1. Therefore, these colourless zones around the oyster shells can present a pH ≤ 10.

It was not found in the literature a possible reason for this pH alteration in the cement matrix around the crushed oyster shells, and further investigation should be conducted to understand this phenomenon.

5.5 Synthesis of the experimental results of CAC – PA, OSC and CAC – NPA

Figure 5-27 summarise all results obtained to characterise CAC – PA, OSC and CAC – NPA at the fresh state. Figure 5-28 summarise all results of the mechanical properties of CAC – PA, OSC and CAC – NPA. Figure 5-29 summarise all results of the durability properties of CAC – PA, OSC and CAC – NPA

The use of crushed oyster shells as aggregate replacement decreased the workability in the concrete OSC when compared to the CAC – PA but increased whe compared to the CAC - NPA. The loss in workability of the oyster shell concrete is usually associated with the shape of the crushed seashell. The lighter oyster shells resulted in a lighter density concrete as well (1787 kg/m3). The thresholds for slump-flow and sieve segregation for producing self-compacting concrete were attended for the three concretes.

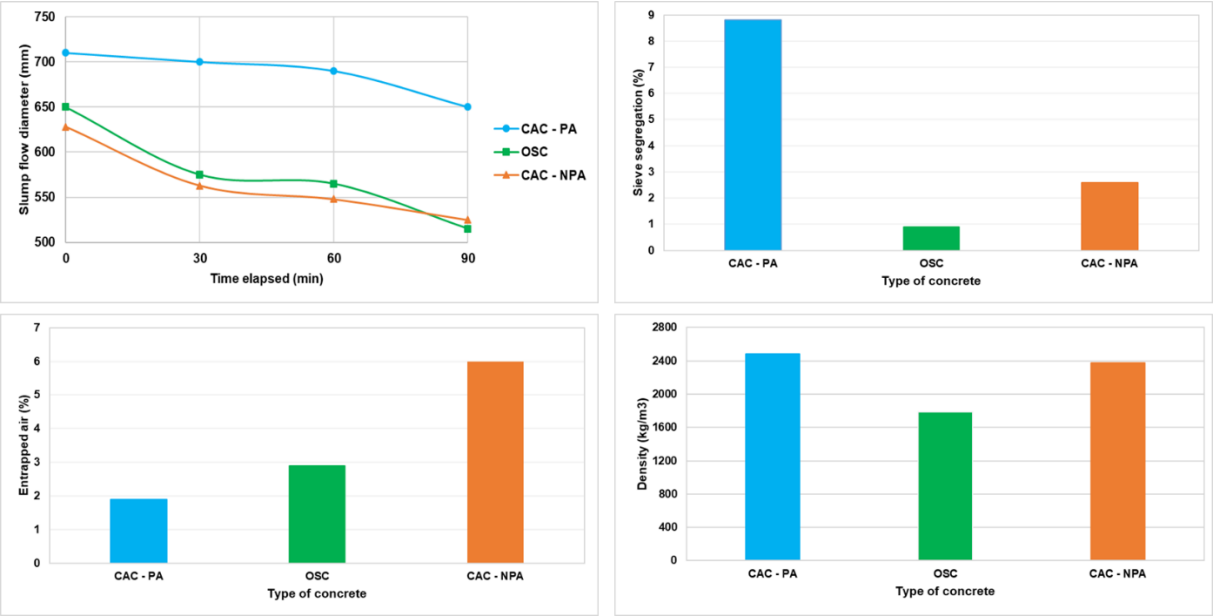

Figure 5-27 – Summary of all results at fresh state for CAC – PA, OSC and CAC – NPA.

From figure 5-28 we can observe that the compressive strength of OSC is lower if compared to CAC – PA and CAC – NPA. However, for a 100% fine and coarse aggregate replacement, we still found very good properties such as the compressive strength of 27.3 ± 1.2 MPa at 90 days for OSC, which is considered enough for several uses and demonstrates that full substitution of conventional aggregate by oyster shell ones could be envisaged. In terms of flexural strength and considering the standard deviation, the OSC is equal in performance to the concretes made with conventional aggregates and may be even better. The elastic modulus of the OSC has sharply decreased compared to the other concretes because the seashells are more deformable than sand and gravel. However, a smaller elastic modulus can be an interesting property depending on the intended use.

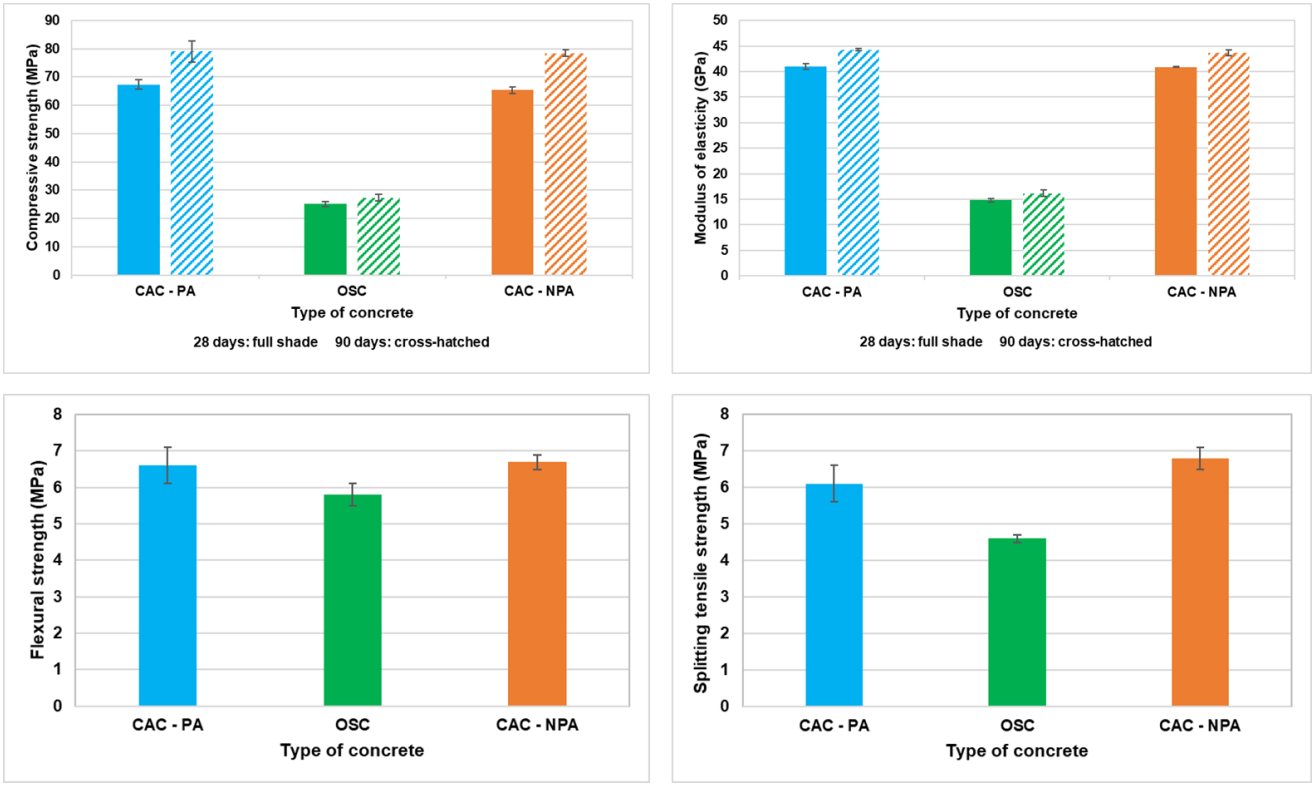

Figure 5-28 - Summary of all results of the mechanical properties of CAC – PA, OSC and CAC – NPA.

From figure 5-29, we can observe that although OSC has a high porosity accessible to water (29.8%) and capillary water absorption (3.1 kg/m^2 at 24 hours), the resistance to chloride penetration is as good as the one of the concretes made with conventional aggregates (CAC – PA and CAC – NPA). This is explained by the use of the cement CEM V/A, which is a blended cement with pozzolanic additions. Usually, these types of blends contribute to modifying the porous media of the cement matrix (smaller porosity, constrictivity). Additionally, the cement CEM V/A is adapted to marine environment which make the concrete made with it more resistant to the chloride penetration. We can see a trend between the carbonation rate and the porosity accessible to water and capillary water absorption. We observe a more significant rate of carbonation for OSC since the CO_2 penetrates the concrete through the porous media and cracks. Additionally, the gas permeability values corroborate this trend since OSC is the most permeable concrete.

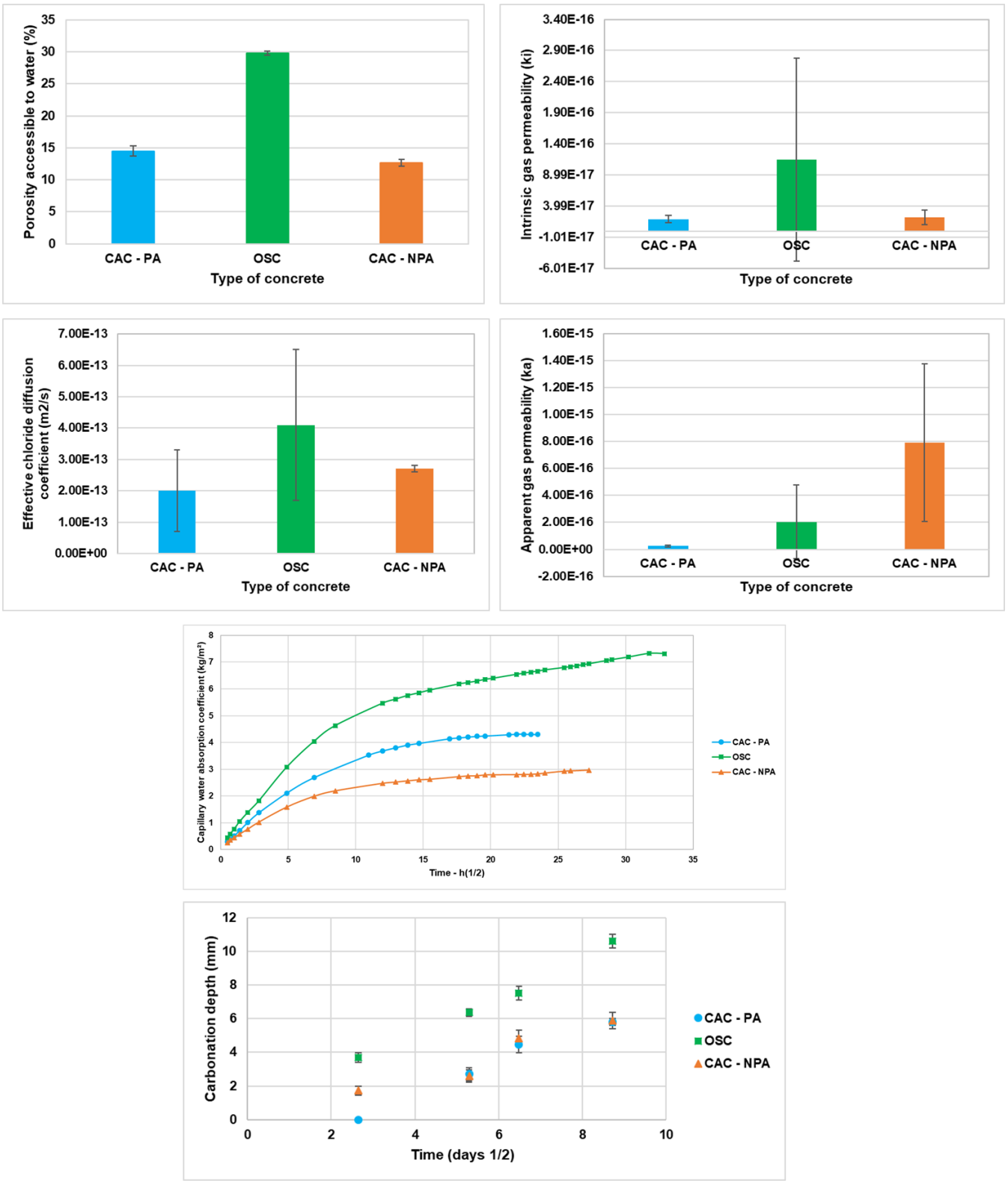

Figure 5-29 – Summary of of all results of the mechanical properties of CAC – PA, OSC and CAC – NPA.

5.6 Synthesis of the potential durability analysis by performance-based approach

Figure 5-30 presents a synthesis of the potential durability qualification of CAC – PA, OSC and CAC – NPA, according to (AFGC, 2004) and based on the performance-based approach. This panorama gathers the general indicators (porosity accessible to water, apparent gas permeability and effective chloride diffusion) with their values and qualification. The substitution indicator (capillary water absorption) and carbonation rate values are also provided although the guide does not establish thresholds for these indicators.

The porosity accessible to water is an important and global indicator but is not enough for qualifying the material's durability. The different types of transport of materials (permeation, diffusion) under different gradients (pressure, concentration) will occur in different types of porosity, depending on the pore size, connectivity, and tortuosity. Therefore, transport properties are also very important when assessing the durability of material.

Figure 5-30 – Summary of the potential durability qualification of CAC – PA, OSC and CAC – NPA.

Potential durability (AFGC, 2004)	
Very low	
Low	
Medium	
High	
Very high	

	CAC - PA	OSC	CAC - NPA
Porosity accessible to water (%)	14.5 ± 0.8	29.8 ± 0.3	12.7 ± 0.5
Apparent gas permeability at 0.2 MPa (10^{-18} m^2)	23.8 ± 6.4	202 ± 273	792 ± 585*
Chloride effective diffusion coefficient (10^{-12} $m^2.s^{-1}$)	0.20 ± 0.13	0.41 ± 0.24	0.27 ± 0.01

* Due to the significant standard deviation, the gas permeability test with CAC – NPA specimens must be redone.

The AFGC guide does not provide thresholds for the capillary water absorption or carbonation

	CAC - PA	OSC	CAC - NPA
Capillary water absorption (kg/m^2) at 24 hours *	2.1	3.1	1.6
Carbonation rate ($mm/day^{1/2}$)	0.98	1.13	0.73

From figure 5-30, we can conclude that the OSC has very low potential durability to porosity accessible to water whereas medium potential durability to apparent gas permeability and high to the chloride diffusivity. The CAC – PA presents low potential durability to porosity accessible to water, and high for apparent gas permeability and chloride diffusivity. The CAC – NPA presents medium potential durability to porosity accessible to water, low for apparent gas permeability and high for chloride diffusivity. Therefore, all concrete provides interesting performances and can be used as long as the final use and durability required are adapted to it.

5.7 Conclusions

This chapter was dedicated to study the use of crushed oyster shells to replace 100% of the fine and coarse aggregate in concrete. To conduct this study, we started with a conventional aggregate (sand and gravel) concrete formulation designed according to the traditional prescriptive approach (CAC – PA). The CAC – PA was the starting formulation for designing an oyster shell concrete (OSC) and then, a conventional concrete beyond the traditional prescriptive approach (CAC – NPA) was formulated.

An analysis of the fresh state properties suggests that the use of crushed oyster shells in concrete decrease the workability and density even though the entrapped air and resistance to segregation were limited. Besides the loss in workability, the OSC is still classified as a self-compacting concrete for using straight after mixing and if not, retarding admixtures can be used to keep the workability for longer until the concrete pouring.

In terms of mechanical properties, the OSC shows a loss of over 50% in compressive strength compared to CAC – PA and CAC – NPA. This is possible because of several factors: the higher intergranular porosity of the granular skeleton; the lack of cement paste to cover all this porosity; the oyster shells themselves that are more fragile than sand and gravel, and the replacement rate (100% of fine and coarse aggregate). However, the flexural strength of OSC is similar to CAC – PA and CAC – NPA, suggesting that the orientation of the shells in the concrete could improve this property somehow.

In terms of durability, we observed higher porosity accessible to water, capillary water absorption and carbonation rate for OSC. These values can be explained by the reasons aforementioned. Conversely, the OSC demonstrate good resistance to chloride penetration

and gas permeability, equating to the other concretes and being classified as high and medium potential durability, respectively.

An interesting observation is that the loss in compressive strength of OSC is directly related to the higher porosity observed in the porosity accessible to water and capillary water absorption results. A higher porosity results in a weaker material. Conversely, for transport properties (gas permeability and chloride diffusion), we found good performance results for OSC demonstrating that the transport properties are more related to the pore size, tortuosity and constrictivity than the general porosity measured by the previously mentioned tests. Additionally, the use of CEM V/A (suitable for marine environment) improved the resistance to aggressive agents in the Oyster Shell Concrete evidenced by the chloride diffusion coefficient of this concrete.

After investigating the properties of the concretes made with crushed oyster shells and conventional aggregates (sand and gravel), we could conclude that the aggregates replacement is viable. However, we want to assess whether the use of crushed oyster shells as aggregate replacement brings environmental benefits or not compared to the process to obtain sand and gravel. For this, we are going to carry out a preliminary environmental analysis of the production process to obtain sand and gravel, and the crushing process to obtain the oyster shells as aggregate for concrete.

CHAPTER 6 - A PRELIMINARY ENVIRONMENTAL ANALYSIS

In this chapter, we present a preliminary environmental analysis concerning the production process of conventional aggregates and crushed oyster shells and a comparison of their potential environmental impacts.

6.1 Context of the environmental analysis

In this thesis, we aimed to develop an environmentally-friendly concrete with shellfish farming by-product (oyster shells) as aggregate replacement. The project was created due to the need for sustainable management of the oyster farming waste in Arcachon Bay in France, to align with the principles of Blue Growth and circularity. Many studies were carried out (chapter 2) showing the feasibility of adding value to this "waste" as a by-product of the concrete industry. At the same time, local quarries in the Nouvelle Aquitaine region have been facing a rapid decrease in their capacities, giving rise to the need to find alternative solutions. Ideally, concrete plants and quarries must be close enough to limit the carbon footprint associated with transportation. Within this context, the potential use of the shells “waste” from the oyster farming activity for producing concrete in the region brings up several benefits like:

- Valorisation of a “waste” into a by-product of another activity;
- Alternative solution for producing an environmentally-friendly concrete, by replacing partially or totally the granular skeleton;
- Application of circularity principles by recycling the shells into concrete in the region area of Arcachon bay;
- Decrease of shells "waste" to be send to landfills or incinerated.

The pillars of sustainable development gather the social, ecological and economical aspects. The use of oyster shells as aggregate in concrete is in line of these pillars. It is social because the concrete made with crushed oyster shells is supposed to be used in the region, showing the inhabitants how the local resources are being used and the commitment of local authorities to recycling "waste", generating awareness among people. Ecological because what was considered initially as waste is now a valued by-product, being recycled, continuing to be used in other processes escaping for the end of life in landfill or incineration. Economical because

the environmentally friendly concrete with oyster shells got value-added for using a more sustainable material and can be commercialised.

Another benefit of using the seashells “waste” is that the process of building shells captures CO_2 from the ocean. The shells are formated of calcium carbonates (calcite and aragonite). In the marine environment, the shells capture CO_2 and calcium ions to build their shells (see equations) When recycling the shells, we avoid that the CO_2 captured is returned to the atmosphere and hence, is stored in concrete with the shells. Figure 6-1 illustrates the reactions involved in the dissolution of CO_2 in water until the calcium carbonate is formated (La Plante et al., 2021; Matrose et al., 2022).

1st phase: The carbon dioxide pass from the gas state to liquid state

$$CO_2(g) + H_2O \longleftrightarrow H_2CO_3$$

2nd phase: Acid-base reactions to obtain carbonate ions in water

$$H_2CO_3 + OH^- \longleftrightarrow HCO^{3-} + H_2O$$

$$HCO^{-3} + OH^- \longleftrightarrow CO_3^{2-} + H_2O$$

3rd phase: Formation of calcium carbonate

$$Ca^{2+} + CO_3^{2-} \longleftrightarrow CaCO_3$$

Figure 6-1 – Chemical reactions involved in the formation of calcium carbonate (main compound of shells).

With this in mind, we found it relevant to carry out a qualitative analysis concerning the potential environmental impacts related to the production process of conventional aggregates and oyster shell aggregates. This analysis was not extended to the concrete because, in this study, the cement, filler and superplasticizer of the concrete mix and the casting procedure adopted was the same for CAC – PA, OSC and CAC - NPA. Although the cement paste volume was not the same for the three formulations, we are going to focus only in the aggregate type .

6.2 Objectives

This preliminary environmental analysis aims to investigate the process of production of the aggregates used in the concrete in this study, and the potential environmental impacts related to it. Two types of aggregates were used: a conventional one (sand 0/4 mm and gravel 4/10 mm – both from alluvial deposit – limestone) and crushed oyster shells (OSFA 0/4 mm and OSCA 4/10 mm). The production processes are different since the conventional aggregates are raw materials and the crushed oyster shells are a by-product of the shellfish farming activity. At the end of this analysis, we aim to answer the questions below:

- What are the main environmental impacts related to each aggregate production process?
- What is the average energy consumption per process of each aggregate production?
- What can be done to decrease the environmental impact of the production process of these aggregates?

6.3 Production process of the studied aggregates

6.3.1 Crushed oyster shells

The oyster shell farming occupies an area about 680 hectares in Arcachon Bay (France). The farming cleaning activity is carried out by a boat that collect the waste and dead shells and takes place during the low tide. This process generates about 9500 tonnes of shell waste per year and currently, management practices of this waste were not implemented yet and only 16% of this shells are recycled and valorised. Management pratices were implemented the 16% (about 1600 tonnes per year) is bought by a company that uses the oyster shells as a "raw resource" for their business. In this company, there is a processing facility where shells pass through stages of cleaning and crushing to then, be commercialised as animal food supply and decoration. In addition to that, the company also has crushed the oyster shells to produce the aggregates we have used in this study. Therefore, the previous "waste" became a by-product/resource for another industry, gaining value and being considered an avoided burden of the oyster shell farming activity. This company has a processing capacity of 1 tonne/ hour, about 1600 tonnes/year.

To understand the processing of crushing oyster shells for producing aggregates, we visited a company located near to La Rochelle, France. From this company, we acquired the primary

data used in this study. Figure 6-2 illustrates the production process of the crushed oyster shell in this company. Currently, the shells are transported from Arcachon Bay to this facility for processing since they are their “raw material”. Once the shells arrive in the company, they are stored in outdoor piles and are naturally washed by rain, so no extra water is used in the current process. To start the processing, the shells are loaded in the facility by front loader equipment (transportation < 100 metres). Once the processing facility is loaded, the process is continuous and sequential and the shells are transported between the equipment by electric conveyors.

The first stage of crushing is composed of selective sorting (hand picking) to remove any waste that is mixed with the shells (fishnet, small pieces of wood, cigarette butt etc). After this stage, the shells are taken to a rotary kiln at low speed and temperature (about 130ºC) where the shells pass continuously for 30 minutes. The kiln is a stage necessary for the products that this company commercialise (eliminate organic matter and pathogens), but it is not mandatory and/or can be adapted for the aggregates process. After the kiln, the shells go into the impact crusher machine and just after being crushed, the material will pass through a vibrating screen for sieving. The particles that are not of the right size are redirected to the crusher and go in the process again. Several crushed oyster shells sizes are obtained for the different products of this company, but we focus on the ones we used for concrete: 0/4 mm and 4/10 mm. The all process is a closed circuit, and the powder emission from the equipment is collected through pipes and redirected to filters. This powder is also commercialised by the company, being the only waste of the process the waste that was collected in the selective sorting.

The transportation at the beginning of the process is made by a grader (diesel). The solid waste recovered from the selective sorting is disposed of in a landfill. The conveyors, rotary kiln, crusher machine and vibrating screening are electric-based. The waste from the packaging of materials used for the processing facility maintenance is not considered in this study.

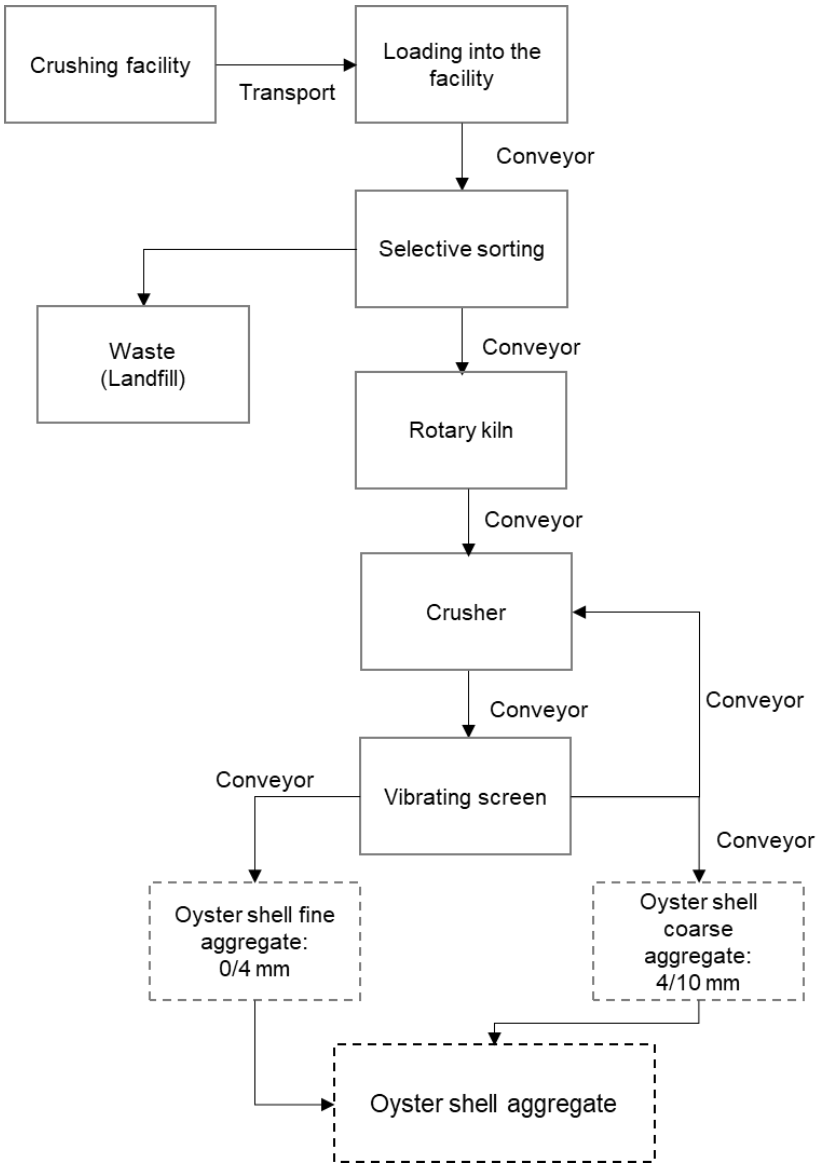

Figure 6-2 – Crushed oyster shell aggregate production process.

To evaluate the potential environmental impacts related to the transformation of the shells into aggregates for concrete, we are taking a few assumptions:

- The oyster shell farming activity is not going to be included in the analysis;
- The treatment process for the shells that are being analysed is based on the one used in the company we visited;
- The transportation from Arcachon Bay to the company was not taken into account in the study since the process of transforming the shells into aggregates is supposed to

be located at the place where the shells are produced, as it is envisioned in Arcachon by the syndicate in charge of shellfish farming to develop this valorisation way;

- The company we visited to acquire the primary data is small compared to a quarry that produces conventional aggregates. Therefore, their capacity is 1 tonne per hour;
- To simplify, we assumed that the current processing facility will be used exclusively for producing oyster shells aggregates and the production proportion between fine (0/4 mm) and coarse (4/10 mm) will be 50/50%;
- The only solid waste consider was the one related to the shells processing. Packaging of products used for maintenance of the machines or waste from the office was not taken into account.

6.3.2 Conventional aggregates: sand and gravel

To evaluate the process of sand and gravel production, we visited a quarry in the Nouvelle Aquitaine region, in France. The quarry production capacity is 400 tonnes/hour and produces fine and coarse aggregate for concrete, in a proportion of 50,4% and 49,6% respectively. Figure 6-3 details the process production.

The mixed grade material is dug out of an alluvial plan deposit by a dragline excavator. Front loader equipment places the material extracted onto a conveyor that is directed to the processing facility. The first stage in the facility is a vibrating screen + washing. The material bigger than 80 cm is separated and the smaller than 80 cm goes for a second vibrating screen. The material bigger than 22 cm is sent to a primary cone crusher that is followed by a vibrating screen. If the material is still not in the desired size, it is then directed to a secondary cone crusher followed by a vibrating screen. Hydrocyclone is used to separate the finer particles and obtain the aggregates 0/2 mm and 0/4 mm. The material is transported between stages by an electric conveyor. At the end of the process, 6 aggregates sizes are obtained: 0/2 mm, 0/4 mm, 6/10 mm, 10/14 mm, 4/16 mm and 11/22 mm.

The processing is in an open-air area but it can be considered that no dust is emitted since the material is wet during all the processing. The water used for washing the material is 80% recycled and reused. A decantation process is used and the slime recovered from this process is used for land restoration inside the site. The 20% of water not reused is considered wastewater. The process does not generate solid waste other than the packaging of materials used for maintenance and they were not considered in this study. All equipment in the

processing facility is electric-based. All the heavy equipment (dragline and front loader) uses diesel as fuel.

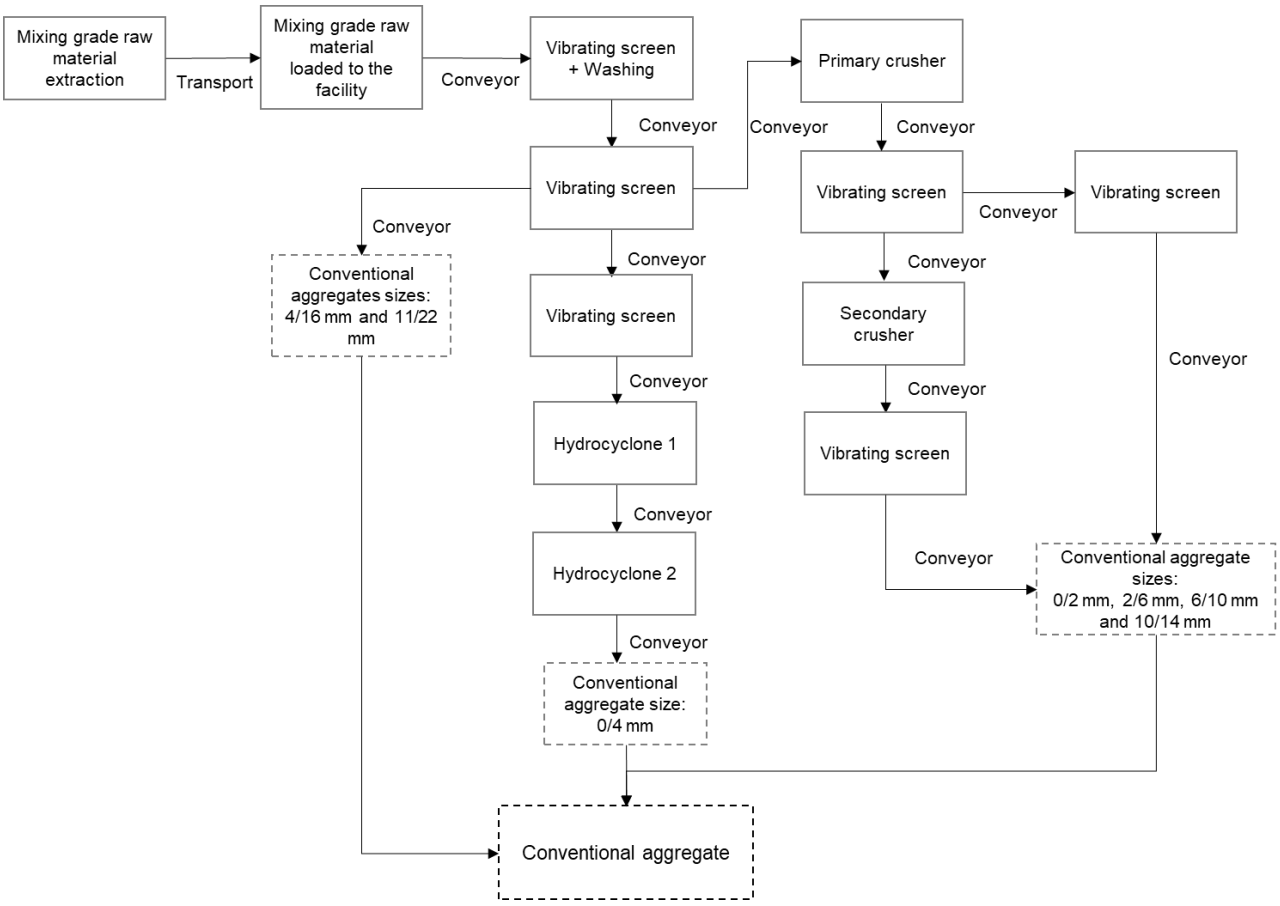

Figure 6-3 – Conventional aggregate production process.

To evaluate the potential environmental impacts related to the production of conventional aggregates for concrete, we are taking a few assumptions:

- Although the quarry produces different sizes of aggregates, we obtained the production proportion between fine (0/6 mm) and coarse (6/22 mm) aggregates to distribute the direct burdens for each of them. This proportion was 50.4% off (0/6 mm) and 49.6% of (6/22 mm);

- It was assumed that no solid waste was produced directly from the material's extraction and processing. The packaging of products used for maintenance of the machines and office waste was not taken into account.

6.4 Environmental analysis of the production process of the studied aggregates

The direct burdens analysed for the production of aggregates are energy, water and fuel consumption. The energy because it is the main source for the equipment in the processing facilities. The water because it is consumed during the conventional aggregates processing. The fuel because it is used in the heavy equipment in both processes.

To analyse these burdens, primary data was collected directly from the oyster shell crushing company and a quarry. We chose to use only primary data to be more accurate when assessing these processes and be more realistic to the scenario and representative of the region studied.

The energy consumption (kWh/t) was estimated considering the total energy consumed per hour for producing 1 tonne of aggregate. The total energy consumed per hour (kWh) was estimated based on the total power consumption per equipment. However, a correction coefficient was applied to the energy consumption since the equipment stops for maintenance, loading and unloading, occupying about 30% of the time (Coelho and Brito, 2013). Only primary data was used for estimating the energy consumption and was obtained directly from the quarry and the company that processes oyster shells.

The water consumption data were obtained directly from the quarry and the company that processes oyster shells, being primary data as well and representative of these two processes in the conditions of this study. The water consumption was estimated at m^3 per tonne of aggregate produced.

The fuel consumption was calculated based on primary data obtained at the quarry and the company that processes oyster shells. The fuel used for transportation within the processing facility is considered indirect primary energy and hence, calculated in megajoules (MJ). Therefore, the fuel consumption was calculated for producing 1 tonne of aggregate (MJ/t).

The wastewater was estimated based on primary data obtained from the quarry (total water consumption per year) and is calculated in m^3 per tonne of aggregate produced. No water is used in the shells processing.

The solid waste was estimated based on the primary data obtained at the shells processing company. The solid waste was calculated in tonnes per tonne of aggregate produced.

With that being said, we are going to proceed with the different preliminary environmental analyses.

6.4.1 Analysis 1 – Direct burdens per 1 tonne of aggregate produced

Figure 6-4 shows the direct burdens (energy, water and fuel consumptions; wastewater and solid waste) per 1 tonne of aggregate produced (gravel, sand, OSFA – Oyster Shell Fine Aggregate, OSCA – Oyster Shell Coarse Aggregate).

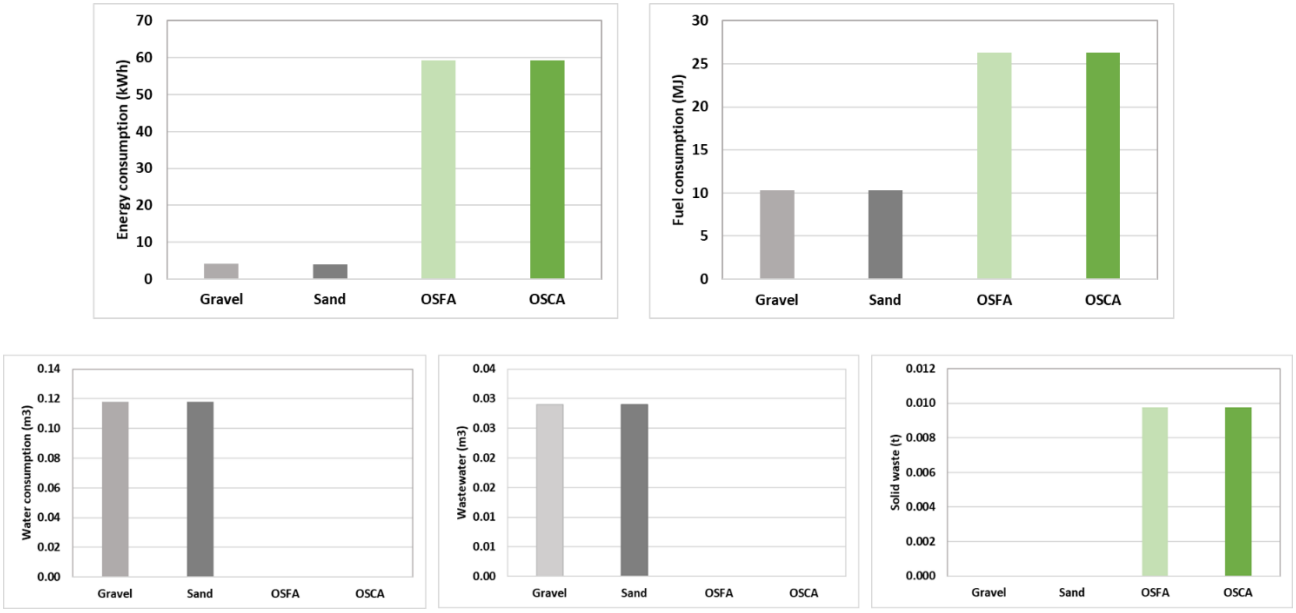

Figure 6-4 – Direct burdens per tonne of aggregate production (gravel, sand, OSFA, OSCA).

It can be seen that the highest consumptions in both types of aggregates (conventional or oyster shells) are concentrated on the energy and fuel demands. Additionally, the oyster shell aggregate production has a higher demand for energy (about 15 times greater) and fuel (about 2.5 times greater) consumption per tonne of production compared to the conventional aggregates. This is possible because of the process efficiency. The quarry capacity is about 400 tonnes/hour whereas the oyster shell processing is 1 tonne/hour. The quarry processing

facility is also optimised to work at the highest capacity and the raw resource extraction is within the size limits and is a constant resource while the quarry is in operation. The oyster shells are a by-product of another process, which means that the constancy of the production cannot be ensured and the volume of production is far from those of the quarry for the current scenario. However, tonnes of oyster shell waste are produced from the cleaning process and were dumped in the past in another area of the bay. If companies with bigger treatment facilities start crushing these oyster shells, the volume of shells being crushed can increase and be more compatible with the new production capacity, potentially decreasing the environmental and economical costs.

Hence, the direct burdens related to the production per tonne will be affected by the aforementioned reasons. Air pollution, global warming, and fossil resources are one of the main environmental impacts related to energy and fuel consumption. Hence, it is necessary to find ways to optimise the process to decrease these consumptions, especially for the oyster shell aggregate production.

In terms of water consumption, the current oyster shell processing does not include water whereas the quarry one does. Although the water consumption is relatively low per tonne of aggregate ($2.9x10^{-2}$ m^3/t aggregate), it is still consumption of a raw resource that was avoided in the shells processing. The main environmental impact related to this is water depletion, and although the process has a high recyclable percentage (80%), wastewater is still a sub-product of the process in the quarry. The potential environmental impacts related to wastewater are damage to the ecosystems if not correctly treated.

In terms of solid waste, the oyster shell processing produces a very low quantity per tonne of oyster shell aggregate ($9.75x10^{-3}$ t waste/t OS aggregate) whereas the quarry was considered as no solid waste was produced. The main environmental impacts related to solid waste are generally associated with land use/transformation, global warming, air pollution.

6.4.2 Analysis 2 – Energy consumption for each process of aggregate production

In this second analysis, we aimed to investigate the energy consumption of the process of aggregate production. This analysis will allow us to identify what are the process that increases the most energy demand and find opportunities for improvement.

Figure 6-4 shows the energy consumption for each process used in the processing facility to produce the oyster shell aggregate. It can be seen that the rotary kiln is the process of the highest energy-consuming. This phase is important to remove the organic matter from the shells since they are not washed before. Furthermore, it is crucial for other products that the company produces like animal food supply. However, this process can be adapted for oyster shell aggregate production since other ways to remove the organic matter can be implemented with less energy demand since less purity is required. Dust system control is the second most energy-consuming process. This system is based on many pipes connected to the equipment for collecting the dust in a closed circuit. This dust is directed to a cyclone and a filter. The energy demand for keeping this circuit is high because it is connected to all equipment of the processing, resulting in higher energy demand. Perharps, to produce the crushed oyster shells aggregates a washing phase can be added, removing the kiln and decreasing the dust since the shells will be wet. This phase could potentially decrease the energy demand but increase the water demand, but should be further investigated.

Conversely, the crusher, vibrating screen and the conveyors that connect the equipment are the processes that have the lower energetical demands. Althought the shells are easier to crush than conventional aggregates, the higher demand is possibly due to the smaller processing capacity of these equipments. The selective sorting does not contribute to the energy consumption since is a handpicking phase.

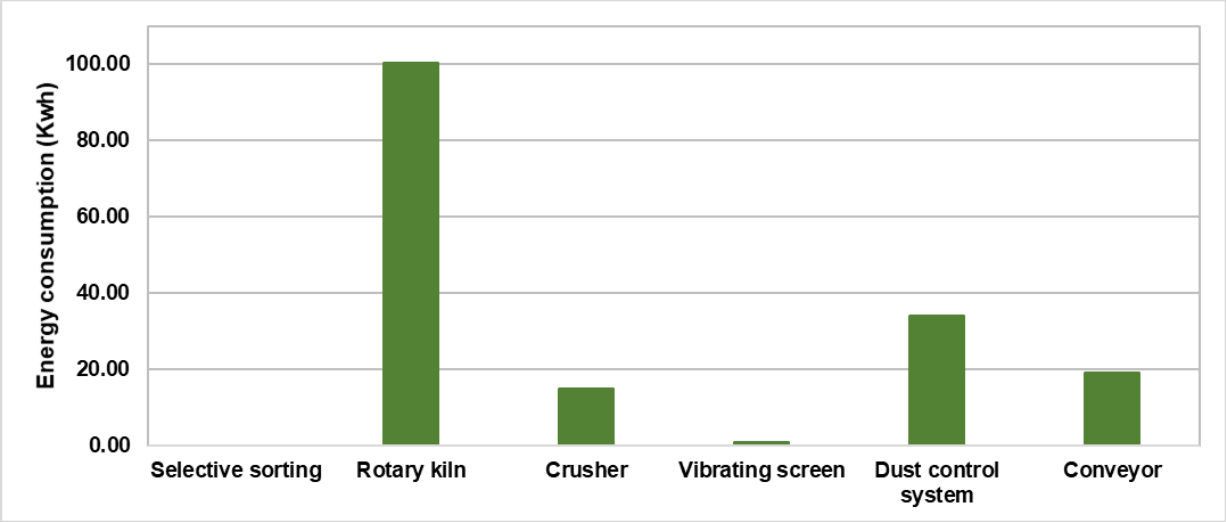

Figure 6-5 – Energy consumption (kWh) per process per tonne of oyster shell aggregate production.

Figure 6-5 shows the energy consumption per process used in the quarry processing facility to produce the conventional aggregates (fine and coarse). It can be seen that the conveyors are the highest energy-consuming in the process. This is possibly due to the distance the material is transported from the extraction to the processing facility and their weight. In this quarry, there are 3000 metres of conveyors only to transport the material from the extraction to the processing facility. Besides that, there are all the conveyors connecting the equipment during the processing. Hence, the conveyors are the equipment with the highest energy demand.

The vibrating screens and crushers are the second most consuming equipment after the conveyors. This is possibly because of the number of equipment (5 vibrating screens and 2 crushers) and their capacity to operate (to process 400 tonnes of aggregates per hour), increasing the energy demand. The 5 vibrating screens were used in this quarry due to their need of providing different grading. However, if we consider that the material produced will have only two sizes (0/4 mm and 4/10 mm), the process should be adapted and probably certain phases will not be necessary. However, based on the assumption we made in section 6.4.2 and to facilitate the analysis, we are considering the global production of a fine (0/6 mm) and coarse (6/22 mm) aggregates.

The washing process and hydrocyclones are the lower energy-consuming phase in the quarry processing and are probably related to their lower operation capacities too.

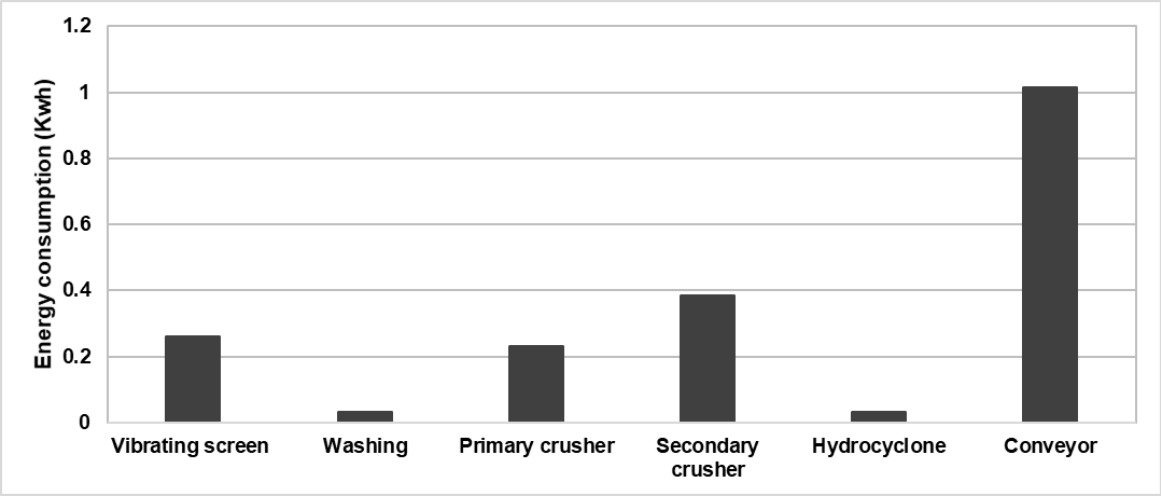

Figure 6-6 – Energy consumption (kWh) per process per tonne of conventional aggregate production.

6.5 Concluding remarks

A preliminary environmental analysis of the production process of aggregates (conventional and oyster shells) was carried out. After visiting a quarry and a company that currently process the oyster shells from Arcachon Bay (France) and collecting primary data concerning their processes, we were able to answer the questions proposed in this brief study.

Environmental impacts

The oyster shells can be considered as an avoided burden since they were supposed to be waste from Shellfish farming and were turned into a by-product for another process, avoiding waste disposal. In terms of the current processing, the main environmental impacts related to it are global warming (energy and fuel consumption, and waste disposal).

For the quarry process, we can estimate that some of the environmental impacts related to their activities are resource depletion (extraction of raw resources and water use), include global warming (due to energy and fuel consumption), and land transformation.

Process energy consumption

In the oyster shell company, the rotary kiln is the process most energy-consuming. This was expected since kilns are high electric demanding due to the capacity and heating process. This is an essential process for the company to produce different products, but adaptable if the production is completely directed to aggregate production.

In the quarry, the conveyors are the equipment the most energy-consuming. This was due to the distance between the extraction site and the processing facility, which is connected by 3000 metres of electric conveyors.

Opportunities for improvement

In the quarry case of study, the processing facility is very well organised for operating with the highest capacity and practices of recycling were also observed. Unfortunately, it is not always possible to install the treatment facility very close to the extraction site. In this quarry, the solution found to transport the mixing grade material from the extraction site to the processing

facility through conveyors (3000 metres of transporting conveyors) was probably less pollutant than transporting by lorries. The transport by lorries would increase carbon footprint due to the fuel consumption of lorries, besides the noise in the region and emissions to the air like particulate matter. Therefore, the conveyors used seemed to be a less impactful measure although the high energy consumption. The only opportunity for improvement we would suggest was regarding water recycling although the recycling rate is already high (80%).

In the case of oyster shell processing, there are a few opportunities to improve the process. Although organic matter in concrete is harmful, we believe that the rotary kiln process is not necessary and other types of the process can be used instead. Perhaps, a washing process (washing + vibrating screen) with a high water recycling rate can be an option. However, the impact of water depletion must be assessed in order to guarantee that this process is less harmful than the energy consumption of the kiln, resulting in an environmental benefit.

Another point is that the transportation from Arcachon Bay to the company that does the processing was not taken into account in this study because the best scenario is the processing *in-loco*. Material transportation through long distances should always be avoided since increases the carbon footprint of the material. Hence, to have an oyster shell processing facility close to the source of the material, in Arcachon Bay, can increase circularity and decrease the environmental impacts related to transportation.

A third point in the process concerns the processing capacity. Since the current processing operation capacity is about 1 tonne per day, the environmental impacts are more significant because of higher energy and fuel demands for lower production. If the treatment capacity is increased, the energy cost is divided by the greater amount of material treated, reducing the environmental impact per tonne of material.

Finally, increasing the production process of the crushed shells will also allow the recycling of all the waste that has been collected from the farming area and dumped at another point in the Arcachon bay. This waste is estimated at 9500 tonnes of shells per year and has a high potential to be used as aggregate for construction materials. Hence, the resource availability will increase as well as the processing decreasing the environmental impacts per tonne of crushed oyster shell aggregate production. The installation of a crushing facility in Arcachon Bay will also decrease environmental impacts related to the transportation of shells to other crushing facilities and will allow the recycling of this by-product locally.

CHAPTER 7 - GENERAL CONCLUSIONS AND PERSPECTIVES

In the context of sustainable development and looking for recycling by-products, this study aimed to fully replace conventional aggregates in concrete by crushed oyster shells (OS). Previous research investigated the feasibility of using crushed seashells as an aggregate replacement at different replacement rates. However, a full replacement of fine and coarse aggregate at the same time was not found in the literature and most studies recommended lower replacement rates (≤ 30%). Conversely, the urge for decreasing the extraction of raw materials and increase circularity practices converge to the need of changing habits and designing more sustainable materials by recycling resources already used in other processes. Hence, we developed a strategy to replace the raw resource (conventional aggregate) at the highest level (100%). General conclusions of this project are presented below:

Granular skeleton optimisation

It was necessary to optimise the granular skeleton of crushed oyster shells to fully replace conventional aggregates in concrete. This was necessary because the shells are non-spherical particles and hence, a direct replacement mimicking the conventional aggregate's gradation curve is not suitable. A general methodology was proposed to optimise the granular skeleton based on physical properties (loose bulk and oven-dried densities) to decrease its intergranular porosity. The main advantage of the method consists in its simplicity (easy laboratory measures – loose bulk and oven-dried densities, and intergranular porosity) and it does not rely on the geometry of the particle, which allows a better spread of the method for other bio-based materials. The experimental plan of optimisation was designed using statistical software (Minitab 17®) but any other statistical software can be used instead.

It was also observed a certain inaccuracy in sieving crushed oyster shells (already mentioned in previous studies) that led to adaptations in the particle groups selected for the optimisation process. Another important point in this method of skeleton optimisation is that we applied it separately to obtain a fine and coarse crushed oyster shell granular skeleton. Then, using the same approach of mixture design we optimised the best proportion between the fine and coarse aggregate for producing oyster shell granular skeleton of concrete.

The oyster shell optimised granular skeleton was compared to other oyster shell granular skeletons. A relative decrease of 20% was found for the intergranular porosity of the oyster

shell granular skeleton that was optimised with our method. It was also noted that when the particles are not proportionally distributed, the intergranular porosity tends to increase (the OS granular skeleton with the highest content of finer particles presents the higher intergranular porosity). Additionally, the OS granular skeleton mimicking sand provided higher intergranular porosity than the optimised OS skeleton (63.6% against 54.1%), confirming the interest on adapting the optimistion to the type of material.

Mortar study

In terms of mechanical performance, a relative decrease in compressive strength of 80% was observed from mortar with OS optimised skeleton (MOS 1) to mortar with the OS skeleton with high content of finer particles (MOS 4), highlighting the importance of the granular skeleton optimisation method. In terms of flexural strength, the MOS 1 provided similar performance to the mortar made with sand (8.3 ± 1 MPa for MOS 1 100% and 9.3 ± 1 MPa for MS 100% at 28 days) Therefore, MOS 1 mechanical performance demonstrates that the aggregate full replacement could be envisaged.

The crushed oyster shell particles being flaky and elongated also increase the demand for cement paste to cover them out. The lack of cement paste directly affects the workability and mechanical performance. Another important result from this study is that the filling rate (how much the intergranular porosity is filled with cement paste) should be take into consideration, especially for the oyster shell mortar formulations, and the variation of it will have a direct impact in mechanical properties.

Concrete study

A oyster shell concrete (OSC) and two conventional aggregate concretes were investigated (CAC – PA designed within the traditional prescriptive approach NF EN 206/CN; CAC – NPA designed beyond the traditional prescriptive approach – less cement content). The crushed oyster shells replaced 100% of the fine and coarse aggregate in concrete. The concretes had different filling rates: CAC – PA: 139%, OSC: 96%, CAC – NPA: 109%.

In terms of fresh properties, the crushed oyster shells decrease the concrete workability by about 8% although still providing a self-compacting concrete. The oyster shell concrete was

lighter as well (1787 kg/m^3) due to the lighter density of crushed oyster shells. Segregation and air entrapped were limited in the oyster shell concrete (OSC).

In terms of mechanical properties, the OSC shows a loss of over 50% in compressive strength compared to CAC – PA and CAC – NPA. This is possible because of several factors: the higher intergranular porosity of the granular skeleton; the lack of cement paste to cover all this porosity; the oyster shells are more fragile than sand and gravel, and the replacement rate (100% of fine and coarse aggregate). Conversely, OSC presented flexural strength similar to these of conventional aggregate concretes indicating a potential improvement of this property by the orientation of shells in the concrete.

In terms of durability, OSC shows higher porosity, capillary water absorption coefficient and carbonation rate. These properties were probably affected by the greater porosity as aforementioned. Conversely, the gas permeability and the chloride diffusion coefficient were similar to those found for the concrete with conventional aggregates.

The loss in compressive strength of OSC is directly related to the higher porosity observed in the porosity accessible to water and capillary water absorption results. A higher porosity results in a weaker material. Conversely, we found good results for transport properties (gas permeability and chloride diffusion) of OSC, demonstrating that the transport properties are more related to the pore size, tortuosity and constrictivity than the general porosity measured by the previously mentioned tests. Additionally, the use of CEM V/A (suitable for marine environment) improved the resistance to aggressive agents in the Oyster Shell Concrete evidenced by the chloride diffusion coefficient of this concrete.

The performance-based approach was used to evaluate the potential durability of the OSC, and CAC – PA and CAC – NPA for comparison purpose with traditional concrete. General and substitution indicators were selected. The CAC – PA presents low potential durability to porosity accessible to water, and high for gas permeability and chloride diffusivity. The OSC presents very low potential durability to porosity accessible to water, medium to gas permeability and high to the chloride diffusivity. The CAC – NPA presents medium potential durability to porosity accessible to water, low for gas permeability and high for chloride diffusivity. Therefore, all concrete provides interesting performances and can be used as long as the final use and durability required are adapted to it.

Another interesting point is that CAC – NPA contains a lower quantity of cement paste and still provides similar or better performance than CAC – PA. This demonstrates the importance of studying further the properties of materials and not focusing only on a prescriptive formulation.

From the results of this study, we can say that the full replacement of conventional aggregates per crushed oyster shells in concrete is envisaged and viable. Although the loss in compressive strength and increase of porosity, the Oyster Shell Concrete provided interesting performance for low load bearing and short life service. Being this concrete is a bio-based material, recycling at the end of life can also be envisaged within circularity practices.

Environmental analysis

From the environmental analysis, we could see that the oyster shell crushing process seems to be more energy consuming than the process in the quarry to obtain conventional aggregates. However, the current production capacity of the oyster shell crushing company is about 400 times smaller than the quarry. Tonnes of oyster shell waste from Arcachon Bay can be recycled and if bigger companies start processing this material. Hence, the impact of the process per tonne of crushed oyster shell will probably decrease.

The oyster shell crushing process can be adapted to produce aggregates, since the current process aims to produce other products with certain purity level (animal food supply). Therefore, a high energy consuming phase (rotary kiln) can be replaced for other processes to remove organic matter from the shells that are less energy demanding. We suggested adding a washing phase to replace the rotary kiln phase but the environmental impact should be assessed.

Perspectives and future recommendations

This study aimed to contribute to the development of environmentally-friendly construction materials. The experimental investigation carried out demonstrated the feasibility of the recycling of crushed oyster shells in concrete and the durability properties of this material. Throughout this thesis, many research points of interest were found and we believe they deserve further investigation:

- The transition of the optimisation method to an industrial scale;
- Evaluation of the feasibility of applying the optimisation method to other seashells and bio-based materials;
- Investigation of seashell concrete performances with 100% of the intergranular porosity filled with cement paste;
- Study of the life cycle assessment of the oyster shell concrete to investigate the carbon footprint and other environmental impacts compared to conventional concretes.

REFERENCES

AFGC, 2018a. Recommandations : Bien Prescrire Les Bétons Choix Des Classes D'Exposition Selon La Norme Nf En 206 / Cn 1–12.

AFGC, 2018b. Recommandations : bien prescrire les bétons - Approche performantielle des bétons.

AFGC, 2004. Conception des bétons pour une durée de vie - Donnée des ouvrages: Maîtrise de la durabilité vis-à-vis de la corrosion des armatures et de l'alcali-réaction, Association Française de Génie Civil. Paris.

AFPC - AFREM a, 1997. Compte-rendu des journées techniques AFPC - AFREM - Durabilité des bétons: Méthodes recommandées pour la mesure des grandeurs associées à la durabilité: determination de la masse volumique apparante et de la porosité accessible à l'eau. Toulouse.

AFPC - AFREM b, 1997. Compte-rendu des journées techniques AFPC - AFREM - Durabilité des bétons: Méthodes recommandées pour la mesure des grandeurs associées à la durabilité: mesure de l'absorption capillaire d'eau. Toulouse.

Alexander, M., Mindess, S., 2010. Aggregate in Concrete, Civil Engineering.

Alvarenga, R.A.F. de, Galindro, B.M., Helpa, C. de F., Soares, S.R., 2012. The recycling of oyster shells: An environmental analysis using Life Cycle Assessment. J. Environ. Manage. 106, 102–109. https://doi.org/10.1016/j.jenvman.2012.04.017

Association française de normalisation, NF EN 1097-3:1998 – Test for mechanical and physical properties of aggregates – Part 3: Determination of loose bulk density and voids, AFNOR – Association française de normalisation, Saint Denis, France (Aug. 1998).

Association française de normalisation, NF EN 12620+A1:2008 – Aggregates for concrete, AFNOR – Association française de normalisation, Saint Denis, France (Jun. 2008).

Association française de normalisation, NF EN 1097-5:2008 – Test for mechanical and physical properties of aggregates – Part 6: Determination of the water content by drying in a ventilated oven, AFNOR – Association française de normalisation, Saint Denis, France (Oct. 2008).

Association française de normalisation, NF EN 12350-11:2010 – Testing fresh concrete – Part 11: self-compacting concrete – sieve segregation test, AFNOR – Association française de normalisation, Saint Denis, France (Nov. 2010).

Association française de normalisation, XP P18-463:2011 – Testing gas permeability on hardened concrete, AFNOR – Association française de normalisation, Saint Denis, France (Nov. 2011).

Association française de normalisation, NF EN 12390-6:2012 – Testing hardened concrete – Part 6: tensile splitting strength of test specimens, AFNOR – Association française de normalisation, Saint Denis, France (Apr. 2012).

Association française de normalisation, NF EN 206/CN – Béton – Spécification, performance, production et conformité – Complément national à la norme NF EN 206, Standard, AFNOR – Association française de normalisation, Saint Denis, France (Dec. 2014).

Association française de normalisation, NF EN 196-1:2016 – Methods for testing cement – Part 1: Determination of strength, Standard, AFNOR – Association française de normalisation, Saint Denis, France (Sep. 2016).

Association française de normalisation, NF EN 12350-8:2019 – Testing fresh concrete – Part 8: self-compacting concrete – Slump-flow test, Standard, AFNOR – Association française de normalisation, Saint Denis, France (Jun. 2019).

Association française de normalisation, NF EN 12350-7:2019 – Testing fresh concrete – Part 7: air content – Pressure methods, AFNOR – Association française de normalisation, Saint Denis, France (Jun. 2019).

Association française de normalisation, NF EN 12350-6:2019 – Testing fresh concrete – Part 6: density, AFNOR – Association française de normalisation, Saint Denis, France (Jun. 2019).

Association française de normalisation, NF EN 12390-3:2019 – Testing hardened concrete – Part 3: compressive strength of test specimens, AFNOR – Association française de normalisation, Saint Denis, France (Jun. 2019).

Association française de normalisation, NF EN 12390-5:2019 – Testing hardened concrete – Part 5: flexural strength of test specimens, AFNOR – Association française de normalisation, Saint Denis, France (Jun. 2019).

Association française de normalisation, NF EN 12390-13:2021 – Testing hardened concrete – Part 13: determination of secant modulus of elasticity in compression, AFNOR – Association française de normalisation, Saint Denis, France (Jul. 2021).

Association française de normalisation, NF EN 1097-6:2022 – Test for mechanical and physical properties of aggregates – Part 6: Determination of particle density and water absorption, AFNOR – Association française de normalisation, Saint Denis, France (Feb. 2022).

Auroy, M., Poyet, S., Le Bescop, P., Torrenti, J.M., Charpentier, T., Moskura, M., Bourbon, X., 2015. Impact of carbonation on unsaturated water transport properties of cement-based materials. Cem. Concr. Res. 74, 44–58. https://doi.org/10.1016/j.cemconres.2015.04.002

Bamigboye, G.O., Nworgu, A.T., Odetoyan, A.O., Kareem, M., Enabulele, D.O., Bassey, D.E., 2021. Sustainable use of seashells as binder in concrete production: Prospect and challenges. J. Build. Eng. 34, 101864. https://doi.org/10.1016/j.jobe.2020.101864

Benaicha, M., Hafidi Alaoui, A., Jalbaud, O., Burtschell, Y., 2019. Dosage effect of superplasticizer on self-compacting concrete: Correlation between rheology and strength. J. Mater. Res. Technol. 8, 2063–2069. https://doi.org/10.1016/j.jmrt.2019.01.015

Beushausen, H., Torrent, R., Alexander, M.G., 2019. Performance-based approaches for concrete durability: State of the art and future research needs. Cem. Concr. Res. 119, 11–20. https://doi.org/10.1016/j.cemconres.2019.01.003

Boel, V., Audenaert, K., De Schutter, G., 2008. Gas permeability and capillary porosity of self-compacting concrete. Mater. Struct. Constr. 41, 1283–1290. https://doi.org/10.1617/s11527-007-9326-x

Carcasses, M., Linger, L., Cussigh, F., Rougeau, P., Barberon, F., Thauvin, B., Cassagnabere, F., Mai-Nhu, J., Dierkens, M., Cubaynes, M.P., 2015. Setting up of a database dedicated to durability indicators by the civil works French Association (AFGC) to support the implementation of concrete performance-based approach. Concr. - Innov. Des. fib Symp. Proc. 355–357.

Chabil, F.-Z.D., 2009. Carbonatation de betons adjuvantes a base de ressources locales algeriennes. Universite Mentouri Constantine.

Chaussadent, T., 1999. Etat des lieux et réflexions sur la carbonatation du béton armé 80.

Chen, D., Zhang, P., Pan, T., Liao, Y., Zhao, H., 2019. Evaluation of the eco-friendly crushed waste oyster shell mortars containing supplementary cementitious materials. J. Clean. Prod. 237, 117811. https://doi.org/10.1016/j.jclepro.2019.117811

Coelho, A., Brito, J. de, 2013. Environmental analysis of a construction and demolition waste recycling plant in Portugal - Part I: Energy consumption and CO2 emissions. Waste Manag. 33, 1258–1267. https://doi.org/10.1016/j.wasman.2013.01.025

Cuadrado-Rica, H., 2016. Étude Du Comportement De Bétons De Coproduits Coquilliers Pour Une Utilisation En Récifs Artificiels. Université de Caen Normandie.

Cuadrado-Rica, H., Sebaibi, N., Boutouil, M., Boudart, B., 2016. Properties of ordinary concretes incorporating crushed queen scallop shells. Mater. Struct. Constr. 49, 1805–1816. https://doi.org/10.1617/s11527-015-0613-7

C. Furnas, 1931. Grading Aggregates; Mathematical Relations for Beds of Broken Solids of Maximum Density, Industrial and Engineering Chemistry, 23 (9), 1052-1058

De Larrard, F., 1999. Structures granulaires et formulation des bétons. Londres.

Drouet, E., 2010. Impact de la température sur la carbonatation des matériaux cimentaires : prise en compte des transferts hydriques. École normale supérieure de Cachan.

Eo, S.-H., Yi, S.-T., 2015. Effect of oyster shell as an aggregate replacement on the characteristics of concrete. Mag. Concr. Res. 67, 833–842. https://doi.org/10.1680/macr.14.00383

Eziefula, U.G., Ezeh, J.C., Eziefula, B.I., 2018. Properties of seashell aggregate concrete: A review. Constr. Build. Mater. 192, 287–300. https://doi.org/10.1016/j.conbuildmat.2018.10.096

Fennis, S.A.A.M., Walraven, J.C., Den Uijl, J.A., 2009. The use of particle packing models to design ecological concrete. Heron 54, 183–202.

FNTP, 2009. Méthodologie d'application du concept de performance équivalente des bétons.

Foti, D., Cavallo, D., 2018. Mechanical behavior of concretes made with non-conventional organic origin calcareous aggregates. Constr. Build. Mater. 179, 100–106. https://doi.org/10.1016/j.conbuildmat.2018.05.042

Georges, M., Bourguiba, A., Chateigner, D., Sebaibi, N., Boutouil, M., 2021. The study of long-term durability and bio-colonization of concrete in marine environment. Environ. Sustain. Indic. 10, 100120. https://doi.org/10.1016/j.indic.2021.100120

Georges, M., Bourguiba, A., Sebaibi, N., Chateigner, D., Boutouil, M., 2020. Concrete Durability Probed Using Compressive Strength, Chloride Penetration and Porosity Measurements on CEMII and CEMV Concretes Incorporating Mollusc Shell Spares in Artificial and Natural Seawaters. https://doi.org/10.23967/dbmc.2020.025

Goodier, C.I., 2019. Development of self-compacting concrete. Loughborough, UK.

Hasnaoui, A., Bourguiba, A., El Mendili, Y., Sebaibi, N., Boutouil, M., 2021. A preliminary investigation of a novel mortar based on alkali-activated seashell waste powder. Powder Technol. 389, 471–481. https://doi.org/10.1016/j.powtec.2021.05.069

Ilgar, A., 2015. Approche performantielle des bétons: vers une meilleure caractérisation des indicateurs de durabilité. Université Paul Sabatier - Toulouse III.

IREX, 2014. Projet National Approche performantielle de la durabilité des ouvrages en béton (PERFDUB) 1–88.

Kumar, S. V., Santhanam, M., 2003. Particle packing theories and their application in concrete mixture proportioning: A review. Indian Concr. J. 77, 1324–1331.

Kuo, W. Ten, Wang, H.Y., Shu, C.Y., Su, D.S., 2013. Engineering properties of controlled low-strength materials containing waste oyster shells. Constr. Build. Mater. 46, 128–133. https://doi.org/10.1016/j.conbuildmat.2013.04.020

La Plante, E.C., Simonetti, D.A., Wang, J., Al-Turki, A., Chen, X., Jassby, D., Sant, G.N., 2021. Saline Water-Based Mineralization Pathway for Gigatonne-Scale CO2 Management. ACS Sustain. Chem. Eng. 9, 1073–1089. https://doi.org/10.1021/acssuschemeng.0c08561

LCPC, 2010. Maîtrise de la durabilité des ouvrages d ' art en béton.

Liao, Y., Fan, J., Li, R., Da, B., Chen, D., Zhang, Y., 2022. Influence of the usage of waste oyster shell powder on mechanical properties and durability of mortar. Adv. Powder Technol. 33. https://doi.org/10.1016/j.apt.2022.103503

Linger, L.; Cussigh, F., 2017. PERFDUB: A new French research project on performance-based approach for justifying concrete structures durability. High Tech Concr. Where

Technol. Eng. Meet - Proc. 2017 fib Symp. 10. https://doi.org/10.1007/978-3-319-59471-2

Ma, K., Feng, J., Long, G., Xie, Y., Chen, X., 2017. Improved mix design method of self-compacting concrete based on coarse aggregate average diameter and slump flow. Constr. Build. Mater. 143, 566–573. https://doi.org/10.1016/j.conbuildmat.2017.03.142

Marinkovic, S.B., 2013. Life cycle assessment (LCA) aspects of concrete, Eco-Efficient Concrete. https://doi.org/10.1533/9780857098993.1.45

Martínez-García, C., González-Fonteboa, B., Carro-López, D., Martínez-Abella, F., 2019. Impact of mussel shell aggregates on air lime mortars. Pore structure and carbonation. J. Clean. Prod. 215, 650–668. https://doi.org/10.1016/j.jclepro.2019.01.121

Martínez-García, C., González-Fonteboa, B., Martínez-Abella, F., Carro- López, D., 2017. Performance of mussel shell as aggregate in plain concrete. Constr. Build. Mater. 139, 570–583. https://doi.org/10.1016/j.conbuildmat.2016.09.091

Matrose, N.A., Obikese, K., Belay, Z.A., Caleb, O.J., 2022. A calcification-related calmodulin-like protein in the oyster Crassostrea gigas mediates the enhanced calcium deposition induced by CO2 exposure. Sci. Total Environ. https://doi.org/10.1016/j.scitotenv.2022.155114

Mehdipour, I., Khayat, K.H., 2018. Understanding the role of particle packing characteristics in rheo-physical properties of cementitious suspensions: A literature review. Constr. Build. Mater. 161, 340–353. https://doi.org/10.1016/j.conbuildmat.2017.11.147

Metha, P. K.; Monteiro, P.J.M., 2001. CONCRETE: Microstructure, Properties and Materials.

Mo, K.H., Alengaram, U.J., Jumaat, M.Z., Lee, S.C., Goh, W.I., Yuen, C.W., 2018. Recycling of seashell waste in concrete: A review. Constr. Build. Mater. 162, 751–764. https://doi.org/10.1016/j.conbuildmat.2017.12.009

Monneron-Gyurits, M., Joussein, E., Soubrand, M., Fondanèche, P., Rossignol, S., 2018. Valorization of mussel and oyster shells toward metakaolin-based alkaline activated material. Appl. Clay Sci. 162, 15–26. https://doi.org/10.1016/j.clay.2018.05.027

Neville, A.M., Brooks, J.J., 2010. Concrete Technology. https://doi.org/10.6004/jnccn.2015.0201

Nguyen, D.H., Boutouil, M., Sebaibi, N., Baraud, F., Leleyter, L., 2017. Durability of pervious concrete using crushed seashells. Constr. Build. Mater. 135, 137–150. https://doi.org/10.1016/j.conbuildmat.2016.12.219

Nguyen, D.H., Boutouil, M., Sebaibi, N., Leleyter, L., Baraud, F., 2013. Valorization of seashell by-products in pervious concrete pavers. Constr. Build. Mater. 49, 151–160. https://doi.org/10.1016/j.conbuildmat.2013.08.017

Olivia, M., Mifshella, A.A., Darmayanti, L., 2015. Mechanical properties of seashell concrete. Procedia Eng. 125, 760–764. https://doi.org/10.1016/j.proeng.2015.11.127

Perlot, C., 2005. Influence de la décalcification de matériaux cimentaires sur les propriétpés de transfert: application au stockage profond de déchets radioactifs. Université Paul Sabatier - Toulouse III.

P. Andersen, B. Johansen, 1991. Particle packing and concrete properties, Materials Science of Concrete II, 111-147

P. Goltermann, V. Johansen, L. Palbol, 1997. Packing aggregates: An Alternative Tool to Determine the Optimal Aggregate Mix, ACI Materials Journal, 94 (5), 435-443

Rozière, E., Loukili, A., Cussigh, F., 2009. A performance based approach for durability of concrete exposed to carbonation. Constr. Build. Mater. 23, 190–199. https://doi.org/10.1016/j.conbuildmat.2008.01.006

Safi, B., Saidi, M., Daoui, A., Bellal, A., Mechekak, A., Toumi, K., 2015. The use of seashells as a fine aggregate (by sand substitution) in self-compacting mortar (SCM). Constr. Build. Mater. 78, 430–438. https://doi.org/10.1016/j.conbuildmat.2015.01.009

Saiyouri, Nadia, Bouasker, Marwen, Khelidj, Abdelhafid, Saiyouri, Nadia, Bouasker, Marwen, Khelidj, Abdelhafid, Permeability, G., Saiyouri, N, Bouasker, M, Khelidj, A, 2007. Gas Permeability measurement on injected soils with cement grout. Cem. Concr. Res. 38, 95–103.

San Nicolas, R., Cyr, M., Escadeillas, G., 2014. Performance-based approach to durability of concrete containing flash-calcined metakaolin as cement replacement. Constr. Build. Mater. 55, 313–322. https://doi.org/10.1016/j.conbuildmat.2014.01.063

Sebaibi, N., Benzerzour, M., Sebaibi, Y., Abriak, N.E., 2013. Composition of self compacting

concrete (SCC) using the compressible packing model, the Chinese method and the European standard. Constr. Build. Mater. 43, 382–388. https://doi.org/10.1016/j.conbuildmat.2013.02.028

Shi, C., Wu, Z., Lv, K., Wu, L., 2015a. A review on mixture design methods for self-compacting concrete. Constr. Build. Mater. 84, 387–398. https://doi.org/10.1016/j.conbuildmat.2015.03.079

Shi, C., Wu, Z., Lv, K., Wu, L., 2015b. A review on mixture design methods for self-compacting concrete. Constr. Build. Mater. 84, 387–398. https://doi.org/10.1016/j.conbuildmat.2015.03.079

Silva, T.H., Mesquita-Guimarães, J., Henriques, B., Silva, F.S., Fredel, M.C., 2019. The Potential Use of Oyster Shell Waste in New Value-Added By-Product. Resources 8, 1–15. https://doi.org/10.3390/resources8010013

Su, N., Hsu, K.C., Chai, H.W., 2001. A simple mix design method for self-compacting concrete. Cem. Concr. Res. 31, 1799–1807. https://doi.org/10.1016/S0008-8846(01)00566-X

Tayeh, B.A., Hasaniyah, M.W., Zeyad, A.M., Yusuf, M.O., 2019. Properties of concrete containing recycled seashells as cement partial replacement: A review. J. Clean. Prod. 237, 117723. https://doi.org/10.1016/j.jclepro.2019.117723

Thiery, M., 2005. Modelling of atmospheric carbonation of cement based materials considering the kinetic effects and modifications of the microstructure and the hydric state. Ecole des Ponts Paris Tech.

Truc, O., Ollivier, J.P., Carcassès, M., 2000. New way for determining the chloride diffusion coefficient in concrete from steady state migration test. Cem. Concr. Res. 30, 217–226. https://doi.org/10.1016/S0008-8846(99)00232-X

Van Den Heede, P., De Belie, N., 2012. Environmental impact and life cycle assessment (LCA) of traditional and “green” concretes: Literature review and theoretical calculations. Cem. Concr. Compos. 34, 431–442. https://doi.org/10.1016/j.cemconcomp.2012.01.004

Varhen, C., Carrillo, S., Ruiz, G., 2017. Experimental investigation of Peruvian scallop used as fine aggregate in concrete. Constr. Build. Mater. 136, 533–540. https://doi.org/10.1016/j.conbuildmat.2017.01.067

Wang, J., Liu, E., Li, L., 2019. Characterization on the recycling of waste seashells with Portland cement towards sustainable cementitious materials. J. Clean. Prod. 220, 235–252. https://doi.org/10.1016/j.jclepro.2019.02.122

W. Fuller, S. Thompson, 1907. The laws of proportioning concrete, ASCE J. Transport, 59, 67-143

Yang, E.I., Kim, M.Y., Park, H.G., Yi, S.T., 2010. Effect of partial replacement of sand with dry oyster shell on the long-term performance of concrete. Constr. Build. Mater. 24, 758–765. https://doi.org/10.1016/j.conbuildmat.2009.10.032

Yang, E.I., Yi, S.T., Leem, Y.M., 2005. Effect of oyster shell substituted for fine aggregate on concrete characteristics: Part I. Fundamental properties. Cem. Concr. Res. 35, 2175–2182. https://doi.org/10.1016/j.cemconres.2005.03.016

Yoon, G.L., Kim, B.T., Kim, B.O., Han, S.H., 2003. Chemical-mechanical characteristics of crushed oyster-shell. Waste Manag. 23, 825–834. https://doi.org/10.1016/S0956-053X(02)00159-9

Yoon, H., Park, S., Lee, K., Park, J., 2004. Oyster shell as substitute for aggregate in mortar. Waste Manag. Res. 22, 158–170. https://doi.org/10.1177/0734242X04042456

Yu, A., Standish, N., Mclean, A., 1993. Porosity calculation of binary mixtures of nonspherical particles. J. Am. Ceram. Soc. 76, 2813–2816.

Yu, A.B., Standish, N., 1992. Characterisation of non-spherical particles from their packing behaviour. Powder Technol. 74, 205–213.